COMPARISON OF SHEAR CAPACITY OF T-BEAMS USING STRUT AND TIE ANALYSIS

By
Alexandra A. Hofer
Steven L. McCabe

Structural Engineering and Engineering Materials
SM Report No. 48

UNIVERSITY OF KANSAS CENTER FOR RESEARCH, INC.
LAWRENCE, KANSAS
January 1998

ABSTRACT

Comparison of Shear Capacity of T-Beams Using Strut and Tie Analysis

The objective of this research was to study the shear strength of continuous lightly reinforced concrete beams which are widely used in practice in North America.

In 1990 six two-span T-beams were tested at the University of Kansas. The research was focused on the primary variables of longitudinal reinforcement ratio and nominal stirrup strength. The tests indicated that the shear provisions of ACI 318-89 overpredicted the concrete shear capacity of lightly reinforced beams in negative moment regions, and underestimated the stirrup contribution to shear strength which increases with higher flexural reinforcement ratios.

These experimental results were reevaluated and analyzed with the shear provisions obtained from existing codes and theories from Europe and Canada including EC 2, DIN 1045, CEB Model Code 1990, ACI 318-95, and Modified Compression Field Theory. In addition a Strut and Tie analysis for these tests also was conducted.

The study indicates that the shear strength may be determined by Strut and Tie approaches with variable inclination θ of the compression field based on the theory of plasticity to derive the interaction between bending moment and shear . The comparison shows that the shear capacity based on a clear truss model and the theory of plasticity gives results that correspond to the experimental results and lead to an economic design. Moreover, the results of this study also reveal the limitation of the present ACI provisions and show that codes formulated on a rigorous theoretical foundation provides excellent results when compared the test data.

ACKNOWLEDGEMENTS

This report was supported by the Department of Civil and Environmental Engineering at the University of Kansas. The authors gratefully acknowledge this support.

TABLE OF CONTENTS

TABLE OF CONTENTS CONTINUED

LIST OF TABLES

LIST OF TABLES CONTINUED

LIST OF FIGURES

LIST OF FIGURES CONTINUED

CHAPTER 1
Introduction

1.1 General

The nature of shear failures in flexural members is usually abrupt and nonductile with little indication of distress prior to rapid reduction in the load carrying capacity of the member. Thus, the accurate determination of the shear capacity of reinforced concrete members is important to maintain a consistent level of safety in the structure. At the same time, analysis methods must not be so conservative that the economy of the section is compromised, Lastly, while analysis procedures must be accurate they also must be relatively easy for designers to apply in real situations.

In the present state of the art, there is a wide range of accuracy and complexity involved in predicting shear capacities and designing shear reinforcement. Present ACI methods are empirical in nature and have been in place for thirty years. In Europe, nearly all of the applicable codes and standards apply some form of strut and tie method (STM) analysis based on work done at the turn of the century in Germany. The Canadians also have developed a promising approach related the STM that currently has been adopted by AASHTO in the latest Bridge Specification.

The point is that there is not a common agreement on how to determine the shear capacity of reinforced concrete members. However, the methods found elsewhere are founded on a more sound analytical foundation than is the present ACI 318 approach. The question is, therefore, how well these other approaches and

philosophies would do in predicting capacities of a "typical" US reinforced concrete system where the capacities were known.

The purpose of this study is to reevaluate the results obtained from a recent study of shear capacities of continuous T-beams that was conducted at the University of Kansas by Pasley et al. in 1990 (21). This experimental study revealed that the capacities predicted by ACI 318 were unconservative in the negative moment regions, while at the same time the stirrup contributions were underestimated. The question is, how would code procedures from Europe and Canada do in predicting capacities for this same series of tests? In addition, one can inquire as to how well a general non-code based strut and tie analysis would do in predicting the capacities for this test setup. Since the STM methods are widely used, the ease and accuracy of this approach in important to assess for future implementation in ACI 318 procedures.

What will follow is a discussion of the historical development of shear analysis and design procedures and a detailed summary of these approaches. Application of these techniques to a set of typical sample beams as well as to the Pasley test beams will be performed. An STM approach also will be derived and applied to these test beams as well and the results compared with test results and with results from other code procedures.

The thesis will conclude with an assessment of these methods in comparison with those found in the ACI 318 Building Code and with recommendations for the development of new procedures for the 2001 version of the ACI Building Code.

1.2 Previous Research

Since the beginning of this century many investigators have experimentally studied the behavior of reinforced concrete beams in shear. The available results are numerous but most of the investigations are not related to each other. The test data is mainly based on simply supported beams and often test setups did not meet real conditions.

In 1899 and 1902, the Swiss engineer Ritter (22) and the German engineer Mörsch[1] (19) published papers proposing the truss analogy for the design of reinforced concrete beams for shear. These first truss models neglected the contribution of the concrete tensile strength and implied an inclination, θ of 45°. In the 1960's Leonhardt and Walther[2] did numerous beam tests at the University of Stuttgart, Germany. They concluded that the angle between the compression strut and the axis of the member, θ, is less that 45° as assumed by Mörsch and that the compression chord was inclined. Leonhardt's approach was adopted by the DIN 1045[3] (25, 26) which is still the current design code in Germany. In the 1970's European engineers developed the CEB-FIB Model Code[4] synthesizing technical developments over the past decades. Based on the CEB-FIB Model Code 1990 (9, 10, 11) the Eurocode 2[5] (23, 26) was developed. The basis for the used Strut and Tie Model is the classical truss model by Mörsch. The standard method implies an

[1] More information is given in section 2.3.
[2] More information is given in section 2.4.
[3] More information is given in section 2.5.
[4] More information is given in section 2.6.

inclination of 45° and the more detailed approach an inclination ranging in 29.7° and 60.3°.

In North America Ritter's truss model was introduced by Witney in 1906. Testing by Whitney (32, 33) and Talbot (27), independently, proced that the results were conservatice in comparison with the test data. In 1920 ACI Standard Specification No. 23 (1) represented the American shear design philosophy considering a truss model, a concrete contribution term, V_c, and inclination, θ of 45°. In the period until 1940 the first testing was conducted concerning shear strength, f_c', length to depth ratios, l/d, and percentage of longitudinal reinforcement, ρ_w.

In 1955 a warehouse roof collapsed at Wilkins Air Force Depot in Shelby, Ohio, USA, indicating a shear induced failure and questioning the current shear design procedures. In 1973 the ACI-ASCE Committee 426 Report presented a summary of experimental investigations synthesizing technical development over the past decades (3). The provisions for shear found in the current ACI 318 are based on the report of Committee 426 noted in references 2-5. Since the 1960's, investigations have implied Strut and Tie Models (STM) for shear and torsion and an inclination, θ, less than 45° (24). In 1974 Mitchell and Collins defined the Compression Field Theory (CFT) (18), an iterative procedure. Linear elasticity which is a main assumption for Strut and Tie approaches is neglected in the CFT. In 1986 Vecchio

[5] More information is given in section 2.7.

and Collins developed the Modified Compression Field Theory[6] (28, 29), an iterative procedure for members with little or no amount of shear reinforcement. In 1995 the ACI-ASCE Committee 445 began work on a state-of-the-art report for shear and torsion. This report is intended to summarize past and current shear design procedures and experimental investigations as well as to concentrate on STM.

The current interest in shear capacity and accurate prediction can be illustrated by examining a study conducted an the University of Kansas where the shear strength of continuous lightly reinforced concrete T-beams was studied by Pasley et al. (21). These members were designed to reflect actual member configuration and to study the effects of negative moments on shear. The study was important since lightly reinforced T-beams are widely used in practice in North America and provide the most economical section in many cases. Six two-span T-beams of approximately 7 meters in span length, with and without web reinforcement were tested. The primary variables were longitudinal reinforcement ratio (0.75% and 1.0%) and nominal stirrup strength (0 to 574 MPa, 0 to 82 psi). The tests indicated that ACI 318-89 overpredicted the concrete shear capacity of lightly reinforced beams without shear reinforcement and thus produced unconservative results. In this study there were only small difference between shear cracking stresses in positive and negative moment regions of the beams. In both regions the stirrup contribution to shear strength

[6] More information is given in section 2.8.
6

exceeded the values predicted per ACI 318-89 primarily because the shear mode geometries were flatter than 45° assumed in the ACI Building Code.

Pasley et al. (21) noted in the report that the results were consistent with previous research that found that the shear cracking load predicted by the ACI 318 Building Code shear provisions were unconservative for beams having longitudinal reinforcement ratios, ρ_w, less than 1%.

It is important to note that the American Concrete Institute is in progress of changing the shear provisions in the ACI Building Code for the 2001 edition. The preferred method under study is a truss model based on Strut and Tie Theory which has been widely used in Europe since 1900. This research gives some insight into the current European practice concerning shear provisions.

1.3 Scope and Objectives of the Investigation

The purpose of this thesis was to study the shear strength of continuous lightly reinforced T-beams and the effects of flexural reinforcement ratio and degree of shear reinforcement on shear capacity using alternative analysis approaches not employed in the original research by Pasley et al.

The predicted shear response of beams obtained using the ACI 318-95, DIN 1045, EC 2, CEB Model 1990, Modified Compression Field Theory, Strut and Tie Theory and the predictive equations of other investigators were compared with the experimental test results obtained by Pasley et al. (21) at the University of Kansas.

The goal was to utilize the experimental data to calibrate these other analysis approaches in particular Strut and Tie approaches and to assess how well other code approaches predict the capacity of these members. STM derived herein are of particular interest since ACI is moving to adopt a form of STM approach for the 2001 version of the ACI 318 Building Code.

CHAPTER 2
Summary of Shear Provisions Found in North American and European Building Codes

2.1 Introduction

Building codes are designed to cover a wide range of structural analysis and design problems. As such their view is general in nature and is designed to produce structures that are safe, yet economical to construct. In addition, building codes have to take into account the individual differences that exist in the types of construction practices in a particular region or country, as well as the differences in approaches taken by the engineers who will use the codes. This fact is particularly true in the case of shear design provisions. The range of approaches vary from an empirical approach as taken by the ACI 318 to a rigorous iterative procedure as advocated by the MCFT and AASHTO[7]. It is the purpose of this chapter to summarize these various approaches and point out how engineers would apply these various codes to the design of reinforced concrete structures.

Accordingly, this chapter contains a detailed summary of the procedures for the building codes to be used in reevaluating the Pasley data. The codes include the ACI 318-95, noting that the ACI 318-89 provisions used by Pasley are unchanged in the '95 version of the ACI Building Code. European codes include the Eurocode 2 developed in Europe by consensus process and CEB Model Code 90 also developed in Europe but a more theoretical and less "realistic" design code than the EC 2. The

[7] AASHTO Bridge Specification.

CEB MC 90 is not a code that is actually enforced directly but is used as a basis for developing the Eurocode and the various national codes. The German national building code for reinforced concrete structures, the DIN 1045, also is described in this chapter. Finally the Modified Compression Field Theory is described. This theory has been recently adopted by AASHTO as an alternate means of predicting the shear capacity of reinforced concrete bridge systems.

Each of these building codes will be discussed in turn and the approach required in the design of reinforced concrete structures for shear will be summarized. This chapter will provide background information for the reevaluation of the Pasley data that will be discussed in Chapter 4.

2.2 Shear Provisions Found in ACI 318-89

2.2.1 General

The equations for the concrete shear capacity given by ACI 318-89 were established through experimental and analytical studies of typical flexural members. The concrete shear strength is represented in terms of concrete compressive strength, beam size, flexural reinforcement ratio and the applied load. The shear strength provided by shear reinforcement is based on the assumptions that (1) the critical diagonal crack is inclined at an angle of about 45° and (2) that the shear reinforcement will yield under design loading.

The ACI shear equations make no adjustments for the design of continuous beams in negative moment regions. These deficiencies are accounted for, to some extent, by the ACI equations underestimating the contribution of shear reinforcement and requiring its use in beams where the shear load exceeds one-half of the design shear capacity of the concrete. ACI-318 also makes no adjustment in the nominal shear capacity of members based on member depth as is done by EC 2 and other codes.

As per ACI 318-89, Chapter 9 defines the basic strength and serviceability for reinforced concrete members as follows

Design Strength $\geq$ Required Strength

$\Leftrightarrow$ ϕ[Nominal Strength] $\geq$ U

The required strength U to resist only dead load D and live load L shall be at least equal to U=1.4D+1.7 L. Other load cases and load combinations are given in the ACI 318-95, Chapter 9. The largest value of these equations will govern. In the case of shear, the equations are $\phi V_n \geq V_u = 1.4V_D + 1.7V_L$ where $\phi = 0.85$ for shear.

2.2.2 Members Not Requiring Design Shear Reinforcement

The strength at which inclined cracking forms is taken to be the shear strength of a beam without shear reinforcement according to the ACI Building Code. The following relationships are assumed in the following equations and list of analysis.

$$f_t \propto \frac{E_s f_s}{E_s} \propto \frac{E_c M_n}{E_s d A_s} \propto \frac{M_n \sqrt{f_c'}}{E_s d A_s} \propto \frac{M_n}{b d^2}\left[\frac{\sqrt{f_c'}}{\rho A_s}\right]^8 \qquad (2.1)$$

where

f_t tensile stress [MPa]

$f_{t,max}$ principal tensile stress [MPa]

f_c' characteristic compressive strength of concrete [MPa]

The following assumptions were made:

1. The strength is reached when the principal tensile stress reaches the tensile strength of the concrete.
2. The flexural tensile stress f_t varies as E_c/E_s times the tensile stress in the reinforcement.
3. The tensile strength f_t of the concrete is proportional to $\sqrt{f_c'}$.
4. The shear stress, v, varies as the average shear stress.
5. E_c is proportional to $\sqrt{f_c'}$.
6. M_n and V_n are the nominal capacities at the section where the inclined crack forms.

The shear stress may be expressed as $v = k_1 V_n / (b_w d)$. (2.2)

[8] More information is given by ACI-ACSE Committee 326.

The stress in the steel f_s is proportional to $M_n/(A_s d)$ and the tensile stress f_t in the concrete.

Rewrite f_t and f_{tmax} as:

$$f_t = \frac{k_4}{E_s}\frac{\sqrt{f_c'}}{\rho}\frac{M_n}{bd^2} \tag{2.3}$$

$$f_{t\max} = k_5\sqrt{f_c'} \tag{2.4}$$

The principal tensile stress, the derivation of $f_{t,max}$ is available in mechanics of materials textbooks, is given by

$$f_{t\max} = \frac{1}{2}f_t + \sqrt{\left[\left(\frac{1}{2}f_t\right)^2 + v^2\right]} \tag{2.5}$$

Substituting Eq. (2.2) through (2.4) into the above Eq. (2.5)

$$f_{t\max} = k_5\sqrt{f_c'} = \frac{V_n}{bd}\left[\frac{1}{2}\frac{k_4}{E_s}\frac{M_n}{V_n d}\frac{\sqrt{f_c'}}{\rho} + \sqrt{\left[\left[\frac{1}{2}\frac{k_4}{E_s}\frac{M_n}{V_n d}\frac{\sqrt{f_c'}}{\rho}\right]^2 + k_1^2\right]}\right] \tag{2.6}$$

$$\frac{V_n}{bd\sqrt{f_c'}} = \frac{k_5}{\left[\frac{1}{2}\frac{k_4}{E_s}\frac{M_n}{V_n d}\frac{\sqrt{f_c'}}{\rho} + \sqrt{\left[\left[\frac{1}{2}\frac{k_4}{E_s}\frac{M_n}{V_n d}\frac{\sqrt{f_c'}}{\rho}\right]^2 + k_1^2\right]}\right]} \tag{2.7}$$

where k_i are the unknown variables.

On the basis of 440 tests[9] the relationship between the nondimensional quantities $\frac{V_n}{bd\sqrt{f_c'}}$ and $\frac{M_n}{V_n d}\frac{\sqrt{f_c'}}{\rho}$ was obtained as

[9] More information is given by ACI-ASCE Committee 326 (2).

$$\frac{V_n}{bd\sqrt{f_c'}} = \frac{1}{7}\left[1 + 120\frac{\rho_w V_u d}{M_n\sqrt{f_c'}}\right] \le 0.3 \tag{2.8}$$

$$V_c = \frac{1}{7}\left[\sqrt{f_c'} + 120\rho_w\frac{V_u d}{M_u}\right]b_w d \le 0.3\sqrt{f_c'}b_w d \qquad \text{(SI units)} \tag{2.9}$$

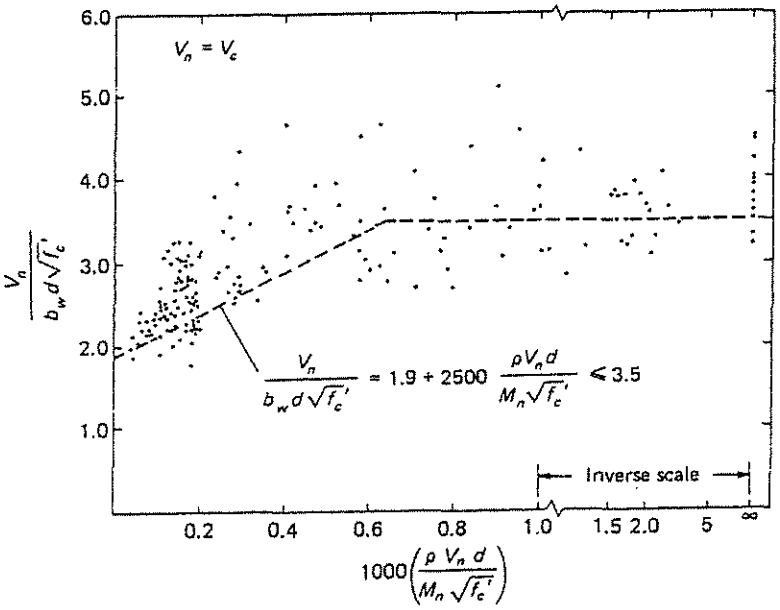

Fig. 2.1: Derivation of ACI shear strength equation for beams without shear reinforcement, $V_n = V_s$ in US Customary Units (adapted from 2).

In 1963, the ACI Building Code accepted the relationship found in Eq. 2.9 representing the shear capacity of beams without shear reinforcement. Expressing the given equation in terms of V_n and substituting $V_c = V_n$, $b = b_w$, $\rho = \rho_w$, $M_n = M_u$ and $V_n = V_u$ Eq. 11.6 from the ACI 318-95 is obtained.

ACI provides two means to complete the shear capacity.

Standard approach: $$V_c = \frac{1}{6}\sqrt{f_c'}b_w d \tag{2.10}$$

More detailed approach: $$V_c = \left[\left[\sqrt{f_c'} + 120\rho_w \frac{V_u d}{M_u}\right]\frac{1}{7}\right] b_w d \le 0.3\sqrt{f_c'} b_w d \qquad (2.11)$$

where $$\frac{V_u d}{M_u} \le 1.0$$

where

f_c' specified compressive strength of concrete [MPa]

[17, 21, 24, 28, 31, 34] per ACI 318-95, Table 5.4

b_w web width of the beam [mm]

d distance from the center of the tension steel to the outer compression fiber of the concrete [mm]

ρ_w $\rho_w = A_s / (b_w d)$, reinforcement ratio

M_u factored moment occurring simultaneously with V_u at the section considered [kNm]

Note that the ratio V_u/M_u is slightly different than V_n/M_n because the ϕ factors for shear and flexure are different. ACI Building Code limits the value $V_u d/M_u$ to be smaller than or equal to 1.0 to limit V_c and its effect on inflection points or regions with high shear and low moment values.

For continuous beams, the ACI-ASCE Committee 426 recommended that the

$$V_c = \frac{1}{6}\sqrt{f'_c}\, b_w d \ \text{[MPa]},$$

this is known herein as the standard procedure and corresponds to ACI 318-95 Eq. 11-2.

2.2.3 Members Requiring Design Shear Reinforcement

The ACI Building Code offers two procedures, a standard procedure and a more detailed procedure, to calculate the required shear reinforcement.

The design of a cross section subjected to shear shall be based on

$$V_u \le \phi V_n \text{ where } V_n = V_c + V_s . \qquad (2.12)$$

V_u factored shear force at section considered [kN]

V_n nominal shear strength [kN]

V_c nominal shear strength provided by concrete [kN]

V_s nominal shear strength provided by shear reinforcement [kN]

The maximum factored shear force V_u shall be computed in accordance with ACI 318-95, Chapter 11. In experimental work the critical section for computing the nominal shear strength was found to be the location of the first inclined shear crack located at approximately d off the face of the support. Since most testing was performed on simply supported beams under simple loading arrangements, extension to generalized loading on continuous structures can prove difficult.

Two assumptions based on observations were made by ACI-ASCE 426:

(1) For shear span to depth ratio (a/d) greater than 2, the critical inclined crack is expected to be at a distance d form the section of the maximum moment

(2) for (a/d) less than 2, an inclined crack is expected to be at the center of the shear span.

Therefore, the critical section for nonprestressed members will be at a distance d from the face of the support if the support reaction introduces compression into the end region of the member. In other words sections located less than a distance d from the face of the support may be designed for the same shear as that at a distance d. For members loaded such that the shear at sections between the support and a distance d differs radically from the shear at a distance d, V_u, at the face of the support is to be used.

2.2.4 Design Categories and Requirements

The design for shear can be separated into the following categories per ACI 318-95:

(A) $\phi V_c \le V_u$: In general for flexural members the predicted shear capacity in form of stirrups is given by

$\phi V_s = V_u - \phi V_c = \phi A_v f_y d / s$ for $\alpha = 90°$ with $s \le d/2 \le 600\text{mm}$ (24 in).

When $V_s > \frac{1}{3}\sqrt{f_c'} b_w d$ the spacing limits have to be divided by 2.

(B) $0.5\phi V_c \le V_u \le \phi V_c$: per the ACI Building Code, minimum shear reinforcement is required except for thin slablike flexural members as slabs, footings, floor joist constructions and beams where the total depth does not exceed 250 mm (10 in), 2.5 times the flange thickness for T-shapes sections or 0.5 times of the web width. The minimum shear reinforcement is given by

$\min V_s = \phi \frac{1}{3} b_w d$ [MPa] with maximum spacing of $s \le d/2 \le 600$ mm (24 in)

per ACI 318-95, 11.5.5.3 and 11.5.4.1.

(C) $V_u \le 0.5\phi V_c$: Per ACI 318-95, 11.5.5.1, no shear reinforcement is required.

2.2.5 Shear Reinforcement

An expression for V_s may be developed from the crack model analogy with the assumption that an inclined shear crack will occur at a 45 degree angle extending from the steel reinforcement to the compression surface. This crack will intersect a number, n, of stirrups as shown in Fig. 2.2 below. The use of 45° inclined crack assumption has been traditional since the early twentieth century and is generally conservative.

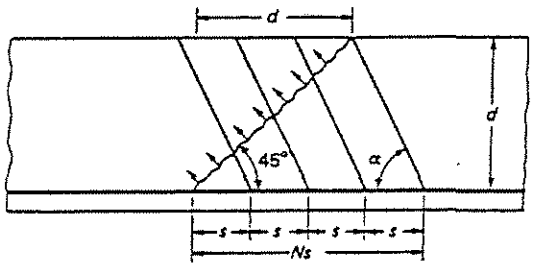

Fig. 2.2: Shear strength V_s attributable to shear reinforcement (adapted from 30).

The development of the equation is as follows

$$\tan 45^\circ = d / x \text{ and } \tan\alpha = d / y \tag{2.13}$$

$$ns = x + y = \frac{d}{\tan 45^\circ} + \frac{d}{\tan\alpha} = d(\cot 45^\circ + \cot\alpha) = d(1 + \cot\alpha) \tag{2.14}$$

$$\sin\alpha = \frac{V_s}{nA_v f_y} \tag{2.15}$$

$$\Rightarrow V_s = nA_s f_y \sin\alpha = \frac{ns}{s} A_v f_y \sin\alpha \tag{2.16}$$

$$\Rightarrow V_s = \frac{d(1+\cot\alpha)}{s} A_v f_y \sin\alpha$$
$$\Rightarrow V_s = A_v f_y \frac{d}{s}(\sin\alpha + \cos\alpha) \quad (2.17)$$

$$\text{if } \alpha = 90° \text{ then } V_s = \frac{A_v f_y d}{s} \quad (2.18)$$

$$\text{if } V_u \geq 0.5(\phi V_c) \text{ then } A_v = \frac{b_w s}{3 f_y}. \quad (2.19)$$

Design of shear reinforcement perpendicular to the x axis of a member:

$$V_s = \frac{A_v f_y d}{s} \leq \frac{2}{3}\sqrt{f'_c} b_w d \quad (2.20)$$

where

A_v sum of area of shear reinforcement within a distance s

Lower and Upper Limits for Amount of Shear Reinforcement

The ACI Building Code requires a minimum shear reinforcement area, A_v, equal to

$$A_{v\min} = \frac{b_w s}{3 f_y}. \tag{2.21}$$

As derived before the expression can be rewritten in terms of nominal shear force or nominal unit stress

$$V_s = \frac{A_v f_y d}{s} = \frac{f_y d}{s}\left[\frac{1}{3}\frac{b_w s}{f_y}\right] = \frac{1}{3} b_w d \text{ or } v_s = \frac{V_s}{b_w d} = \frac{\frac{1}{3} b_w d}{b_w d} = \frac{1}{3} \text{ [MPa]}. \tag{2.22}$$

The upper limit can be represented by the following:

$$V_s \le \frac{2}{3}\sqrt{f_c'}\, b_w d \tag{2.23}$$

2.3 Classical Truss Analogy by Ritter (1899) and Mörsch (1902)

In 1899 and 1902, respectively, the Swiss engineer Ritter (22) and the German engineer Mörsch (19) independently published papers proposing the truss analogy for the design of reinforced concrete beams for shear. Mörsch analyzed the angle of inclination on two simply supported T-beams subjected to increasing uniformly distributed load. He concluded that the shear cracking angle, θ, was variable and not mathematically defined. Consequently, Mörsch derived an equation for the required amount of shear reinforcement assuming $\theta = 45°$. This model consists of a tension tie (longitudinal bars), a top concrete compression chord, vertical or inclined tension tie between 45° and 90° (stirrups), and 45° inclined concrete compression struts. The truss is referred to as the plastic truss model depending on plasticity in the nodes leading to a system which is statically determinate.

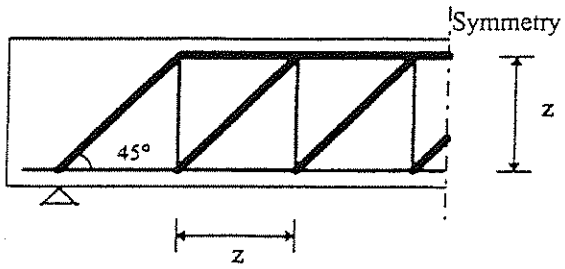

Fig. 2.3 Truss action in a simply supported reinforced concrete beam by Mörsch.

This mechanical model of a reinforced beam in cracked condition is called "volle Schubsicherung durch Bewehrung". Later it was just called "volle

Schubdeckung". The meaning is that the shear resisting force is given only by the shear reinforcement.

The required shear reinforcement, a_s, is represented by

$$a_s = \tau_0 b_0 / \text{zul}\sigma_s \qquad [\text{cm}^2/\text{m}] \qquad (2.24)$$

where

τ_0 $\tau_0 = V / b_0 z$, shear stress [MPa]

V unfactored shear force [N]

b_o width of beam width [mm]

z $z = 0.85\ d$ lever arm for rectangular cross section [mm]

$z = d - t_f/2$ lever arm for T-beams [mm]

d distance from the outer compression fiber to the centerline of the tension steel [mm]

h height of the beam [mm]

t_f depth of the flange [mm]

zul σ_s factored specified yield strength for shear reinforcement, generally

zul $\sigma_s = 500/\gamma = 500/1.75 = 286$ MPa

Therefore, the required shear reinforcement area, a_s, can be computed as

$a_s = \tau_0 b_0 / 2.86$ [cm^2/m].

The "volle Schubdeckung" was commonly used until the introduction of the DIN 1045 (1972) and is still used for the analysis of the shear reinforcement for high

shear stresses called "Schubbereich 3" (region 3)[9], in the DIN 1045 (1988) in Germany.

[9] As further discussed in Section 2.4 three different shear regions are defined per DIN 1045 which are minimum shear reinforcement, intermediate shear reinforcement, and maximum allowable shear reinforcement.

2.4 Expanded Truss Analogy by Leonhardt (1965)

In the 1960's Leonhardt (14) and Walther did numerous beam tests called the "Stuttgarter Schubversuche" at the University of Stuttgart, Germany. Based on these test series, they came to the conclusion that Mörsch's truss analogy was too conservative and had to be modified. They concluded that the actual top compression chord should be inclined and that the angle θ between the compression strut and the x axis of the member is less than 45° . A frame effect was considered concerning the flexural stiffness of compression members and a dowel action of the longitudinal reinforcement. Consequently, the forces in the tension ties are reduced but the forces in the tension chord are increased.

Leonhardt's approach was adopted by the DIN 1045 and is still the current design approach for shear in Germany.

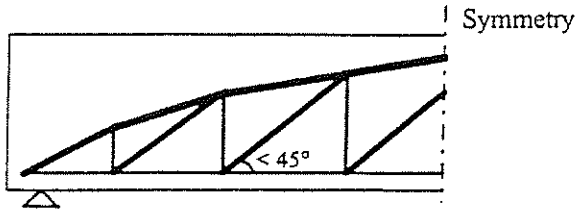

Fig. 2.4 Modified truss action in a simply supported reinforced concrete beam by Leonhardt.

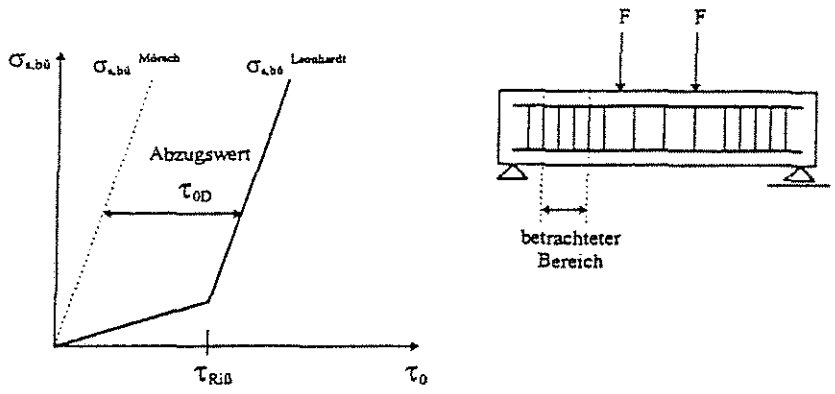

Fig. 2.5 More realistic curve of the shear stresses versus stresses in the stirrups (adopted from 23).

The "Abzugsglied" (reduction term) is called τ_{0D} and is taken off by the compression struts. The modified truss theory thus reduces the shear reinforcement and increases the shear stresses in the compression struts due to the smaller θ.

Then the required shear reinforcement, a_s, is

$$a_s = (\tau_0 - \tau_{0D}) b_0 / \text{zul}\sigma_s . \qquad (2.25)$$

2.5 Truss Analogy by DIN 1045

Based on Leonhardt's theory the DIN design procedure for shear is defined by three shear regions which are given in Table 2.1. The limit τ_{011} is applicable for plates where generally no shear reinforcement is required which is not listed in Table 2.1. The limit τ_{012} is applicable for beams where the design shear stress, τ, is below τ_{012} and a minimum amount of shear reinforcement has to be provided. The second limit τ_{02} is for beams where the shear force is intermediate. τ_{03} is the upper limit of the allowable amount of shear reinforcement.

The critical section may be located at a distance 0.5h from the face of the support (column, wall) if no concentrated load occurs between the face of the support and the location of the critical section. For point loads at a distance $a \leq 2h$ from the centerline of the support a factor to reduce the required amount of shear reinforcement is given by a/2h for the shear force, V, due to a point load, F. This reduction factor does not apply for region 3. For other support conditions where support reaction in direction of applied shear introduce no compression into the end regions of the member the critical section may be at the face of the support.

The shear stress, τ_0, is defined by the following equation:

$\tau_0 = V / b_0 z$ shear stress [MPa]

where

V unfactored shear force [N]

b_o smallest width of beam width [mm]

z z = 0.85 d, lever arm for rectangular cross section [mm]

z = d - t_f/2, lever arm for T-beams [mm]

h distance from the outer compression fiber to the centerline of the tension steel [mm]

d height of the beam [mm]

t_f flange depth [mm]

Table 2.1 Limits of τ_0 [MPa] and the required shear reinforcement per DIN 1045 with vertical stirrups is tabulated.[10]

Region	max τ_0	B15	B25	B35	B45	B55	shear reinforcement
1	τ_{012}	0.50	0.75	1.00	1.10	1.25	$a_s = \frac{0.4\tau_0 b}{2.86}$
2	τ_{02}	1.20	1.80	2.40	2.70	3.00	$a_s = \frac{\tau_0^2 b}{\tau_{02} 2.86}$
3	τ_{03}	2.00	3.00	4.00	4.50	5.00	$a_s = \frac{\tau_0 b}{2.86}$

where τ_0 in [MN/m^2], b [cm], a_s [cm^2/m]

Table 2.2 Spacing requirements in longitudinal direction.

Region	Spacing Requirement	Maximum Spacing
1	0.8 h	≤ 25 cm
2	0.6 h	≤ 20 cm
3	0.3 h	≤ 15 cm

Table 2.3 Spacing requirement perpendicular to the longitudinal direction.

h ≤ 40 cm	40 cm
h > 40 cm	h or 80 cm, smaller value governs

[10] For T-beams b has to be substituted by the width of the web, b_0.

2.6 Expanded Truss Analogy by Eurocode (1990)

2.6.1 General

The structural Eurocodes compromise a group of standards for the structural and geotechnical design of buildings and civil engineering works in Europe. Consequently, Eurocode 2 (EC 2) is intended to provide the necessary technical basis to prove compliance of buildings and civil engineering works made with plain, reinforced or prestressed concrete with the essential requirements.

Besides the EC 2, each country has design modifications and/or references which govern over the general EC 2. In Germany the additional specification is the DAfStb-Rili[11]. This specification will be referred to in this document later.

The general safety concept of the EC 2 is $S_d \leq R_d$ where R_d is the design resistance force and S_d the design load. This concept implies factored loads and reduced material properties.

The EC 2 offers standard procedure to calculate the required shear reinforcement as well as more detailed procedure.

The standard procedure is based on the truss analogy by Mörsch. The truss model consists of an inclined compression strut with $\theta = 45°$ and two parallel chords (top and bottom). In contrast to Leonhardt, the EC 2 assumes that the shear mechanism is represented by the shear capacity of a cross section without shear reinforcement plus the shear capacity of the shear reinforcement.

The more detailed procedure also considers a variable angle θ which is enclosed by the axis of the member and the compression strut. The design of a cross section subjected to shear is based on $V_{sd} \leq V_{rd}$, where V_{sd} is the factored shear force at the considered section and V_{rd} is the nominal shear strength of the cross section.

Maximum factored shear force V_{sd} may be computed in accordance with EC 2.

(a1) If support reaction of nonprestressed members in the direction of applied shear introducing compression into the end regions of the member and no concentrated load occurs between the face of the support and the location of the critical section the critical section may be at a distance d from the face of the support. Sections located less than a distance d from the face of the support may be designed for the same shear V_{sd} as that computed at a distance d.

(a2) If concentrated loads occur at the distance $x \leq 2.5d$ from the face of the support it is not allowed to reduce V_{sd}. The allowable shear stress may be factored by β, where $\beta = 2.5(d/x)$ with $1.0 \leq \beta \leq 3.0$. The enlargement of V_{rdl} implies that the standard shear procedure is used. In cases where uniformly distributed and concentrated loads occur simultaneously, a linear interaction relationship may be used per EC 2 [4.3.2.2.(9)2.].

---

[11] DAfStb-Rili stands for Deutscher Ausschuss fur Stahlbetonbau Richtlinie (German Committee of Concrete Design Regulations).

(b) If support reaction in direction of applied shear introduces no compression into the end regions of the beam the shear force at the face of the support may be used.

2.6.2 Members Not Requiring Design Shear Reinforcement

Members without shear reinforcement are represented by two mechanical models which are an arch and/or a "Sprengwerk" with a tension tie. The shear mechanisms are the shear strength of the arch or strut provided by the concrete and the dowel reaction of the longitudinal bars.

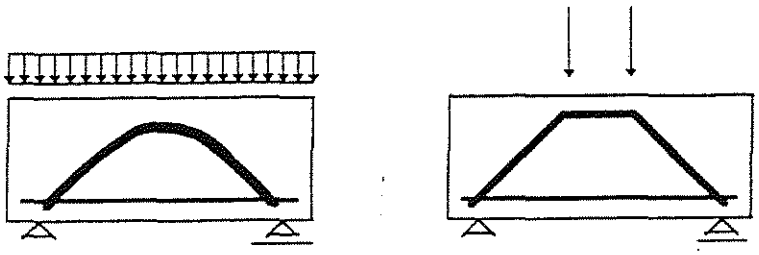

Fig. 2.6 Models.

The design shear resistance of a member not requiring design shear reinforcement, is given by

$$V_{sd} \leq V_{rd1}$$

$$V_{rd1} = \tau_{rd} k(1.2 + 40\rho_1) b_w d \qquad (2.26)$$

where

V_{sd} design shear force

V_{rd1} design shear resistance of a member not requiring design shear reinforcement

τ_{rd} basic design shear strength; values are given in Table 2.4.

k constant relating to effective depth d and curtailment of reinforcement; values of k are:

$k = 1.6 - d \geq 1$, d [m] or,

$k = 1$ for members where more than 50% of the bottom reinforcement is curtailed

ρ_1 reinforcement ratio related to A_s; $\rho_1 = \frac{A_s}{b_w d} \leq 0.02$

A_s area of tension reinforcement effective at a section

b_w minimum width of the member

d distance from the extreme compression fiber to the centroid of the tension steel

Table 2.4 Design shear strength

C[MPa][12]	12/15	16/20	20/25	25/30	30/37	35/45	40/50	45/45	50/60
$\tau_{rd,EC\,2}$	0.18	0.22	0.26	0.30	0.34	0.37	0.41	0.44	0.48
$\tau_{rd,DAfStb}$	0.20	0.22	0.24	0.26	0.28	0.30	0.31	0.32	0.33

The basic values τ_{rd} are given in Eurocode 2 (EC 2). These values are based on the characteristic cylinder strength $\tau_{rd} = 0.035 \times f_{cd}^{2/3}$. The basic τ_{rd} is calculated

by $\tau_{rd} = 0.09 \times f_{cd}^{1/3}$ (per DAfStb-Rili 5). These τ_{rd} values already include the material safety factor for concrete $\gamma_c = 1.5$. In Table 2.4 the basic values are tabulated. It is shown that the values per DAfStb-Rili 5 are reduced in comparison to the EC 4.

If the shear forces are smaller than V_{rd1}, slabs are permitted to have no shear reinforcement. For beams, minimum amount of shear reinforcement is required which depends on the characteristic concrete strength f_{ck}. The minimum web reinforcement ratios, ρ_w, are given in EC 2 Table [3.5.3.1-1] and may be calculated by the equation $\rho_w = \frac{A_{sw}}{s b_w \sin\alpha}$.

where

A_{sw} cross section of the shear reinforcement [mm^2]

(e.g. one U-shaped stirrup $A_{sw} = 2A_{s,bar}$)

s distance of shear reinforcement in x direction [mm]

α angle between shear reinforcement and x axis of the beam; α should not be less than 45°

When checking members without design shear reinforcement, the design resistance V_{rd2} is given by $V_{rd2} = 0.5 \nu f_{cd} b_w z$ (2.27)

---

[12] As an example: C 12/15 means that the cylinder compressive strength is 12 [MPa] and the cube compressive strength is 15 [MPa].

where

V_{rd2} design shear resistance of the compression strut [kN]

ν efficiency factor defined as $\nu = 0.7 - f_{ck} / 200 \geq 0.5$

f_{ck} characteristic compressive strength of concrete [MPa]

f_{cd} $f_{cd} = f_{ck} / \gamma_c$, specified compressive strength of concrete [MPa]

γ_c $\gamma_c = 1.5$ material safety factor of concrete

2.6.3 Members Requiring Design Shear Reinforcement

If the factored shear force V_{sd} is greater than the limit V_{rd1}, then EC 2 requires a check of the shear reinforcement and the compression struts for capacity.

$V_{sd} \leq V_{rd3}$ (check of the shear reinforcement)

$V_{sd} \leq V_{rd2}$ (check of the compression strut)

Theoretically, the most favorable design result is achieved by $V_{sd} = V_{rd2} = V_{rd3}$.

Standard Procedure

The standard procedure for nonprestressed members is based on the truss analogy by Mörsch. The factored shear force may be reduced by the term that represent a cross section without shear reinforcement. The remaining shear force will be covered by the 45° truss model with parallel chords. The standard procedure is effective for point loads near the support or for beams with high longitudinal loads.

$$V_{sd} \le V_{rd3} = V_{cd} + V_{wd} \tag{2.28}$$

$$V_{cd} = V_{rd1} = \tau_{rd} k(1.2 + 40\rho_l) b_w d \tag{2.29}$$

$$V_{wd} = \frac{A_{sw}}{s} z f_{ywd} (1 + \cot\alpha) \sin\alpha \tag{2.30}$$

$$V_{wd} = \frac{A_{sw}}{s} z f_{ywd} \qquad \text{(for 90° stirrups)}$$

where

V_{rd3} design shear resistance of the inclined/vertical shear reinforcement

V_{cd} design shear resistance provided by concrete [kN]

V_{wd} design shear resistance provided by shear reinforcement due to a 45° truss model with parallel chords [kN]

z lever arm may be taken as $z = 0.9d$ [mm]

f_{ywk} characteristic yield strength of nonprestressed reinforcement [MPa]

220, 400, 500 [MPa]

f_{ywd} specified yield strength of nonprestressed reinforcement [MPa]

$f_{ywd} = f_{ywk} / \gamma_s$

γ_s $\gamma_s = 1.15$ material safety factor for nonprestressed reinforcement

The required amount of shear reinforcement may be calculated by equating V_{sd} and V_{rd3}.

$$a_{sw} = \frac{A_{sw}}{s} = \left(V_{sd} - V_{rd1}\right) / \left(f_{ywd} z(1 + \cot\alpha)\sin\alpha\right) \ge \min.a_{sw} \tag{2.31}$$

$$a_{sw} = \frac{A_{sw}}{s} = \left(V_{sd} - V_{rd1}\right) / \left(f_{ywd} z\right) \geq \min.a_{sw} \quad \text{(for 90° stirrups)}$$

The minimum amount of shear reinforcement, a_{sw}, is given by

$$a_{sw} = \min \rho_w b_w \sin\alpha \qquad [cm^2/m] \tag{2.32}$$

$\min \rho_w$ is given in Table 2.5.

Table 2.5 Minimum shear reinforcement ratios.

Concrete Classes [MPa]	Steel Classes [MPa]		
	S 220	S 400	S 500
C12/15-C20/25	0.0016	0.0009	0.0007
C25/30-C35/45	0.0024	0.0013	0.0011
C40/50-C50/60	0.0030	0.0016	0.0013

The nominal resistance force of the compression strut can be calculated by

$$V_{rd2} = 0.5 \nu f_{cd} b_w z(1 + \cot\alpha)$$

$$V_{rd2} = 0.5 \nu f_{cd} b_w z \qquad \text{(for 90° stirrups)}$$

where

ν efficiency factor defined as $\nu = 0.7 - f_{ck} / 200 \geq 0.5$

f_{ck} characteristic compressive strength of concrete [MPa]

f_{cd} $f_{cd} = f_{ck} / \gamma_c$, specified compressive strength of concrete [MPa]

γ_c $\gamma_c = 1.5$ material safety factor of concrete

It is recommended in DAfStb to check the compression strut angle, θ, using the standard procedure. It is a combination of the simplified and the more detailed procedure. Using the following equations and equating them, an equation for the inclination of the compression strut can be developed.

$$a_{sw} = \frac{A_{sw}}{s} = \left(V_{sd} - V_{rd1}\right) / \left(f_{ywd} z (1 + \cot\alpha) \sin\alpha\right) \geq \min a_{sw} \tag{2.32}$$

$$a_{sw} = \frac{A_{sw}}{s} = \left(V_{sd} - V_{rd1}\right) / \left(f_{ywd} z\right) \geq \min a_{sw} \qquad \text{(for 90° stirrups)} \tag{2.33}$$

$$\Rightarrow \tan\theta = \frac{1 - \left(V_{cd} / V_{sd}\right)}{1 + \left(V_{cd} / V_{sd}\right) \cot\alpha} \tag{2.34}$$

$$\Rightarrow \tan\theta = 1 - \left(V_{cd} / V_{sd}\right) \qquad \text{(for 90° stirrups)}$$

The angle θ has the limits as discussed in the next paragraph. If the angle is not within the limits using the above equation, then the limits on θ will govern and it is recommended to use the more detailed procedure discussed below.

More Detailed Procedure

The more detailed procedure allows more freedom in the arrangement and detailing of the shear reinforcement than the standard method. It will frequently lead to substantial economies in shear reinforcement but require an increase in the longitudinal tension steel. This method considers a variable angle θ between the axis of the member and the compression strut. The angle θ is limited to $2.5 > \cot\theta > 0.4$ ($21.8° < \theta < 68.2°$) for beams with full length flexural reinforcement and by

$2.0 > \cot\theta > 0.5$ $(26.6^\circ < \theta < 63.4^\circ)$ for beams with curtailed flexural reinforcement. The DAfStb limits the angle θ to a range of $7/4 > \cot\theta > 4/7$ $(29.7^\circ < \theta < 60.3^\circ)$ for both cases. This procedure is intended for beams with a load combination of shear and torsion and for load cases using low values of θ; it provides more accurate results for these conditions than the simplified method.

The equilibrium conditions lead to the following expressions:

$$V_{rd2} = b_w z \nu f_{cd} (\cot\theta + \cot\alpha) / (1 + \cot^2\theta) \qquad (2.35)$$

$$V_{rd2} = \frac{b_w z \nu f_{cd}}{(\cot\theta + \tan\theta)} \qquad \text{(for 90° stirrups)}$$

$$V_{rd3} = \frac{A_{sw}}{s} z f_{ywd} (\cot\theta + \cot\alpha) \sin\alpha \qquad (2.36)$$

$$V_{rd3} = \frac{A_{sw}}{s} z f_{ywd} \cot\theta \qquad \text{(for 90° stirrups)}$$

The required amount of shear reinforcement, a_{sw}, is given by

$$a_{sw} = \frac{A_{sw}}{s} = V_{sd} / \left(z f_{ywd} \sin\alpha (\cot\theta + \cot\alpha) \right) \geq \min a_{sw} \qquad (2.37)$$

$$a_{sw} = \frac{A_{sw}}{s} = V_{sd} / \left(z f_{ywd} \cot\theta \right) \geq \min a_{sw} \quad \text{(for 90° stirrups)}$$

The equations are limited by

$$\frac{A_{sw} f_{ywd}}{b_w s} \leq 0.5 \nu f_{cd} \frac{\sin\alpha}{(1 - \cos\alpha)} \qquad (2.38)$$

$$\frac{A_{sw} f_{ywd}}{b_w s} \le 0.5 \nu f_{cd} \qquad \text{(for 90° stirrups)}$$

In a design situation, the actual value of the compression strut angle, θ, will depend on several parameters such as load configuration, load intensity, geometry of the member, detailing of the reinforcement and the pattern of possible shear cracks, etc. A reliable estimate of the angle θ for reinforced or prestressed members is given by

$$\cot\theta = 1.25 - 3\frac{\sigma_{cp.eff}}{f_{cd}} \qquad (2.39)$$

For members without longitudinal forces, i.e. $\sigma_{cp,eff} = 0$ and the above equation leads to $\cot\theta = 1.25 \Leftrightarrow \theta \cong 39°$.

To measure the smallest amount of shear reinforcement for small and/or medium shear stresses generally the upper limit of cot θ is controlling. For high shear stresses it might be advisable to set V_{sd}=V_{rd2} to find the largest possible cot θ. The required area of shear reinforcement may be calculated by V_{sd}=V_{rd3} with θ as derived above.

The equilibrium of forces when $\theta \le 45°$, requires additional tension reinforcement is which is given by

$$\Delta A_s \ge \Delta T_d / f_{ywd}$$

$$\Delta T_d = 0.5|V_{sd}|(\cot\theta - \cot\alpha) \qquad (2.40)$$

This added demand on the tensile reinforcement also is a feature of the MCFT.

Design For Shear Between Web and Flanges

In flanged beams or T-beams, the shear resistance of the flange is calculated assuming a system of compressive struts combined with ties in the form of tensile reinforcement.

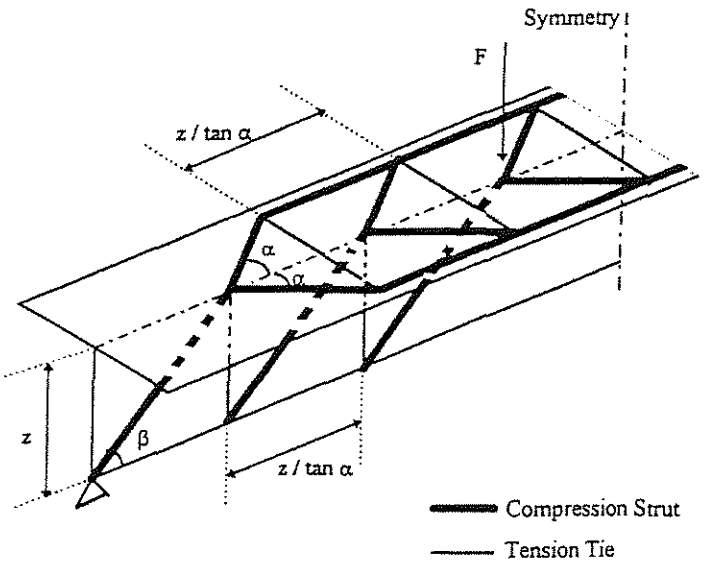

Fig. 2.7 Truss model of a T-beam.

For this system, at the ultimate limit states, it shall be verified that $v_{sd} \leq v_{rd}$.

where

v_{rd} denotes either the shear resistance of the compression struts or of the ties which ensure the connection between flange and web. In the absence of more rigorous calculations, the following design resistance may be assumed.

v_{sd} mean longitudinal sliding shear per unit length to be resisted

The change of the tension force in the longitudinal direction of the beam is given by

$$Z_L = \delta V_{sd} / z \qquad (2.41)$$

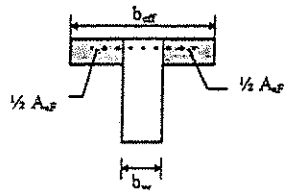

$$\delta = \frac{1}{2}(b_{eff} - b_w) / b_{eff} + \frac{1}{2} A_{sf} / \Sigma A_s$$

where

b_{eff} effective width of the flange

A_{sf} amount of tension steel in the flanges

ΣA_s total amount of longitudinal steel in the tension zone

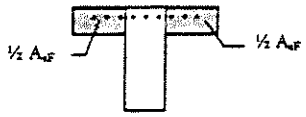

$$\delta = \frac{1}{2} A_{sf} / \Sigma A_s$$

A_{sf} amount of compression steel in the flanges

ΣA_s total amount of longitudinal steel in the compression zone

V_{sd} factored load

z z is assumed to be 0.9 d.

The force in the tension tie in the flange is given by

$$Z_q = Z_L \tan\alpha \tag{2.42}$$

Based on Leonhardt, the following is assumed:

$\alpha = 30^\circ$ for the compression strut in the compression zone (flange)

$\alpha = 45^\circ$ for the compression strut in the tension zone (flange)

Force in the compression strut in the flange is given by

$$D = Z_L / \cos\alpha \tag{2.43}$$

The nominal resistance force of the compression strut may be calculated by

$$v_{rd2} = 0.2 f_{cd} h_f \qquad \text{(for compression struts)} \tag{2.44}$$

where

v_{rd2} design shear resistance of the compression strut and $D \le v_{rd2}$

h_f flange depth [mm]

Calculation of the required amount of shear reinforcement

$$a_{sf} = \left(Z_q - 2.5\tau_{rd} h_f\right) / f_{yd} \ge \min a_{sw} \tag{2.45}$$

where

f_{yd} yield strength of the provided steel, a_{sf} [MPa]

The nominal resistance of the tension tie may be calculated by

$$v_{rd3} = v_{cd} + v_{wd} = 2.5\tau_{rd} h_f + \frac{A_{sf}}{s_f} f_{yd} = 2.5\tau_{rd} h_f + a_{sw} f_{yd} \qquad (2.46)$$

with $Z_q \leq v_{rd3}$

where

v_{rd3} design shear resistance of the inclined/vertical shear reinforcement [kN]

v_{cd} design shear resistance provided by concrete in compression regions only [kN]

v_{wd} design shear resistance provided by shear reinforcement due to a 45° truss model with parallel chords [kN]

Calculation of the required amount of shear reinforcement

$$a_{sf} = \left(V_{sd} - 2.5\tau_{rd} h_f\right) / f_{yd} \geq \min a_{sw}$$

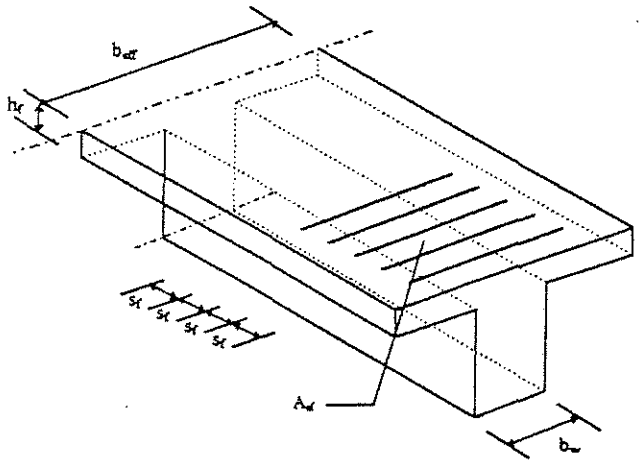

Fig. 2.8 Flange reinforcement.

where

h_f flange depth [mm]

τ_{rd} basic shear strength: Table 2.4

A_{sf} area of reinforcement across the flange of a flange beam [mm^2]

s_f denotes the spacing of the reinforcing bars across the flange [mm]

Thus, the design model for the shear reinforcement is similar of that of the standard method. If at the section with maximum bending moment the flange is subjected to a tensile force, the term $\Delta v_{rd3} = 2.5\tau_{rd} h_f$ in Eq. 2.46 should be taken as zero.

Spacing Requirements for Shear Reinforcement

The spacing limits of the shear reinforcement are according to the utilization of the compression struts. Spacing requirements for shear reinforcement in x direction are

Table 2.6 Spacing requirements in x direction

s_{max} (smaller value governs)	Limits
$s_{max} = 0.8d \leq 300mm$	$V_{sd} \leq 0.2V_{rd2}$
$s_{max} = 0.6d \leq 300mm$	$0.2V_{rd2} < V_{sd} \leq (2/3)V_{rd2}$
$s_{max} = 0.3d \leq 200mm$	$V_{sd} > (2/3)V_{rd2}$

For inclined shear reinforcement there will be an additional requirement

$s_{max} = 0.6d(1 + \cot\theta)$

Table 2.7 Spacing requirements in z direction

s_{max} (smaller value governs)	Limits
$s_{max} = 1.0d \leq 800mm$	$V_{sd} \leq 0.2V_{rd2}$
$s_{max} = 0.6d \leq 300mm$	$0.2V_{rd2} < V_{sd} \leq (2/3)V_{rd2}$
$s_{max} = 0.3d \leq 200mm$	$V_{sd} > (2/3)V_{rd2}$

2.7 CEB-FIP Model Code (1990)

2.7.1 General

The CEB-FIP Model Code for concrete structures synthesizes technical developments over the past decades in the safety analysis and design of concrete structures but does not attempt to cover particular types of civil engineering structures (e.g. bridges) nor gives provisions against certain actions (e.g. seismic loads).

The first CEB-FIB Model Code was published in 1978 following approval by the Euro-International Committee for Concrete (CEB). Since that time the Model Code has had considerable impact on national Codes in Europe and Japan and on the development of the EC 2. As an example, EC 2 "Design of Concrete Structures, Part 1: General Rules for Buildings" used as its basic reference document the Model Code 1978.

The general safety concept of the CEB-FIP, similar to the EC 2, is $S_d \leq R_d$ where R_d is the design resistance force and S_d the design load. This concept implies factored loads and reduced material properties.

The CEB-FIP Model Code also offers two procedures, a standard method and a refined method, to calculate the required shear reinforcement. The design philosophy is similar to that in the EC 2.

2.7.2 Members Not Requiring Design Shear Reinforcement

The design shear resistance of a member not requiring design shear reinforcement is given by

$$V_{rd1} = 2.5\tau_{rd} b_w d \tag{2.47}$$

where

V_{rd1} design shear resistance of a member not requiring shear reinforcement

τ_{rd} basic design shear strength is given by $\tau_{rd} = 0.25 f_{ctd}$

$$f_{ctk,min} = f_{ctko,min}\left[\frac{f_{ck}}{f_{ck,o}}\right]^{\frac{2}{3}} \tag{2.48}$$

$f_{ctk,min}$ minimum characteristic concrete tensile strength

f_{ck} characteristic concrete compression strength

f_{ctd} $f_{ctd} = f_{ctk} / \gamma_c$, design tensile strength of concrete

$f_{cko,min}$ $f_{cko,min} = 0.95$ MPa

f_{cko} $f_{cko} = 10$ MPa

When checking members without design shear reinforcement, the design resistance is given by

$$V_{rd2} = 0.30 f_{cd} b_w d \tag{2.49}$$

where

V_{rd2} design shear resistance of the compression strut

f_{cdl} average stress for uncracked zones

2.7.3 Members Requiring Design Shear Reinforcement

Standard Method

The standard method assumes a truss model consisting of $\theta = 45°$ inclined compression struts and two parallel chords (top and bottom).

(A) $$V_{sd} \le V_{rdl} = V_{cdl} + V_{wdl} \quad (2.50)$$

(B) $$V_{sd} \le V_{rd2} \quad (2.51)$$

$$V_{cdl} = 2.5\tau_{rd} b_w d \quad (2.52)$$

$$V_{wdl} = \frac{A_{sw}}{s}(0.9d) f_{ywd}(1 + \cot\alpha)\sin\alpha \quad (2.53)$$

$$V_{wdl} = \frac{A_{sw}}{s}(0.9d) f_{ywd} \qquad \text{(for 90° stirrups)}$$

where

A_{sw} cross sectional area of web reinforcement [mm^2]

f_{ywk} characteristic yield strength of nonprestressed reinforcement [MPa]

in Grades 220, 400, 500 [MPa]

f_{ywd} specified yield strength of nonprestressed reinforcement [MPa]

$f_{ywd} = f_{ywk} / \gamma_s$

γ_s $\gamma_s = 1.15$ material safety factor for nonprestressed reinforcement

τ_{rd} the basic design shear strength is given by $\tau_{rd} = 0.25 f_{ctd}$ [MPa]

The absolute maximum shear resistance for a given section and concrete strength is obtained with $\theta = 45^{\circ}$.

$$V_{rd2} = 0.30 f_{cd} b_w d \tag{2.54}$$

f_{ck} characteristic compressive strength of concrete [MPa]

f_{cd} $f_{cd} = f_{ck} / \gamma_c$, specified compressive strength of concrete [MPa]

γ_c $\gamma_c = 1.5$ material reduction factor of concrete

Table 2.8 Concrete strengths per CEB.

Grade	C12	C20	C30	C40	C50	C60	C70	C80
$f_{ck}^{cylinder}$	12	20	30	40	50	60	70	80
f_{ck}^{cube}	15	25	37	50	60	70	80	90

Refined Method

The refined method assumes a truss model consisting of variably inclined compression struts and two parallel chords (top and bottom).

$$V_{sd} \leq V_{rd2} \tag{2.55}$$

$$V_{sd} \leq V_{rd3} = V_{wd2} + V_{cd2} \tag{2.56}$$

$$V_{rd2} = 0.30 f_{cd} b_w d \sin 2\theta \tag{2.57}$$

where

V_{rd3} design shear resistance of the tension tie [kN]

V_{rd2} design shear resistance of the compression strut [kN]

Table 2.9 Ranges of resistance force V_{cd2}.

Range	V_{sd}	V_{cd2}
Uncracked	$V_{sd} \le 2.5\tau_{rd} b_w d$	$2.5\tau_{rd} b_w d$
Transition	$2.5\tau_{rd} b_w d < V_{sd} < 7.5\tau_{rd} b_w d$	$0.5(7.5\tau_{rd} b_w d - V_{sd})$
Truss action	$V_{sd} \ge 7.5\tau_{rd} b_w d$	0

$$V_{wd2} = \frac{A_{sw}}{s}(0.9d) f_{ywd} (\cot\theta + \cot\theta)\sin\alpha \qquad (2.58)$$

The value of inclination θ of the concrete compression struts can be varied between $5/3 \ge \cot\theta \ge 3/5$ ($30.96^\circ \le \theta \le 59.04^\circ$ for beams per CEB-FIP 1990. A reliable estimate of the angle θ for reinforced or prestressed members is given by

$$\cot\theta = \sqrt{\left[\frac{b_w s f_{cd2}}{A_{sw} f_{ywd}} - 1\right]} \le 3 \qquad (2.59)$$

where

$$f_{cd2} = 0.60\left[1 - \frac{f_{ck}}{250}\right] f_{cd}$$

f_{cd2} average stress for uncracked zones [MPa]

The value of $\cot\theta$ has a direct influence on the design of the longitudinal reinforcement. The bending reinforcement $A_{sl}(M_{sd})$ has to be increased by an additional longitudinal reinforcement $\Delta A_{sl}(V_{sd})$ due to the design shear force, i.e. the working shear force multiplied by the appropriate load factor.

$$\Delta A_{sl}(V_{sd}) = \frac{V_{sd}^2 s}{2A_{sw} f_{ywd} d f_{yld} (\cot\theta + \cot\alpha)\sin\alpha} \tag{2.60}$$

where

f_{yld} design yield stress of the longitudinal reinforcement

f_{ywd} design yield stress of the web reinforcement

The contribution V_{cd2} varies linearly with the intensity of the nominal shear stress in the transition range between no diagonal cracks and fully developed truss action. Thus, the upper limit of the shear resistance is finally controlled by the crushing of the concrete compression diagonals $V_{rd2} = 0.30 f_{cd} b_w d \sin 2\theta$.

The spacing requirements of the shear reinforcement in longitudinal direction are given in Table 2.19 and are found in CEB 9.2.2.2.

Table 2.10 Spacing requirements

s_{max} (smaller value governs)	Limits
0.7d or 300 mm	for $F_{SEW} \le \frac{1}{5} F_{REW}$
0.6d or 300 mm	for $\frac{1}{5} F_{REW} < F_{SEW} \le \frac{2}{3} F_{REW}$
0.3d or 200 mm	for $\frac{2}{3} F_{REW} < F_{SEW}$

where

$$F_{sew} = \frac{V_{sd}}{\sin\theta}\left[\frac{\cot\theta}{\cot\theta + \cot\alpha}\right]$$

F_{sew} compression force in the web concrete [kN]

$F_{rew} = f_{cd2} b_w z \cos\theta$

F_{rew} compression resistance force in the web concrete [kN]

The transverse spacing of the stirrups should not exceed $s \leq \frac{2}{3} d$ or 800 mm, whichever is smaller.

2.8 Modified Compression Field Theory

2.8.1 General

The Modified Compression Field Theory (MCFT), developed by Vecchio and Collins at the University of Toronto in 1986 (28, 29), is an analytical model which is based largely on experimental results. The theory is able to predict the load deformation response of reinforced concrete elements subjected to inplane shear and normal stresses developed from the Compression Field Theory (18). While the Compression Field Theory ignored tension in the cracked concrete, the MCFT takes it into account. Experimentally verified average stress-strain relationships are used for the cracked concrete.

Two procedures, using an iterative process to reach a solution, were developed applying the MCFT to predict the shear capacity of concrete beams. The first procedure, called the response procedure[11], determines the shear capacity, forces, stresses, and strains of the member subjected to moment and shear. The second procedure, the design procedure[12], uses design tables presented by Collins and Mitchell (18) to obtain the shear capacity of a member.

The experimental program was based on 30 reinforced concrete elements which were subjected to different load combinations as pure shear, uniaxial compression, biaxial compression and shear, biaxial tension and shear, reversed cyclic shear, and changes in load ratios. Additional variables were percentage of

[11] Steps of procedures are given in 21.
[12] Steps of procedures are given in 21.

transverse reinforcement, percentage of longitudinal reinforcement and concrete strength. The test specimens were 890 mm square × 70 mm thick (35 square in × 2.75 in) reinforced with welded wire mesh running parallel to the edges of the test element in x and y direction. A jack-and-link assembly was used to apply shear and normal stresses.

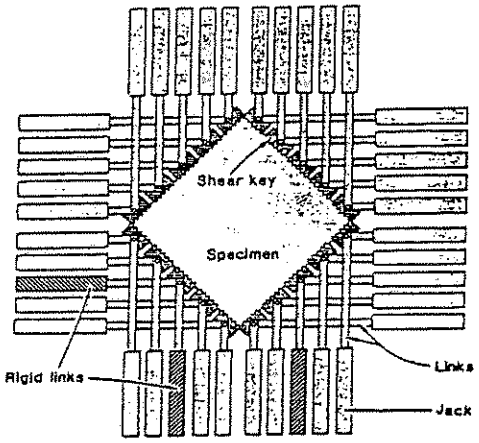

Fig. 2.9 Jack-and-link assembley used to apply shear and normal stresses (adapted from 28).

The analytical model represents a part of a reinforced concrete member to predict the shear response. Loads assumed to consist of uniform axial stresses, f_x and f_y, and uniform shear stresses, v_{xy}, which are acting on the element's edges as shown in Fig. 2.11. Average stresses in the reinforcement were determined from the measured strains in the longitudinal and transverse directions and from the stress-strain characteristics of the reinforcement. Using these steel stresses together with the

known externally applied normal stresses the average concrete stresses in x and y direction may be calculated.

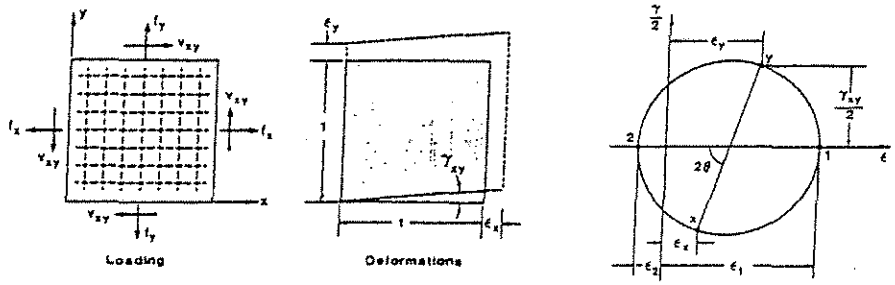

Fig. 2.10 Loading, deformation and average strains (adapted from 28).

The main problem was to determine how inplane stresses f_x, f_y, v_{xy}, are related to the inplane strains ε_x, ε_y, γ_{xy}. Vecchio and Collins made the following assumptions:

1. For each strain state there exists only one stress state.
2. Stresses and strains may be considered in terms of average values when areas are large enough to include several cracks.
3. The concrete and the reinforcing bars are perfectly bonded together at the boundaries of the element.
4. Longitudinal and transverse reinforcement is uniformly distributed over the element.

Based on these assumptions equilibrium, compatibility, and stress-strain relationships are formulated in terms of average stresses and average strains. Cracked concrete is treated as a new material with its own stress-strain characteristics.

Compatibility conditions

It was assumed that the reinforcement and the surrounding concrete have the same initial strain.

$$\varepsilon_x = \varepsilon_{sx} = \varepsilon_{cx} \tag{2.61}$$

$$\varepsilon_y = \varepsilon_{sy} = \varepsilon_{cy}$$

Compatibility conditions for cracked elements

If the strain components ε_x, ε_y, γ_{xy} are known, then the strain in any other direction may be found from geometry using the Mohr's Circle of strain.

Using geometry

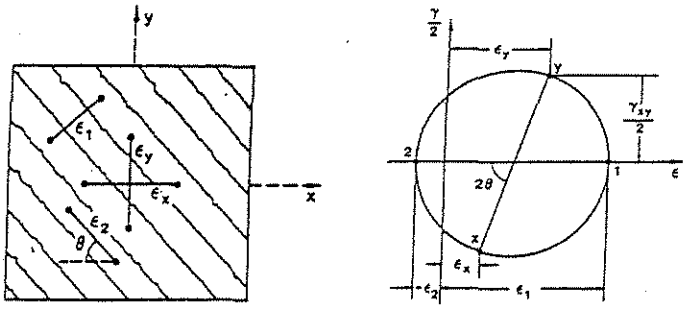

Fig. 2.11 Compatibility conditions for cracked element: average strains in cracked element, Mohr's circle for average strains (adapted from 28).

$$\gamma_{xy} = \frac{2(\varepsilon_x - \varepsilon_2)}{\tan\theta} \tag{2.62}$$

$$\varepsilon_x + \varepsilon_y = \varepsilon_1 + \varepsilon_2 \tag{2.63}$$

$$\tan^2\theta = \frac{\varepsilon_x - \varepsilon_2}{\varepsilon_y - \varepsilon_2} = \frac{\varepsilon_1 - \varepsilon_y}{\varepsilon_1 - \varepsilon_x} = \frac{\varepsilon_1 - \varepsilon_y}{\varepsilon_y - \varepsilon_2} = \frac{\varepsilon_x - \varepsilon_2}{\varepsilon_1 - \varepsilon_x} \tag{2.64}$$

where

ε_x, ε_y strain in x direction, strain in y direction

ε_1 principal tensile strain in concrete (positive quantity)

ε_2 principal compressive strain in concrete (negative quantity)

γ_{xy} shear strain

Equilibrium condition

The equilibrium of the applied forces and the stresses in the concrete and in the reinforcement of the reinforced concrete element is shown in a free body diagram.

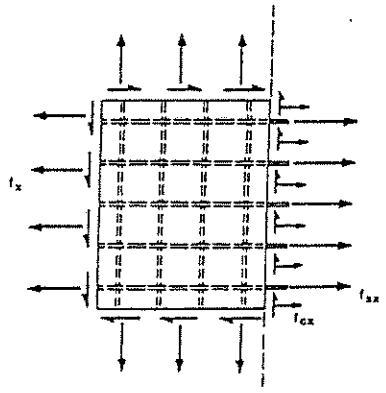

Fig. 2.12 Free-body diagram of part of test element (adapted from 28).

$$\int_A f_x dA - \int_{A_c} f_{cx} dA_c - \int_{A_s} f_{sx} dA_s = 0 \qquad (2.65)$$

Ignoring the small reduction in the concrete cross sectional area due to reinforcement

$$f_x = f_{cx} + \rho_{sx} f_{sx} \qquad (2.66)$$

similarly,

$$f_y = f_{cy} + \rho_{sy} f_{sy} \qquad (2.67)$$

assuming $v_{xy} = v_{cy} = v_{cxy}$

$$v_{xy} = v_{cx} + \rho_{sx} v_{sx} \text{ and } v_{xy} = v_{cy} + \rho_{sy} v_{sy} \qquad (2.68)$$

with v_{cxy} is known and f_{cx}, f_{cy} are defined.

Using the Mohr's Circle for concrete stresses

$$f_{cx} = f_{c1} - v_{cxy} / \tan\theta_c \qquad (2.69)$$

$$f_{cy} = f_{c1} - v_{cxy} \tan\theta_c$$

$$f_{c2} = f_{c1} - v_{cxy} (\tan\theta_c + 1/ \tan\theta_c) = f_{c1} - v_{cxy} (\tan\theta_c + \cot\theta_c) \qquad (2.70)$$

where

f_x, f_y stresses applied to the element [MPa]

f_{cx}, f_{cy} stresses in the concrete [MPa]

f_{sx}, f_{sy} stresses in the reinforcement [MPa]

v_{xy} shear stresses [MPa]

v_{cx}, v_{cy} shear stresses in the concrete [MPa]

v_{sx}, v_{sy} shear stresses in the reinforcement [MPa]

f_{c1} principal tensile stress in the concrete [MPa]

f_{c2} principal compressive stress in the concrete [MPa]

Stress-strain relations

The average stress-average strain relationships for the concrete and for the reinforcement are assumed to be dependent and the axial stress in the steel depends only on the uniaxial strain in the reinforcement. There might be significant differences between local and average stress-strain relations.

$$f_{sx} = E_s \varepsilon_x \leq f_{yx} \tag{2.72}$$

$$f_{sy} = E_s \varepsilon_y \leq f_{yy}$$

$$v_{sx} = v_{sy} = 0 \tag{2.73}$$

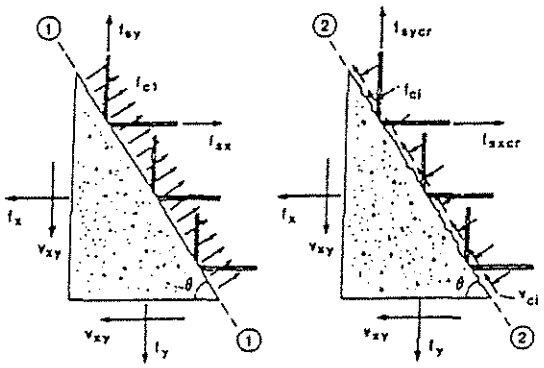

Fig. 2.13 Calculated average stresses (left) and local stresses at a crack (right) (adapted from 28).

Average stress - average strain response of concrete

For the concrete, it was assumed by Vecchio and Collins that the principal axes of strain, θ, and stress, θ_c, coincide. $\Rightarrow \theta_c = \theta$

The direction of principal strains deviates from the direction of principal stresses in the concrete, as shown in Fig. 2.15. For simplification, it was assumed to be the same. The test results showed that the principal compressive strength of the concrete depends on ε_1 and ε_2. The cracked concrete was found to be weaker subjected to high tensile strains normal to the compression than concrete in a standard cylinder test.

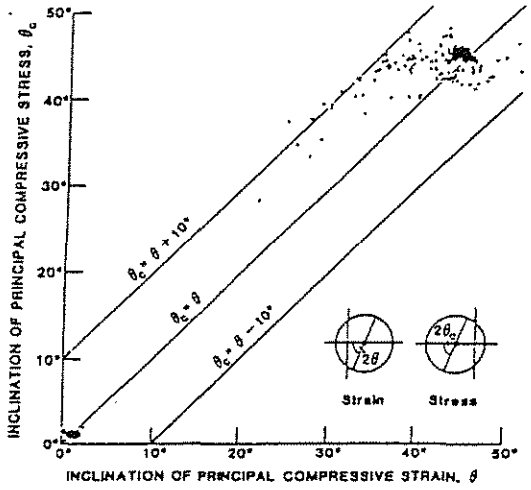

Fig. 2.14 Comparison of principal compressive stress direction with principal compressive strain direction (adapted from 28).

Thus,

$$f_{c2} = f_{c2\,max} = \left[2\left(\frac{\varepsilon_2}{\varepsilon_c'}\right) - \left(\frac{\varepsilon_2}{\varepsilon_c'}\right)^2 \right] \tag{2.74}$$

where

$$\frac{f_{c2\,max}}{f_c'} = \frac{1}{0.8 - 0.34\varepsilon_1 / \varepsilon_c'} \leq 1.0$$

where

f_{c2} principal compressive stress in concrete [MPa]

$f_{c2\,max}$ peak compressive stress of concrete under combined biaxial tension and compression [MPa]

ε_1 principal tensile strain in concrete

ε_c' strain in concrete cylinder at peak stress f_c', usually ε_c' has the value of -0.002

For the reinforcing steel a bilinear uniaxial stress-strain relationship was assumed.

$$f_{c1} = E_c \varepsilon_1 \qquad \text{[MPa] for } \varepsilon_1 < \varepsilon_{cr} \tag{2.75}$$

$$f_{c1} = \frac{f_{cr}}{1 + \sqrt{200\varepsilon_1}} \qquad \text{[MPa] for } \varepsilon_1 \geq \varepsilon_{cr} \tag{2.76}$$

where

E_c Modulus of Elasticity of the concrete assumed as $E_c \cong 2f_c' / \varepsilon_c'$ [MPa]

ε_{cr} cracking strain of concrete

f_{cr} compressive cracking strength of concrete [MPa]

Transmitting Loads Across Cracks

Local stress variations are important. The concrete tensile stresses will be zero at a crack and higher than average between the cracks. Furthermore at a crack the tensile stresses in the reinforcement will be higher than average while lower than average between the cracks. The critical direction was assumed to be normal to the principal tensile strain direction.

As investigated in numerous experimental studies the relationship between shear stress, v_{ci}, the crack width, w, and the required compressive stress on the crack, f_{ci}, is expressed in various equations by many investigators. Based on the research by Walraven (31), Vecchio and Collins developed the following relationships:

$$v_{ci} = 0.18 v_{ci\,max} + 1.64 f_{ci} - 0.82 \frac{f_{ci}^2}{v_{ci\,max}} \tag{2.77}$$

where

$$v_{ci\,max} = \frac{\sqrt{-f_c'}}{0.31 + 24w/(a+16)} \tag{2.78}$$

$$w = \varepsilon_1 s_\theta$$

$$s_\theta = \frac{1}{\frac{\sin\theta}{s_{mx}} + \frac{\cos\theta}{s_{my}}} \tag{2.79}$$

a maximum aggregate size [mm]

w average crack width [mm]

s_θ crack spacing [mm]

s_{mx} , s_{my} average spacing of cracks perpendicular to the x reinforcement / y reinforcement [mm]

f_{vy} yield strength of stirrup [MPa]

f_v stress in the stirrup [MPa]

A_v area of stirrup [mm^2]

s stirrup spacing [mm]

v_{ci} local shear stress on the crack surface [MPa]

b_w web width of the beam [mm]

jd internal flexural moment arm [mm]

The equilibrium of the unbalanced vertical component of diagonal compressive and tensile stresses which is carried by tension in the web reinforcement, can be expresses as:

$$A_v f_v = \left(f_2 \sin^2\theta - f_1 \cos^2\theta\right) b_w s$$

Substituting Eq. 2.70 into above equation

$$A_v f_v = \left[\left\{\left(\tan\theta_c + \cot\theta_c\right)\frac{V}{b_w jd}\sin^2\theta_c - f_1 \sin^2\theta\right\} - f_1 \cos^2\theta\right] b_w s$$

$$A_v f_v = \left[\left(\tan\theta_c + \cot\theta_c\right)\frac{V}{b_w jd}\sin^2\theta_c - f_1\right] b_w s \qquad (2.80)$$

$$A_v f = f_1 b_w jd \cot\theta_c + \frac{A_v f_v}{s} jd \cot\theta_c$$

The above equation represents the shear capacity of a member as a function of principal stress in concrete, f_1, the stress in the stirrup, f_v, and the crack orientation θ_c.

The principal compressive strain, ε_2, is given by

$$\varepsilon_2 = \varepsilon_c'\left(1 - \sqrt{1 - f_2 / f_{2\max}}\right) \tag{2.81}$$

where

$f_{c2\max}$ peak compressive stress of concrete under combined biaxial tension and compression [MPa]

The longitudinal strain in the web, ε_x, is given by

$$\varepsilon_x = \frac{\varepsilon_1 \tan^2\theta_c + \varepsilon_2}{1 + \tan^2\theta_c} \tag{2.82}$$

The strain in the web reinforcement, ε_t, is given by

$$\varepsilon_t = \frac{\varepsilon_1 + \varepsilon_2 \tan^2\theta_c}{1 + \tan^2\theta_c} \tag{2.83}$$

The equilibrium of the unbalanced longitudinal component of the diagonal concrete stresses for a certain crack angle and principal tensile stress is balanced by tensile stresses in the longitudinal where $A_c f_c$ is the force in the concrete and $A_s f_s$ is the force in the longitudinal steel

$$
\begin{aligned}
A_x f_s + A_c f_c &= \left(f_2 \cos^2\theta_c - f_1 \sin^2\theta_c\right) b_w jd \\
A_x f_s + A_c f_c &= \left[\left\{\left(\tan\theta_c + \cot\theta_c\right)v - f_1\right\}\cos^2\theta_c - f_1 \sin^2\theta_c\right] b_w jd \\
A_x f_s + A_c f_c &= \left[\frac{\cos\theta_c}{\sin\theta_c}\left(\sin^2\theta_c + \cos^2\theta_c\right)\frac{V}{b_w s} - f_1\right] b_w jd \\
A_x f_s + A_c f_c &= V\cot\theta_c jd/s + f_1 b_w jd
\end{aligned}
\tag{2.84}
$$

For members with web reinforcement, ε_x is assumed to occur at the midheight of the cross section because of the load redistribution capacity of such members. The shear stresses are transferred from high strain regions to low strain regions of the cross section. Members without web reinforcement have less capacity because they are not ?

CHAPTER 3
Development of a Strut and Tie Model for Analysis of Typical North American Members

3.1 General

Truss models can be used to investigate the equilibrium between internal and external forces. Furthermore stress fields can be developed by replacing the truss members by struts, ties, fans, and arches with finite dimensions. These form a specific form of rational model that can be accurate, simple and general for practical applications. The purpose of this chapter is to derive a strut and tie approach for use in evaluating typical North American reinforced concrete members including the Pasley data (21).

3.2 Members Not Requiring Shear Reinforcement

For a simply supported beam without shear reinforcement, the bending moment M at a section A-A in Fig. 3.1 causes compressive stresses in the concrete above the neutral axis, and tensile stresses below the neutral axis. The concrete is not yet cracked, To satisfy the vertical force equilibrium, the summation of the vertical shear stresses across the section must be equal to the shear force, V. Below the neutral axis there is nearly a state of pure shear. This state implies no tensile or compressive stresses on the faces of the element. The diagonal tension constitutes the main cause of inclined cracking.

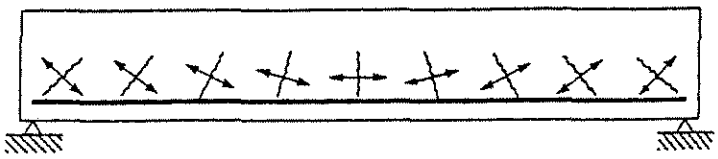

Fig. 3.1: Directions of potential cracks in a simple supported beam.

Thus the failures in beams commonly referred to as "shear failures" are actually 'tension failures" at the inclined cracks. One of the earliest to recognize this was Mörsch (19) in Germany in the early 1900's. Bresler (7) and MacGregor (15) have presented a systematic treatment of the various situations in which shear related cracks develop. Collins and Mitchell (18), Marti (16, 17), Vecchio and Collins (28, 29), and Schlaich, Schäfer and Jennewein (24) all have explained the truss model (or the strut and tie model and compression field theory) as the most rational approach to shear related behavior of beams.

3.3 Members Requiring Shear Reinforcement

The most general accepted model for the behavior of reinforced concrete beams containing shear reinforcement is the truss model originated by Ritter and Mörsch (19). The current thinking related to the truss model is summarized by Schlaich, Schäfer and Jennewein (24) as follows.

In a simply supported steel truss, the upper and the lower chord are in compression and tension respectively and the diagonal and vertical members are

alternately in tension and compression. In the reinforced concrete beam the concrete performs the task of carrying the compressive forces while steel reinforcement is used for the tensile forces.

The shear reinforcement wraps around the longitudinal tension reinforcement and must be anchored in the compression zone, usually by hooking it around longitudinal bars. These bars are either compression reinforcement or are provided solely to hold in place and anchor the shear reinforcement. While shear reinforcement provides shear strength, its contribution to the strength occurs only after inclined cracks form. Prior to the formation of inclined cracks, the concrete performs the task of carrying the shear. The shear reinforcement is necessary in order to allow a redistribution of internal forces across any inclined crack that may form. The primary functions of shear reinforcement are

1. To carry part of the shear.
2. To restrict the growth of the inclined crack and thus to maintain interface shear transfer strength.
3. To tie the longitudinal bars in place and thereby increase their strength V_d to resist transverse forces (dowel action). Additionally dowel action on the stirrups may transfer a small force across a crack and the confirming action of the stirrups on the compression concrete may slightly increase its strength.

If the amount of shear reinforcement is small, it will yield immediately at the formation of an inclined crack, and then will fail if insufficient amount of steel is provided. If the amount of shear reinforcement is too large, there will be a shear compression failure without the yielding of the shear reinforcement under large loads. The optimum amount of shear reinforcement should be such that both the shear reinforcement and the compression zone of the beam each continue to carry increasing shear after the formation of the inclined crack unit the shear reinforcement yields, resulting in a ductile failure.

In zones of a concentrated load or at an abrupt discontinuity in the member the plane section theory is not applicable and the true forces are not those obtained by first order shear and moment diagrams.

3.4 Transfer of Shear

The transfer of shear in reinforced concrete members occurs by a combination of the following mechanisms shown in Fig. 3.2:

1. Shear resistance of the uncracked concrete [ACI:V_{cz}, EC2:V_{cd}]
2. Interface shear transfer [ACI:V_a, EC2:$V_{Friction}$]; other terms are: aggregate interlock, surface roughness shear transfer and shear friction. This force occurs tangentially along a crack and is similar to a frictional force due to irregular interlocking of aggragates along the rough concrete surface on each side of the crack.

3. Dowel action [ACI:V_d, EC2:V_{Dowel}] is the resistance of the longitudinal reinforcement to a transverse force.
4. Arch action on relatively deep beam
5. Shear reinforcement resistance from stirrups [ACI:V_s, EC2:V_{wd}]

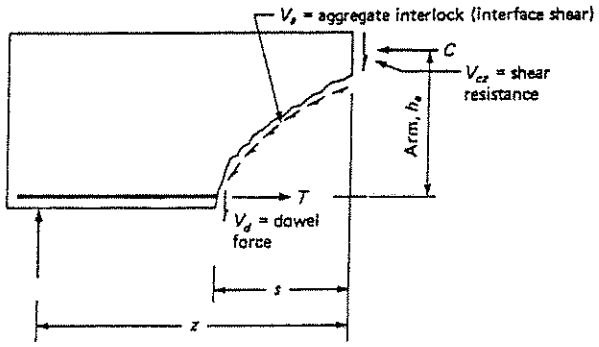

Fig. 3.2: Redistribution of shear resistance after formation of inclined crack, adopted from (30).

As the crack widens, V_a decreases, increasing the fraction of the shear resisted by V_{cz} and V_d (and V_s) until either a splitting (dowel) failure occurs, or the compression zone crushes due to combined shear and compression. Thus stirrups do not prevent inclined cracks forming but they come into play only after the cracks have formed.

The ability of a beam to carry additional load after an inclined crack has formed depends on whether or not the portion of shear formerly carried by uncracked concrete can be redistributed across the inclined crack.

3.5 Strut and Tie Model

As discussed earlier, the shear contribution consists of a combination of several mechanisms. The values of each contribution are not identified but can be combined. An assumption is to adopt the diagonal cracking load of a member without shear reinforcement as the concrete strength of a similar concrete member strength with shear reinforcement.

A beam subjected to shear and bending may be represented by simple truss model with a constant slope angle, θ, as shown in Fig. 3.3.

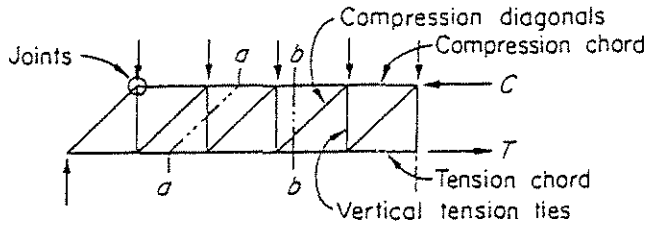

Fig. 3.3: Truss model with constant θ.

The components are:

(a) Struts: uniaxial loaded concrete compression members.

(b) Ties: Steel tension members.

(c) Joints at the intersection of truss members are assumed to be pin connected.

(d) Compression fans, which form at 'distributed' regions as at the supports or under concentrated loads transmitting the forces into the beam.

(e) Diagonal compression fields, occurring where parallel compression struts transmit force form one stirrup to another.

Due to the arrangement of the shear reinforcement, the slope angle, θ, of the diagonal compression struts may range from about 25° to 65° based on analysis and observation. It is assumed that all the stirrups reach the yield stress at failure. Therefore, the truss model becomes statically determinate.

The effective concrete compressive strength, which might be assumed for a truss model, is given by the following table.

Table 3.1: Effective concrete compressive strength (13)

Structural member	f_{ce}
Truss node	
• Joints bounded by compressive struts and bearing areas.	0.85 f_c'
• Joints anchoring one tension tie.	0.65 f_c'
• Joints anchoring tension ties in more than one direction.	0.50 f_c'
Isolated compression struts in deep beams or distributed regions	0.50 f_c'
Severely cracked webs of slender beams.	0.25 f_c' to 0.45 f_c'

The modeling of the truss can be significantly simplified if the top and the bottom chords are parallel. This represents an approximation since the chords may not be parallel in an actual member. However for design purposes, the approximation is sufficiently accurate.

A simplified model is a truss model with parallel chords. For simplification, it is assumed that the beam is a rectangular cross section with constant height. The truss model consists of compression struts, tension ties and pinned joints as shown in

Fig. 3.4. The enclosed angle between the longitudinal axis of the beam and the shear reinforcement (stirrups), α, is equal to or smaller than 90°.

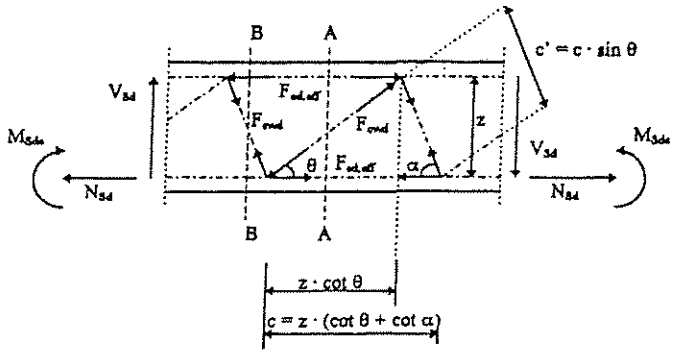

Fig. 3.4: Forces in the positive moment region.

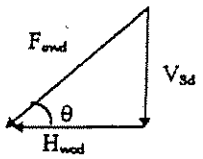

$F_{cwd} = V_{Sd} / \sin \theta$

Fig. 3.5: Cut A-A.

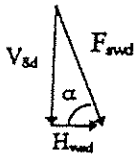

$F_{swd} = V_{Sd} / \sin \alpha$

Fig. 3.6: Cut B-B.

From Fig. 3.5 and 3.6, it is recognizable that the forces F_{cwd} of the compression strut and F_{swd} of the tension tie depend on the acting shear force V_{sd}, but not on the flexural moment. To determine the stresses, the forces F_{cwd} and F_{swd} have to be divided by the appropriate areas on which they act.

Therefore the stresses in the compression strut are given by

$$\sigma_{c2}^{II} = F_{cwd} / \left(c' b_w \right) \tag{3.1}$$

$$\sigma_{c2}^{II} = F_{cwd} / \left(z b_w \sin^2 \theta (\cot\theta + \cot\alpha) \right)$$

σ_{c2}^{II} principal stress of the compression strut

The required shear reinforcement is given by

$$a_{sw} = F_{swd} / \left(c f_{ywd} \right) \tag{3.2}$$

$$a_{sw} = F_{swd} / \left(z f_{ywd} \sin\alpha (\cot\theta + \cot\alpha) \right)$$

$$a_{sw} = A_{sw} / \delta_w$$

$A_{sw} = n\phi_w^2 \pi / 4$ sum of the required shear reinforcement of a cross section of the beam [mm^2]

n number of steel cross sections in a plane perpendicular to the shear reinforcement

ϕ_w diameter of the shear reinforcement bar [mm]

δ_w shear reinforcement spacing in longitudinal direction [mm]

The forces $F_{cd,eff}$ in the compression chord and $F_{sd,eff}$ in the tension chord are given by a combination of moment, longitudinal force and shear.

$$\left|F_{cd,eff}\right| = M_{Sds} / z - \frac{V_{sd}}{2}(\cot\alpha + \cot\theta) \tag{3.3}$$

$$F_{cd,eff} = M_{Sds} / z + N_{sd} + \frac{V_{sd}}{2}(\cot\alpha + \cot\theta) \tag{3.4}$$

The truss model can fail

(a) by yielding of the tie.

(b) by crushing of one of the struts.

(c) by crushing in a model node area.

The addition of stirrups will modify the internal flow of forces in the truss model as shown in Fig. 3.7..

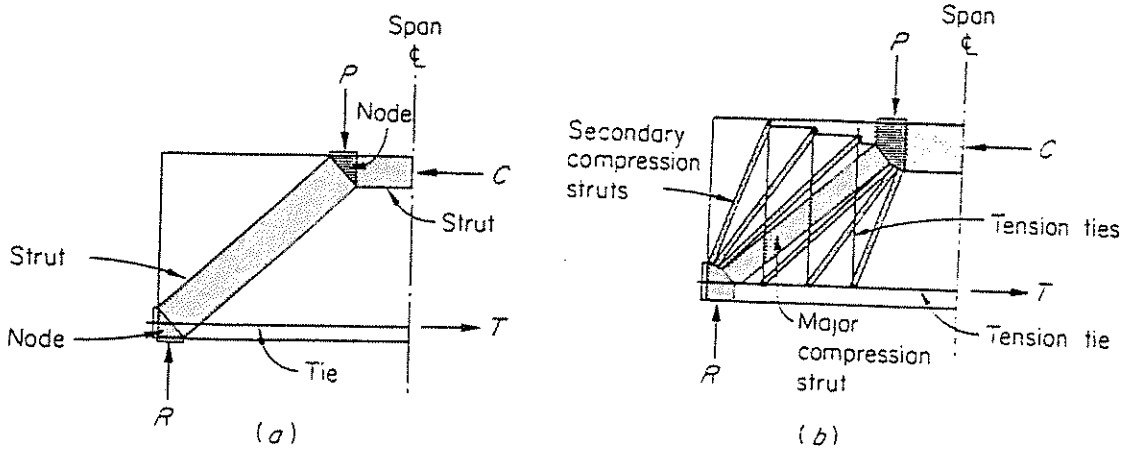

Fig. 3.7: Truss models (a) beam without stirrups and (b) beam with stirrups, adopted from (20).

For a T-beam the truss model for the web is equivalent to the simplified model. The top chord is represented by a horizontal truss model instead by a line. Therefore, the model becomes more complex as shown in Fig. 3.8. The forces in the compression struts and the tension ties are identical with the forces in the simplified model.

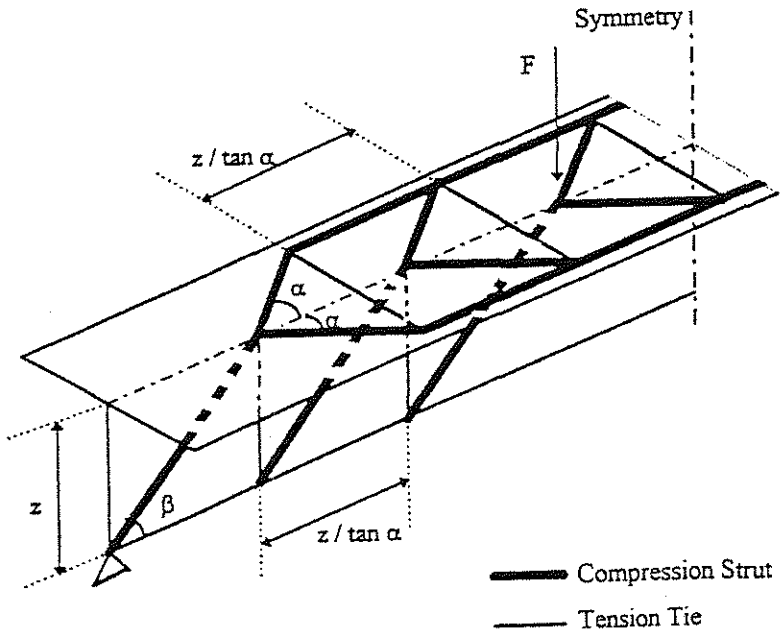

Fig. 3.8: T-beam model.

3.6 Evaluation of Beam Models with Variable Inclination α

Using the test results from Pasley et al. (21) the capacity of an equivalent truss model is analyzed for a range of angles, α, between 35° and 45°. For two variable angles, and , the general equation for the nominal strength of the compression strut is more complex and will be derives as follows using the geometries of a general model

in Fig. 3.9 and the Pasley test beam in Fig. 3.10. The Pasley test data is shown in Table 3.2 for the overall test series.

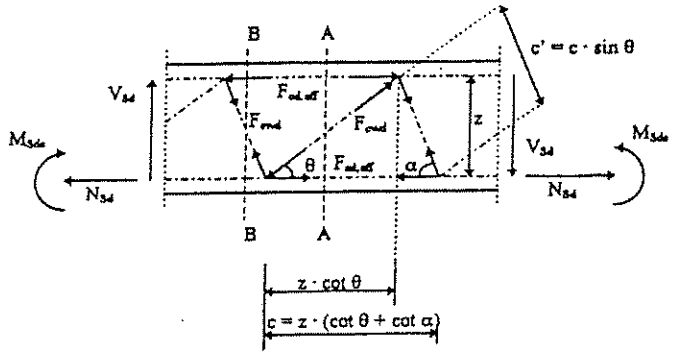

Fig. 3.9: General truss model.

Using principles of geometry and the layout in Fig. 3.9, the horizontal projections of the tension tie, s_1, and the compression strut, s_2, can be computed using the geometry of the strut and tie model. The actual Pasley model is shown in Fig. 3.10. The results for various tension tie angles, α, and compression strut angles, θ, are found in Tables 3.3 through 3.5. The inclination of the tension tie is found in Table 3.6 and 3.7. It can be seen from these results that the geometry itself controls the placement and inclination of the compression struts and tension ties. The overall load carrying mechanism and its strength is then dependent on the strength of these elements oriented in the configurations provided in the tables.

It can be seen that for every compression strut angle, θ, from 35° to 45°, there exist three tension tie angles, α. These generally are different in value and are about at 15°, 40° and 75°, as controlled by the geometry.

$$c = z(\cot\alpha + \cot\theta)$$
$$c' = c\sin\theta = z\sin\theta(\cot\alpha + \cot\theta) \tag{3.5}$$

Where

α angle between the tension tie and the axis of the member

θ angle between the compression strut and the axis of the member

c horizontal distance between two compression struts

c' shortest distance between two compression struts

z lever arm assumed to be $z = c_2 d$, where c_2 is an unknown coefficient to be found

$$F_R = V_R / \sin\theta \tag{3.6}$$

$$\sigma_R = F_R / \left(c' b_w\right) \tag{3.7}$$

$$\sigma_R = \frac{V_R}{z b_w \sin^2\theta(\cot\alpha + \cot\theta)} \tag{3.8}$$

R indice R stands for resistance of the compression strut;

d indice d stands for design

F_R shear force in the compression strut [kN]

V_R vertical component of the shear force in the compression strut [kN]

σ_R shear stress in the compression strut [MPa]

Substituting $\sigma_R = c_1 f_c'$, where c_1 is an unknown coefficient, and solve for V_R

$$\begin{aligned} V_R &= (c_1 f_c')(c_2 d) b_w \sin^2\theta(\cot\alpha + \cot\theta) \\ V_R &= c_3 f_c' d b_w \sin^2\theta(\cot\alpha + \cot\theta) \\ V_R &= c_3 f_c' d b_w (\cot\alpha + \cot\theta)/(1 + \cot^2\theta) \\ V_R &= \nu f_c' d b_w \sin^2\theta(\cot\alpha + \cot\theta) \end{aligned} \tag{3.9}$$

where $c_3 = c_1 c_2$

The unknown variable in this equation is the factor ν which will be assumed to be 0.8 based on EC 2. It is known that the shear resistance of the compression struts has to be larger than the actual shear force for equilibrium.

$$V_R = \nu f_c' d b_w \sin^2\theta(\cot\alpha + \cot\theta) \geq V_{sd}$$

Rearranging and solving

$$V_R \geq V_{sd} \Rightarrow \nu \geq \frac{V_{sd}}{f_c' d b_w \sin^2\theta(\cot\alpha + \cot\theta)}$$

where

V_{sd} actual vertical component of the shear force in the compression strut

For each assumed angle θ, there are several possible values of the angle α which give a different value ν. The smallest value of ν will be determined and substituted as a known variable into the shear resistance of the compression strut equation given by Eq. 3.11.

To calculate the shear resistance force of the tension tie, V_T, it is assumed that the sum of the shear resistance provided by the shear reinforcement, V_s, and the shear resistance provided by an uncracked concrete section, V_{cl}. To determine V_{cl} it was assumed that the shear capacity was equal to the tension tie capacity of a Pasley test beam[1] without shear reinforcement.

$$
\begin{aligned}
&V_{n(test)} \geq V_{cl} = \left(c_1 + c_2\rho_l\right) f_c' b_w d \\
&\Rightarrow k_1 = V_{cl} / \left(f_c' b_w d\right) = \left(c_1 + c_2\rho_l\right) \\
&\Rightarrow k_n = V_{cl} / \left(f_c' b_w d\right) = \left(c_1 + c_2\rho_{l(n)}\right) \\
&\Rightarrow k_n - k_{(n-1)} = \left(c_2\left(\rho_{l(n)} - \rho_{l(n-1)}\right)\right) \Leftrightarrow c_2 = \frac{k_n - k_{(n-1)}}{\left(\rho_{l(n)} - \rho_{l(n-1)}\right)}
\end{aligned}
\qquad (3.12)
$$

where

c_1, c_2 are unknown constants

ρ_l flexural reinforcement ratio

The process can be described as follows. Using the test data from Pasley as the known results, the data can be set equal to the expression for shear capacity shown in the first of Eq. 3.12.

First set min $|c_2| = c_2$, then calculate c_1 for all cases without shear reinforcement. Knowing the shear resistance of the uncracked concrete, V_{cl}, it must be determined if it is appropriate to consider Vc1 for the beams with shear reinforcement. Having low ratios of shear reinforcement for the test beams with shear

[1] The shear capacity of the test beams is given in Appendix A and (21).

reinforcement, it is assumed that the tension tie, consisting of the capacity of the provided stirrups and the uncracked concrete section, will fail first. The calculation of V_{cl} is summarized in Table 3.8. The value of V_{cl} obtained by the process described in Table 3.8 is:

$$V_{cl} = \left(0.0276 + 0.0121\rho_l\right) f_c' b_w d \qquad (3.13a)$$

This equation was used to predict V_{cl} for the various beams tested by Pasley based on no shear reinforcement. The results are shown in Tables 3.9 through 3.11 where the shear force carried by the concrete ΔV is computed by subtracting the computed stirrup force from the measured test load. The predicted concrete strengths are shown at the right of the figure. All data is shown as a function of angle θ for each of the tests.

The results show that the resulting predictions for the concrete strength compare favorably to the test data. The observed results from Pasley indicate that the shear cracks were observed to be at about 39°. The computed results in Tables 3.9 through 3.11 show that the maximum stirrup loads occurs at n=3 and provides corresponding concrete load values that compare close to that of the test values.

This results is shown perhaps better in Tables 3.12 through 3.14 where the computed concrete shear, V_{cl}, is added to the stirrup loads, V_s. The computed values are quite close to the test values. The range of ratios for predicted to test range from 1.00 down to 0.88 all for the strut inclined at 35° and for three tension ties. The other steeper angles produce lower capacity values. It also is important to note that the

error is conservative in that the capacity is slightly underpredicted. In essence the results show a variable ϕ factor that ranges from 1.00 to about 0.90. Use of an ACI factor of $\phi = 0.85$ would produce conservative results across the tests. This agreement is very close to that produced by code methods and points to the strut and tie approach as a viable means to identify the capacity of members like those tested here.

Finally it is possible to plot the nominal capacity of each truss model with different angle combinations, θ and α, versus the inclination θ to show a comparison between the test results and the assumed truss model with different angles θ. The results of these calculations are presented graphically in Figs. 3.11 through 3.22. Here the total load, V_n, computed is plotted for n=1, 2, 3 and 4 plus the test data for the six test beams. The results are present for values of θ from 35° to 45°. The result here confirm that the match to test data is a function of the test configuration, and that the best overall match occurs with a compression strut angle of about 35°. The last plot Fig. 3.22 shows that the overall capacity drops slightly with increasing strut angle indicating that the stirrup capacity is decreasing in response to the increasing strut angle.

The data of the beam model indicated that the capacity of the uncracked concrete, V_{c1}, is around 90% of that for beams with shear reinforcement. The reduced capacity is called V_{c2} for those beams with shear reinforcement and the nominal shear capacity is given by

$$V_w = V_{c2} + V_s \tag{3.13b}$$

$$V_{c2} = \frac{8}{10}\left(0.0233 + 0.909\rho_l\right)f_c' b_w d \tag{3.14}$$

$$V_s = \frac{A_{sw}}{s} z f_y (\cot\alpha + \cot\theta)\sin\alpha \tag{3.15}$$

or

$$V_w = \left(0.0186 + 0.727\rho_l\right)f_c' b_w d + A_{sw}\frac{z f_y}{s}(\cot\alpha + \cot\theta)\sin\alpha \tag{3.16}$$

for beams with shear reinforcement.

The results of this analysis show that the strut and tie model can be used effectively to model the capacity of these members. Even with the simple form of the model, the results are promising and show that the basic mechanics involved in predicting shear failures in these lightly reinforced members produces results that range from 0.90 of the test load to 1.00 of the measured. Thus the conclusion can be reached that with proper "tuning" of design factors that an even better match of behavior to that predicted could be obtained. One such tuning is the use of two sets of predictive equations for V_c. One equation V_{c1} (Eq. 3.13a) is based on beams with no shear reinforcement. A second equation is presented for V_{c2} (Eq. 3.13b) for systems where there is shear reinforcement and the system behave slightly differently. The use of strut and tie models can indeed to be employed to model these systems and to produce accurate results.

3.7 Evaluation of Pasley data with Hofer/McCabe Model

The Pasley data was analyzed using the strut and tie model developed in this study and discussed in Chapter 3. Here the equation was developed by "calibrating" the shear capacity obtained by testing beams without shear reinforcement. This equation, Eq. 3.13, reveals the contribution of the concrete system and includes the dowel action, aggregate interlock and strength of the uncracked concrete into a single equation.

To account for the effects of shear reinforcement, four truss models were assumed. These models, shown in Fig. 3.10, correspond to the four possible arrangement of tension ties that can fit within the load point to the reaction point on the span. This geometric limitation fixed the range of possible tension ties to just these four models. Note that in this set of calculations, no explicit assumption was made as to a 90 ° tension tie as is normally done with stirrups. Instead the analysis was conducted with the concept that the analyzed system would provide the required steel areas that could then be provided in the from of vertical stirrups.

In the analysis, a range of compression strut angles was assumed from 35° up to 45°. This range was selected because of experience and the knowledge that the experimental data appeared to support a 40° angle, as did the CEB results. The angles were incremented in one degree increments and for each compression strut angle, all

four possible tension strut inclinations used in the computed capacities. The results were presented in Tables 3.6 to 3.15 and plotted in Figs. 3.11 to 3.21.

The results show that the strut and tie model does quite well in predicting the capacities of the sections. In most cases the strut and tie model is at or below the actual strength obtained from the test. In only the I-3 test does the strut and tie model overpredict the capacity. These results can be seen in the various figures where the spread in predicted capacities can be seen.

In Fig. 3.22, the results of one test, J-2, is plotted for various angles of compression strut inclination. It can be seen here that the angle has varying amounts of influence on the results. It appears that an angle of 40° does indeed appear to produce good predictions of the capacities. Moreover, the results are about 10% lower than the test points. This difference between test and prediction is in the same order of magnitude as that of the standard EC 2 and the test points. This result would tend to support the concept of a strut and tie model as an alternative to the empirical model currently used by ACI. Of course the trade off from engineering standpoint is the added effort required to produce the possible strut orientations and to evaluate the results. However, this process could easily be automated to produce predictions quickly and efficiently.

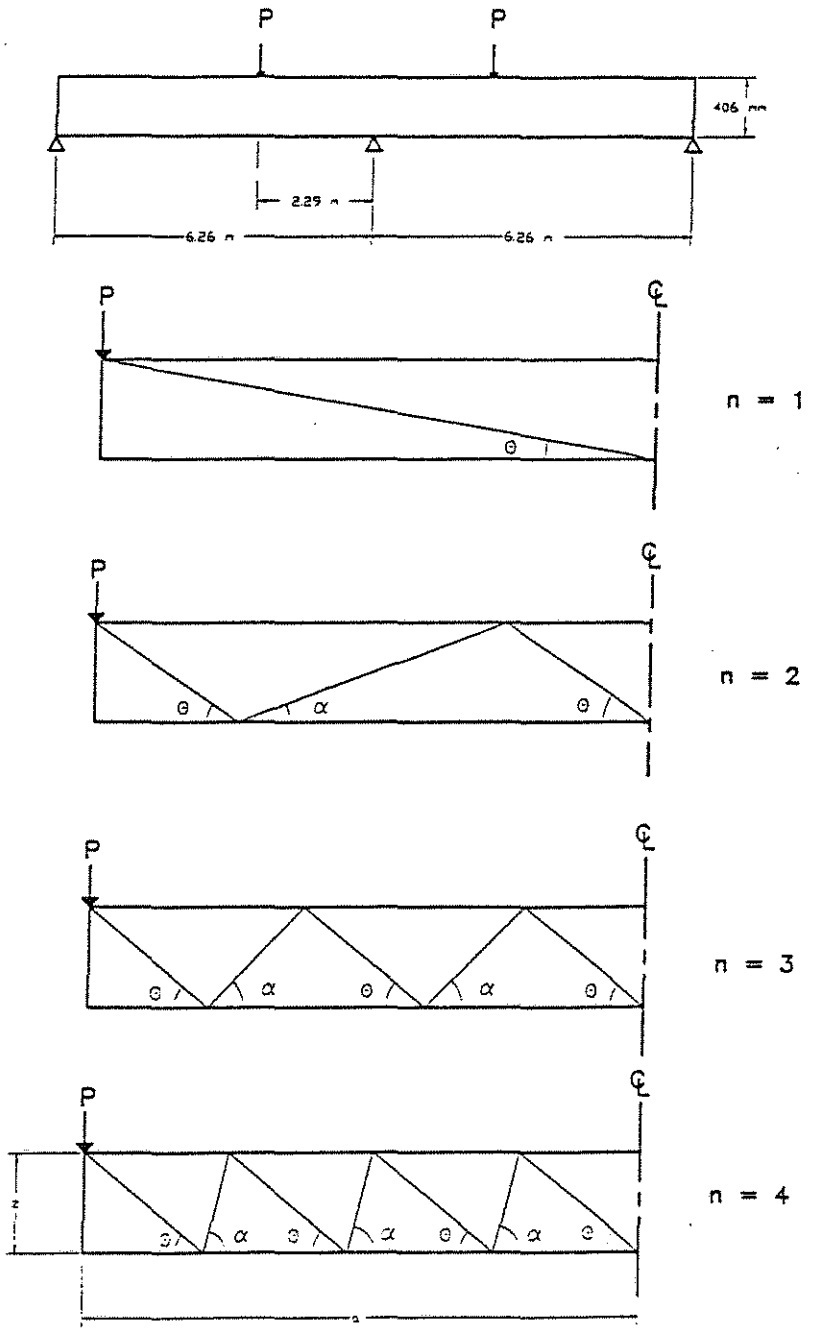

Fig. 3.10 : Truss Models

Table 3.2: Beam Properties for 2-Point Loading on Each Span.

Load	Span	Failure Region	Beam	f'_c [MPa]	$V_{n(test)}$ [kN]	$v_{n(test)}$ [MPa]	d [mm]	Support R [kN]	Load P [kN]	$\rho_v * f_{vy}$ [MPa]	ρ_v [-]	ρ_w [-]
2	west	negative	I-3	30.8207	93.4080	1.2135	403.6060	93.4080	60.9376	0.2337	0.0008	0.0100
2	west	negative	J-2	30.9586	96.0768	1.2480	403.3520	96.0768	62.7168	0.2344	0.0008	0.0074
2	west	negative	J-3	30.5449	138.7776	1.8341	400.0500	138.7776	114.3136	0.5654	0.0015	0.0074
2	east	negative	I-3	30.8207	74.2816	0.9653	403.6060	74.2816	45.8144	0.0000	0.0000	0.0100
2	east	negative	J-2	30.9586	68.9440	0.8964	403.3520	68.9440	41.8112	0.0000	0.0000	0.0074
2	east	negative	J-3	30.5449	109.4208	1.4342	397.0020	109.4208	84.5120	0.3951	0.0008	0.0075

Table 3.3: Horizontal Projection of the Compression Strut, s_2, as Function of θ.

$$s_2 = \frac{0.9d}{\tan\theta}, s_1 = \frac{0.9d}{\tan\alpha}, s_1 + s_2 = s$$

$$35^\circ \le \theta \le 45^\circ$$

$$45^\circ \le \alpha \le 90^\circ$$

$$a = ns_2 + (n-1)s_1 \Rightarrow s_1 = \frac{a - ns_2}{(n-1)}$$

bw= 190.5 [mm]
a= 2.286 [m]

	s2[m]	s2[m]	s2[m]	s2[m]	s2[m]	s2[m]	s2[m]	s2[m]	s2[m]	s2[m]	s2[m]
	θ=35	θ=36	θ=37	θ=38	θ=39	θ=40	θ=41	θ=42	θ=43	θ=44	θ=45
I-3 west	0.5188	0.5000	0.4820	0.4649	0.4486	0.4329	0.4179	0.4034	0.3895	0.3762	0.3632
J-2 west	0.5184	0.4996	0.4817	0.4646	0.4483	0.4326	0.4176	0.4032	0.3893	0.3759	0.3630
J-3 west	0.5142	0.4956	0.4778	0.4608	0.4446	0.4291	0.4142	0.3999	0.3861	0.3728	0.3600
I-3 east	0.5188	0.5000	0.4820	0.4649	0.4486	0.4329	0.4179	0.4034	0.3895	0.3762	0.3632
J-2 east	0.5184	0.4996	0.4817	0.4646	0.4483	0.4326	0.4176	0.4032	0.3893	0.3759	0.3630
J-3 east	0.5103	0.4918	0.4742	0.4573	0.4412	0.4258	0.4110	0.3968	0.3832	0.3700	0.3573

Table 3.4: Horizontal Projection of the Tension Tie, s_1, as Function of θ.

θ=35	s1[m]	s1[m]	s1[m]	θ=36	s1[m]	s1[m]	s1[m]	θ=37	s1[m]	s1[m]	s1[m]
n	2	3	4	n	2	3	4	n	2	3	4
I-3 west	1.2485	0.3648	0.0703	I-3 west	1.2861	0.3931	0.0954	I-3 west	1.3219	0.4199	0.1193
J-2 west	1.2491	0.3653	0.0707	J-2 west	1.2867	0.3935	0.0958	J-2 west	1.3225	0.4204	0.1197
J-3 west	1.2576	0.3717	0.0764	J-3 west	1.2949	0.3997	0.1013	J-3 west	1.3304	0.4263	0.1249
I-3 east	1.2485	0.3648	0.0703	I-3 east	1.2861	0.3931	0.0954	I-3 east	1.3219	0.4199	0.1193
J-2 east	1.2491	0.3653	0.0707	J-2 east	1.2867	0.3935	0.0958	J-2 east	1.3225	0.4204	0.1197
J-3 east	1.2654	0.3776	0.0816	J-3 east	1.3024	0.4053	0.1063	J-3 east	1.3377	0.4318	0.1298
θ=38	s1[m]	s1[m]	s1[m]	θ=39	s1[m]	s1[m]	s1[m]	θ=40	s1[m]	s1[m]	s1[m]
n	2	3	4	n	2	3	4	n	2	3	4
I-3 west	1.3561	0.4456	0.1421	I-3 west	1.3889	0.4701	0.1639	I-3 west	1.4202	0.4937	0.1848
J-2 west	1.3567	0.4460	0.1425	J-2 west	1.3894	0.4706	0.1643	J-2 west	1.4207	0.4941	0.1852
J-3 west	1.3643	0.4517	0.1476	J-3 west	1.3968	0.4761	0.1692	J-3 west	1.4278	0.4994	0.1899
I-3 east	1.3561	0.4456	0.1421	I-3 east	1.3889	0.4701	0.1639	I-3 east	1.4202	0.4937	0.1848
J-2 east	1.3567	0.4460	0.1425	J-2 east	1.3894	0.4706	0.1643	J-2 east	1.4207	0.4941	0.1852
J-3 east	1.3713	0.4570	0.1522	J-3 east	1.4035	0.4812	0.1737	J-3 east	1.4344	0.5043	0.1942

Table 3.5: Horizontal Projection of the Tension Tie, s_1, as Function of θ.

θ=41	sl[m]	sl[m]	sl[m]	θ=42	sl[m]	sl[m]	sl[m]	θ=43	sl[m]	sl[m]	sl[m]
n	2	3	4	n	2	3	4	n	2	3	4
I-3 west	1.4503	0.5162	0.2048	I-3 west	1.4792	0.5379	0.2241	I-3 west	1.5069	0.5587	0.2426
J-2 west	1.4508	0.5166	0.2052	J-2 west	1.4797	0.5382	0.2244	J-2 west	1.5074	0.5591	0.2429
J-3 west	1.4576	0.5217	0.2098	J-3 west	1.4863	0.5432	0.2288	J-3 west	1.5138	0.5638	0.2472
I-3 east	1.4503	0.5162	0.2048	I-3 east	1.4792	0.5379	0.2241	I-3 east	1.5069	0.5587	0.2426
J-2 east	1.4508	0.5166	0.2052	J-2 east	1.4797	0.5382	0.2244	J-2 east	1.5074	0.5591	0.2429
J-3 east	1.4639	0.5265	0.2140	J-3 east	1.4924	0.5478	0.2329	J-3 east	1.5197	0.5683	0.2511

θ=44	sl[m]	sl[m]	sl[m]	θ=45	sl[m]	sl[m]	sl[m]
n	2	3	4	n	2	3	4
I-3 west	1.5337	0.5788	0.2605	I-3 west	1.5595	0.5981	0.2777
J-2 west	1.5342	0.5791	0.2608	J-2 west	1.5600	0.5985	0.2780
J-3 west	1.5403	0.5837	0.2649	J-3 west	1.5659	0.6029	0.2819
I-3 east	1.5337	0.5788	0.2605	I-3 east	1.5595	0.5981	0.2777
J-2 east	1.5342	0.5791	0.2608	J-2 east	1.5600	0.5985	0.2780
J-3 east	1.5460	0.5880	0.2687	J-3 east	1.5714	0.6070	0.2856

Table 3.6: Inclination of the Tension Tie, s_1, as Function of θ.

θ=35	α	α	α	θ=36	α	α	α	θ=37	α	α	α
	degrees	degrees	degrees		degrees	degrees	degrees		degrees	degrees	degrees
I-3 west	16.2226	44.8739	79.0454	I-3 west	15.7721	42.7430	75.2874	I-3 west	15.3649	40.8599	71.8218
J-2 west	16.2049	44.8174	78.9725	J-2 west	15.7554	42.6907	75.2167	J-2 west	15.3490	40.8113	71.7535
J-3 west	15.9761	44.0872	78.0193	J-3 west	15.5387	42.0149	74.2926	J-3 west	15.1431	40.1834	70.8628
I-3 east	16.2226	44.8739	79.0454	I-3 east	15.7721	42.7430	75.2874	I-3 east	15.3649	40.8599	71.8218
J-2 east	16.2049	44.8174	78.9725	J-2 east	15.7554	42.6907	75.2167	J-2 east	15.3490	40.8113	71.7535
J-3 east	15.7672	43.4194	77.1314	J-3 east	15.3408	41.3968	73.4336	J-3 east	14.9548	39.6089	70.0361
0=38	α	α	α	θ=39	α	α	α	θ=40	α	α	α
	degrees	degrees	degrees		degrees	degrees	degrees		degrees	degrees	degrees
I-3 west	14.9949	39.1863	68.6362	I-3 west	14.6570	37.6906	65.7139	I-3 west	14.3470	36.3469	63.0353
J-2 west	14.9797	39.1410	68.5706	J-2 west	14.6424	37.6482	65.6510	J-2 west	14.3331	36.3070	62.9752
J-3 west	14.7833	38.5552	67.7155	J-3 west	14.4545	37.0996	64.8325	J-3 west	14.1528	35.7914	62.1930
I-3 east	14.9949	39.1863	68.6362	I-3 east	14.6570	37.6906	65.7139	I-3 east	14.3470	36.3469	63.0353
J-2 east	14.9797	39.1410	68.5706	J-2 east	14.6424	37.6482	65.6510	J-2 east	14.3331	36.3070	62.9752
J-3 east	14.6036	38.0191	66.9230	J-3 east	14.2825	36.5974	64.0746	J-3 east	13.9877	35.3192	61.4695

Table 3.7: Inclination of the Tension Tie, s_1, as Function of θ.

θ=41	α	α	α	θ=42	α	α	α	θ=43	α	α	α
	degrees	degrees	degrees		degrees	degrees	degrees		degrees	degrees	degrees
I-3 west	14.0615	35.1337	60.5800	I-3 west	13.7975	34.0331	58.3280	I-3 west	13.5526	33.0304	56.2598
J-2 west	14.0481	35.0961	60.5226	J-2 west	13.7846	33.9976	58.2732	J-2 west	13.5401	32.9967	56.2075
J-3 west	13.8747	34.6098	59.7759	J-3 west	13.6175	33.5376	57.5606	J-3 west	13.3788	32.5602	55.5274
I-3 east	14.0615	35.1337	60.5800	I-3 east	13.7975	34.0331	58.3280	I-3 east	13.5526	33.0304	56.2598
J-2 east	14.0481	35.0961	60.5226	J-2 east	13.7846	33.9976	58.2732	J-2 east	13.5401	32.9967	56.2075
J-3 east	13.7159	34.1644	59.0857	J-3 east	13.4644	33.1161	56.9023	J-3 east	13.2309	32.1602	54.8995

θ=44	α	α	α	θ=45	α	α	α
	degrees	degrees	degrees		degrees	degrees	degrees
I-3 west	13.3246	32.1129	54.3576	I-3 west	13.1117	31.2703	52.6049
J-2 west	13.3125	32.0809	54.3077	J-2 west	13.1000	31.2397	52.5572
J-3 west	13.1565	31.6657	53.6583	J-3 west	12.9488	30.8438	51.9366
I-3 east	13.3246	32.1129	54.3576	I-3 east	13.1117	31.2703	52.6049
J-2 east	13.3125	32.0809	54.3077	J-2 east	13.1000	31.2397	52.5572
J-3 east	13.0133	31.2850	53.0589	J-3 east	12.8100	30.4806	51.3640

Table 3.8: Calculation of V_{c1}.

$$V_{tie} = V_c + V_s$$

$$V_c = (c_1 + c_2\rho_1) f_c' b_w d$$

$$V_s = \frac{A_{sv}}{s} z f_y (\cot\theta + \cot\alpha)\sin\alpha$$

V_{tie} = shear resistance provided by tension tie

V_c = shear resistance provided by shear transfer mechanisms

V_s = shear resistance provided by stirrup

n=1 θ= 9.0815 [deg]

n>1 θ= [35:45] [deg]

Shear resistance provided by shear transfer mechanisms **[kN]**

$$V_c = (c_1 + c_2\rho_1) f_c' b_w d$$

$$k_1 = \frac{V_{c(1)}}{f_c' b_w d} = (c_1 - c_2\rho_1), k_2 = \frac{V_{c(2)}}{f_c' b_w d} = (c_1 - c_2\rho_1)$$

$$\ldots k_n = \frac{V_{c(n)}}{f_c' b_w d} = (c_1 - c_2\rho_1)$$

$$k_n - k_{n-1} = [c_2(\rho_{1(n)} - \rho_{1(n-1)}] \Rightarrow c_2$$

Apply it on all combinations and obtain min [c2] = c2, then solve for c1

Shear resistance provided by shear transfer mechanisms **[kN]**
[calculate for beams without shear reinforcement]

$$V_{c1} = (0.0276 + 0.012\rho_1) f_c' b_w d$$

min c2=	0.0121
min c1=	0.0276

c2
n=1
0.0312
0.0289
0.0312
0.0289
0.0312
0.0312
0.0289
0.0312
0.0289
0.0312
0.0312
0.0289
0.0312
0.0289
0.0312
0.0312
0.0289
0.0312
0.0312
0.0289
0.0312
0.0289
0.0312
0.0312
0.0289

Table 3.9: Calculation of V_s, ΔV and V_{cl} for Various Values of θ.

Listing of the nominal forces in the stirrup, V_s						[kN]	Vn (test)	$\Delta V = V_n - V_s$		[kN]	$V_{c\,(predicted)} = V_{cl}$
θ	Beam	θ	n=2	n=3	n=4	[kN]	n=2	n=3	n=4	[kN]
35	I-3 west	θ=35	21.9837	27.7600	25.7522	93.4080	71.4243	65.6480	67.6558	65.6464
35	J-2 west	0.6109	22.0292	27.8195	25.8266	96.0768	74.0476	68.2573	70.2502	65.8239
35	J-3 west		52.5248	66.3870	62.2261	138.7776	86.2528	72.3906	76.5515	64.4126
35	I-3 east		0.0000	0.0000	0.0000	74.2816	74.2816	74.2816	74.2816	65.6464
35	J-2 east		0.0000	0.0000	0.0000	68.9440	68.9440	68.9440	68.9440	65.8239
35	J-3 east		36.3158	45.9299	43.4300	109.4208	73.1050	63.4909	65.9908	63.9247
36	I-3 west	θ=36	21.6166	26.9882	25.6401	93.4080	71.7914	66.4198	67.7679	65.6464
36	J-2 west	0.6283	21.6617	27.0458	25.7119	96.0768	74.4151	69.0310	70.3649	65.8239
36	J-3 west		51.6605	64.5371	61.8804	138.7776	87.1171	74.2405	76.8972	64.4126
36	I-3 east		0.0000	0.0000	0.0000	74.2816	74.2816	74.2816	74.2816	65.6464
36	J-2 east		0.0000	0.0000	0.0000	68.9440	68.9440	68.9440	68.9440	65.8239
36	J-3 east		35.7258	44.6486	43.1444	109.4208	73.6950	64.7722	66.2764	63.9247
37	I-3 west	θ=37	21.2836	26.2750	25.4389	93.4080	72.1244	67.1330	67.9691	65.6464
37	J-2 west	0.6458	21.3284	26.3312	25.5083	96.0768	74.7484	69.7456	70.5685	65.8239
37	J-3 west		50.8761	62.8318	61.3310	138.7776	87.9015	75.9458	77.4466	64.4126
37	I-3 east		0.0000	0.0000	0.0000	74.2816	74.2816	74.2816	74.2816	65.6464
37	J-2 east		0.0000	0.0000	0.0000	68.9440	68.9440	68.9440	68.9440	65.8239
37	J-3 east		35.1901	43.4695	42.7237	109.4208	74.2307	65.9513	66.6971	63.9247
38	I-3 west	θ=38	20.9800	25.6174	25.1720	93.4080	72.4280	67.7906	68.2360	65.6464
38	J-2 west	0.6632	21.0245	25.6721	25.2389	96.0768	75.0523	70.4047	70.8379	65.8239
38	J-3 west		50.1607	61.2618	60.6334	138.7776	88.6169	77.5158	78.1442	64.4126
38	I-3 east		0.0000	0.0000	0.0000	74.2816	74.2816	74.2816	74.2816	65.6464
38	J-2 east		0.0000	0.0000	0.0000	68.9440	68.9440	68.9440	68.9440	65.8239
38	J-3 east		34.7013	42.3855	42.2063	109.4208	74.7195	67.0353	67.2145	63.9247

Table 3.10: Calculation of V_s, ΔV and V_{cl} for Various Values of θ.

Listing of the nominal forces in the stirrup, V_s						[kN]	V_n (test)	$\Delta V = V_n - V_s$		[kN]	$V_{c\,(predicted)} = V_{cl}$
θ	Beam	θ	n=2	n=3	n=4	[kN]	n=2	n=3	n=4	[kN]
39	I-3 west	θ=39	20.7021	25.0111	24.8586	93.4080	72.7059	68.3969	68.5494	65.6464
39	J-2 west	0.6807	20.7462	25.0647	24.9234	96.0768	75.3306	71.0121	71.1534	65.8239
39	J-3 west		49.5053	59.8163	59.8338	138.7776	89.2723	78.9613	78.9438	64.4126
39	I-3 east		0.0000	0.0000	0.0000	74.2816	74.2816	74.2816	74.2816	65.6464
39	J-2 east		0.0000	0.0000	0.0000	68.9440	68.9440	68.9440	68.9440	65.8239
39	J-3 east		34.2532	41.3884	41.6237	109.4208	75.1676	68.0324	67.7971	63.9247
40	I-3 west	θ=40	20.4465	24.4519	24.5145	93.4080	72.9615	68.9561	68.8935	65.6464
40	J-2 west	0.6981	20.4903	24.5045	24.5773	96.0768	75.5865	71.5723	71.4995	65.8239
40	J-3 west		48.9023	58.4843	58.9689	138.7776	89.8753	80.2933	79.8087	64.4126
40	I-3 east		0.0000	0.0000	0.0000	74.2816	74.2816	74.2816	74.2816	65.6464
40	J-2 east		0.0000	0.0000	0.0000	68.9440	68.9440	68.9440	68.9440	65.8239
40	J-3 east		33.8409	40.4703	41.0007	109.4208	75.5799	68.9505	68.4201	63.9247
41	I-3 west	θ=41	20.2105	23.9355	24.1521	93.4080	73.1975	69.4725	69.2559	65.6464
41	J-2 west	0.7156	20.2540	23.9871	24.2131	96.0768	75.8228	72.0897	71.8637	65.8239
41	J-3 west		48.3454	57.2549	58.0671	138.7776	90.4322	81.5227	80.7105	64.4126
41	I-3 east		0.0000	0.0000	0.0000	74.2816	74.2816	74.2816	74.2816	65.6464
41	J-2 east		0.0000	0.0000	0.0000	68.9440	68.9440	68.9440	68.9440	65.8239
41	J-3 east		33.4599	39.6234	40.3564	109.4208	75.9609	69.7974	69.0644	63.9247
42	I-3 west	θ=42	19.9919	23.4577	23.7807	93.4080	73.4161	69.9503	69.6273	65.6464
42	J-2 west	0.7330	20.0351	23.5084	23.8399	96.0768	76.0417	72.5684	72.2369	65.8239
42	J-3 west		47.8293	56.1183	57.1498	138.7776	90.9483	82.6593	81.6278	64.4126
42	I-3 east		0.0000	0.0000	0.0000	74.2816	74.2816	74.2816	74.2816	65.6464
42	J-2 east		0.0000	0.0000	0.0000	68.9440	68.9440	68.9440	68.9440	65.8239
42	J-3 east		33.1067	38.8407	39.7050	109.4208	76.3141	70.5801	69.7158	63.9247

Table 3.11: Calculation of V_s, ΔV and V_{cl} for Various Values of θ.

Listing of the nominal forces in the stirrup, V_s					[kN]	Vn (test)	$\Delta V = V_n - V_s$		[kN]	$V_{c\,(predicted)} = V_{cl}$
θ	Beam	θ	n=2	n=3	n=4	[kN]	n=2	n=3	n=4	[kN]
43	I-3 west	θ=43	19.7886	23.0148	23.4072	93.4080	73.6194	70.3932	70.0008	65.6464
43	J-2 west	0.7505	19.8317	23.0648	23.4649	96.0768	76.2451	73.0120	72.6119	65.8239
43	J-3 west		47.3493	55.0650	56.2327	138.7776	91.4283	83.7126	82.5449	64.4126
43	I-3 east		0.0000	0.0000	0.0000	74.2816	74.2816	74.2816	74.2816	65.6464
43	J-2 east		0.0000	0.0000	0.0000	68.9440	68.9440	68.9440	68.9440	65.8239
43	J-3 east		32.7782	38.1156	39.0566	109.4208	76.6426	71.3052	70.3642	63.9247
44	I-3 west	θ=44	19.5991	22.6034	23.0367	93.4080	73.8089	70.8046	70.3713	65.6464
44	J-2 west	0.7679	19.6419	22.6527	23.0931	96.0768	76.4349	73.4241	72.9837	65.8239
44	J-3 west		46.9016	54.0870	55.3271	138.7776	91.8760	84.6906	83.4505	64.4126
44	I-3 east		0.0000	0.0000	0.0000	74.2816	74.2816	74.2816	74.2816	65.6464
44	J-2 east		0.0000	0.0000	0.0000	68.9440	68.9440	68.9440	68.9440	65.8239
44	J-3 east		32.4717	37.4425	38.4188	109.4208	76.9491	71.9783	71.0020	63.9247
45	I-3 west	θ=45	19.4219	22.2205	22.6729	93.4080	73.9861	71.1875	70.7351	65.6464
45	J-2 west	0.7854	19.4645	22.2691	22.7280	96.0768	76.6123	73.8077	73.3488	65.8239
45	J-3 west		46.4828	53.1768	54.4408	138.7776	92.2948	85.6008	84.3368	64.4126
45	I-3 east		0.0000	0.0000	0.0000	74.2816	74.2816	74.2816	74.2816	65.6464
45	J-2 east		0.0000	0.0000	0.0000	68.9440	68.9440	68.9440	68.9440	65.8239
45	J-3 east		32.1848	36.8161	37.7963	109.4208	77.2360	72.6047	71.6245	63.9247

Table 3.12: Listing of $V_n=V_{cl}+V_s$ and $V_{n(test)}$ as a Function of θ.

	$V_{n\,(predicted)} = V_{cl} + V_s$			[kN]	Vn (test)		
θ	Beam	n=2	n=3	n=4	[kN]		
35	I-3 west	87.6301	93.4064	91.3986	93.4080		1.00
35	J-2 west	87.8531	93.6434	91.6505	96.0768		0.98
35	J-3 west	116.9375	130.7997	126.6387	138.7776		0.94
35	I-3 east	65.6464	65.6464	65.6464	74.2816		0.88
35	J-2 east	65.8239	65.8239	65.8239	68.9440		0.95
35	J-3 east	100.2405	109.8546	107.3547	109.4208	***	1.00
36	I-3 west	87.2630	92.6346	91.2865	93.4080		
36	J-2 west	87.4856	92.8698	91.5358	96.0768		
36	J-3 west	116.0732	128.9498	126.2931	138.7776		
36	I-3 east	65.6464	65.6464	65.6464	74.2816		
36	J-2 east	65.8239	65.8239	65.8239	68.9440		
36	J-3 east	99.6505	108.5733	107.0691	109.4208		
37	I-3 west	86.9300	91.9214	91.0853	93.4080		
37	J-2 west	87.1523	92.1551	91.3322	96.0768		
37	J-3 west	115.2888	127.2444	125.7436	138.7776		
37	I-3 east	65.6464	65.6464	65.6464	74.2816		
37	J-2 east	65.8239	65.8239	65.8239	68.9440		
37	J-3 east	99.1148	107.3942	106.6484	109.4208		
38	I-3 west	86.6264	91.2638	90.8183	93.4080		
38	J-2 west	86.8484	91.4961	91.0628	96.0768		
38	J-3 west	114.5734	125.6744	125.0461	138.7776		
38	I-3 east	65.6464	65.6464	65.6464	74.2816		
38	J-2 east	65.8239	65.8239	65.8239	68.9440		
38	J-3 east	98.6259	106.3102	106.1309	109.4208		

*** Note: One value (θ=35°) is slightly above $V_{n(test)}$. The test results showed that θ is around 39°.

Table 3.13: Listing of $V_n=V_{cl}+V_s$ and $V_{n(test)}$ as a Function of θ.

	$V_{n\ (predicted)} = V_{cl} + V_s$			[kN]	Vn (test)
0	Beam	n=2	n=3	n=4	[kN]
39	I-3 west	86.3485	90.6575	90.5050	93.4080
39	J-2 west	86.5701	90.8886	90.7473	96.0768
39	J-3 west	113.9179	124.2290	124.2465	138.7776
39	I-3 east	65.6464	65.6464	65.6464	74.2816
39	J-2 east	65.8239	65.8239	65.8239	68.9440
39	J-3 east	98.1779	105.3131	105.5483	109.4208
40	I-3 west	86.0928	90.0983	90.1609	93.4080
40	J-2 west	86.3142	90.3284	90.4012	96.0768
40	J-3 west	113.3149	122.8969	123.3816	138.7776
40	I-3 east	65.6464	65.6464	65.6464	74.2816
40	J-2 east	65.8239	65.8239	65.8239	68.9440
40	J-3 east	97.7655	104.3950	104.9254	109.4208
41	I-3 west	85.8569	89.5818	89.7985	93.4080
41	J-2 west	86.0779	89.8110	90.0370	96.0768
41	J-3 west	112.7580	121.6676	122.4798	138.7776
41	I-3 east	65.6464	65.6464	65.6464	74.2816
41	J-2 east	65.8239	65.8239	65.8239	68.9440
41	J-3 east	97.3846	103.5481	104.2811	109.4208
42	I-3 west	85.6383	89.1041	89.4271	93.4080
42	J-2 west	85.8591	89.3323	89.6639	96.0768
42	J-3 west	112.2419	120.5309	121.5624	138.7776
42	I-3 east	65.6464	65.6464	65.6464	74.2816
42	J-2 east	65.8239	65.8239	65.8239	68.9440
42	J-3 east	97.0314	102.7653	103.6296	109.4208

Table 3.14: Listing of $V_n=V_{cl}+V_s$ and $V_{n(test)}$ as a Function of θ.

	$V_{n\,(predicted)} = V_{cl} + V_s$			[kN]	Vn (test)
θ	Beam	n=2	n=3	n=4	[kN]
43	I-3 west	85.4350	88.6612	89.0536	93.4080
43	J-2 west	85.6556	88.8887	89.2888	96.0768
43	J-3 west	111.7619	119.4777	120.6453	138.7776
43	I-3 east	65.6464	65.6464	65.6464	74.2816
43	J-2 east	65.8239	65.8239	65.8239	68.9440
43	J-3 east	96.7029	102.0403	102.9813	109.4208
44	I-3 west	85.2455	88.2498	88.6831	93.4080
44	J-2 west	85.4658	88.4766	88.9170	96.0768
44	J-3 west	111.3143	118.4997	119.7397	138.7776
44	I-3 east	65.6464	65.6464	65.6464	74.2816
44	J-2 east	65.8239	65.8239	65.8239	68.9440
44	J-3 east	96.3963	101.3672	102.3434	109.4208
45	I-3 west	85.0683	87.8669	88.3193	93.4080
45	J-2 west	85.2884	88.0930	88.5519	96.0768
45	J-3 west	110.8955	117.5894	118.8534	138.7776
45	I-3 east	65.6464	65.6464	65.6464	74.2816
45	J-2 east	65.8239	65.8239	65.8239	68.9440
45	J-3 east	96.1095	100.7408	101.7210	109.4208

Table 3.15: Analysis Results.

The test results in the of Table 3.12-3.14 show that it is not conservative to predict 100% of the shear resistance provided by shear transfer mechanisms for beams with shear reinforcement.

Test results showed that the angle between the axis of the member and the compression strut is approximately 39^{o}.

$$\Rightarrow V_{c1} = \left(0.0276 + 0.0121\rho_1\right) f_c' b_w d$$

$$\Rightarrow V_{c2} = V_{c1} + V_s$$

$$\Leftrightarrow V_{c2} = V_{c1} + \left(\frac{A_{sw}}{s}\right) f_y\, 0.9d \cot\theta$$

V_{c1} = shear resistance provided by shear transfer mechanisms used for beams without shear reinforcement

V_{c2} = shear resistance provided by shear transfer mechanisms used for beams with shear reinforcement

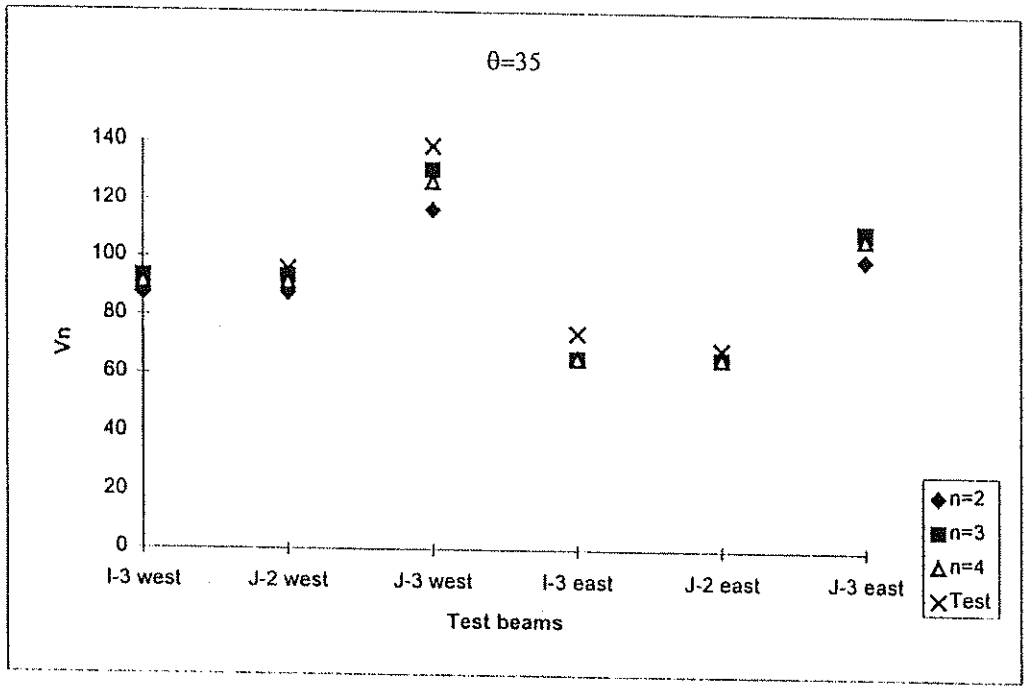

Fig. 3.11: Predicted Nominal Shear Capacity of 3 Truss Models vs. Test Results.

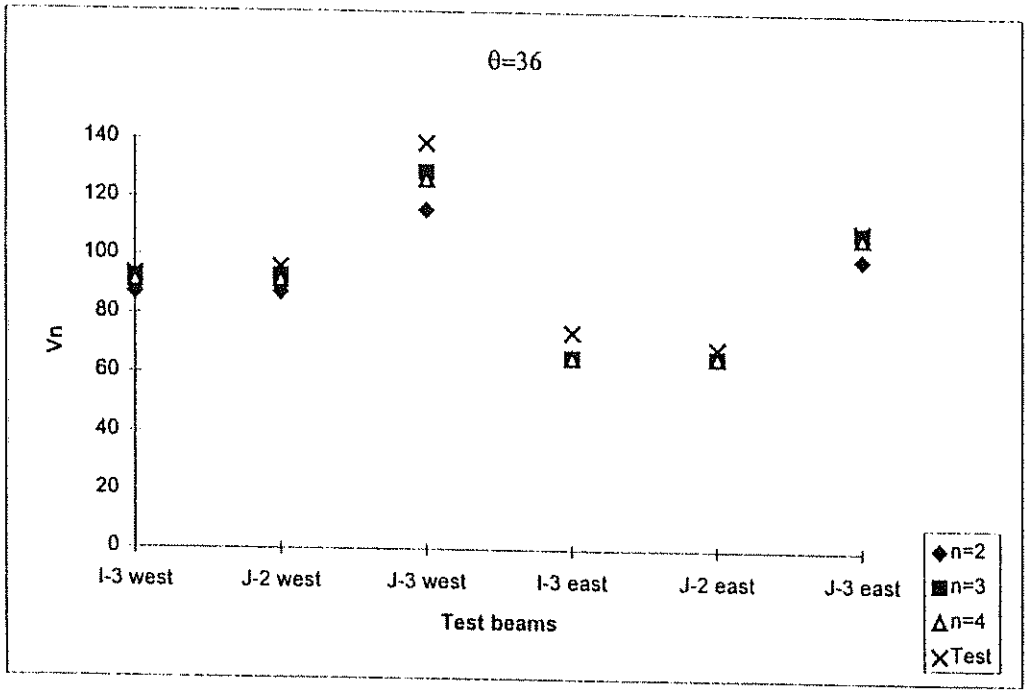

Fig.3.12: Predicted Nominal Shear Capacity of 3 Truss Models vs. Test Results.

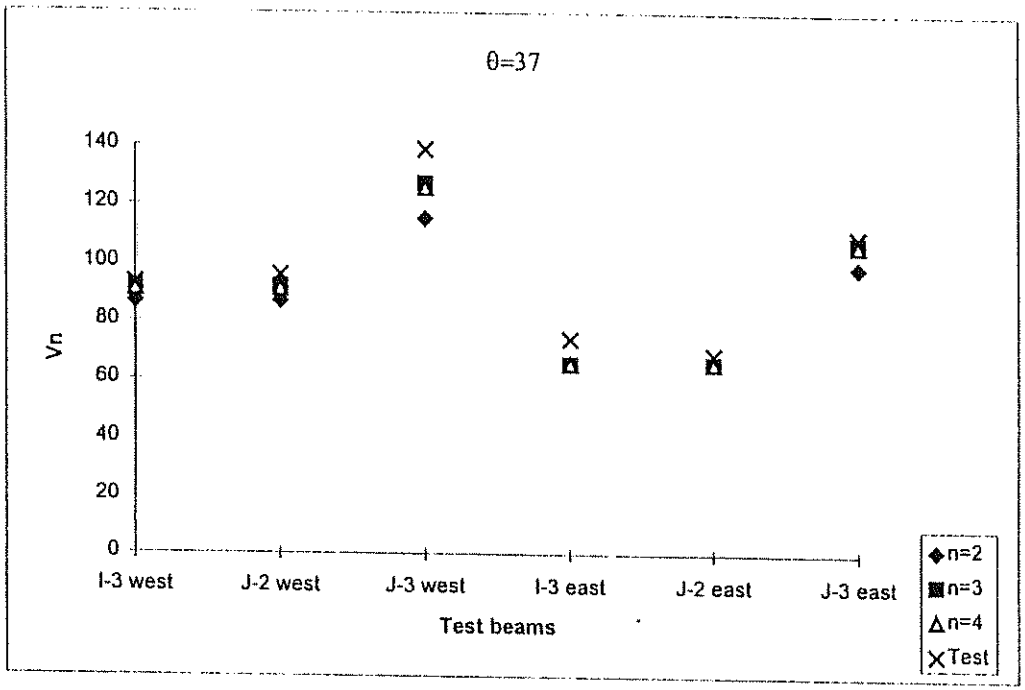

Fig. 3.13: Predicted Nominal Shear Capacity of 3 Truss Models vs. Test Results.

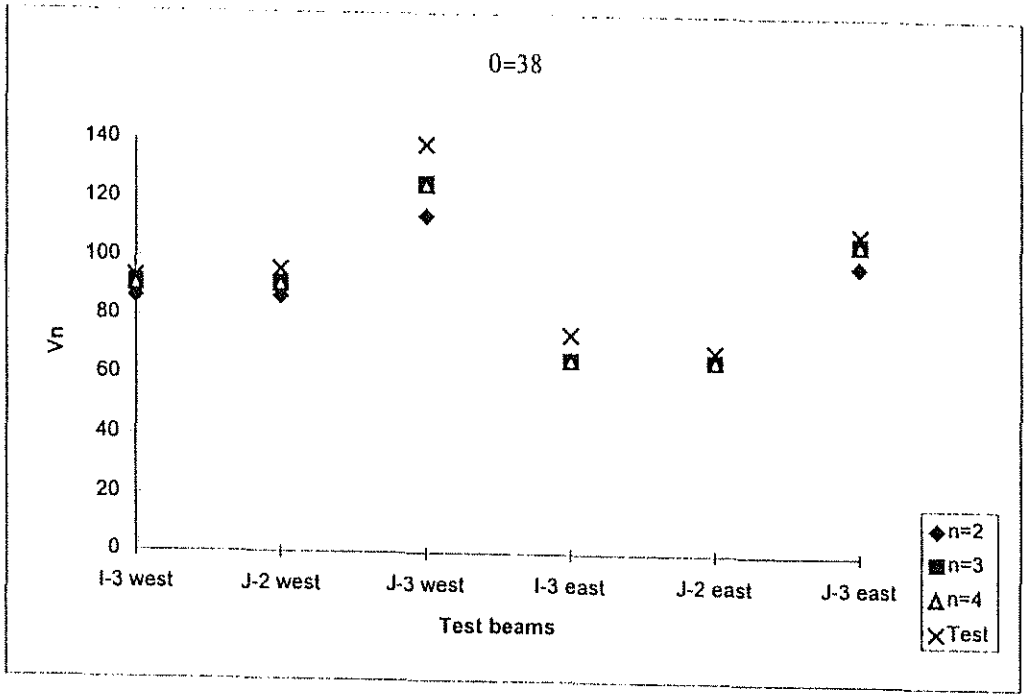

Fig. 3.14: Predicted Nominal Shear Capacity of 3 Truss Models vs. Test Results.

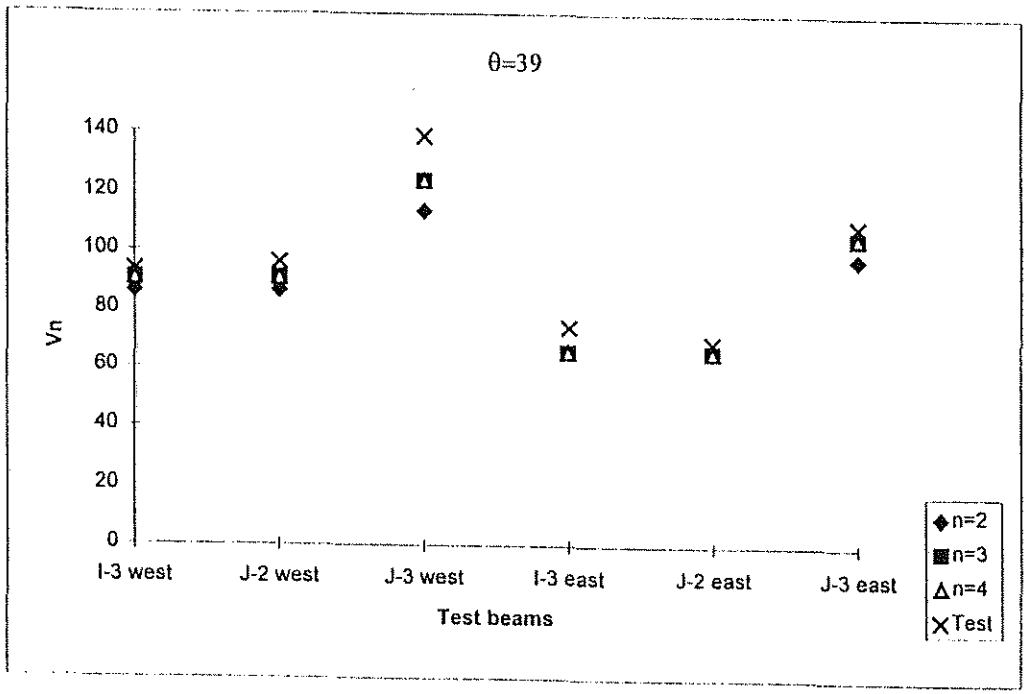

Fig. 3.15: Predicted Nominal Shear Capacity of 3 Truss Models vs. Test Results.

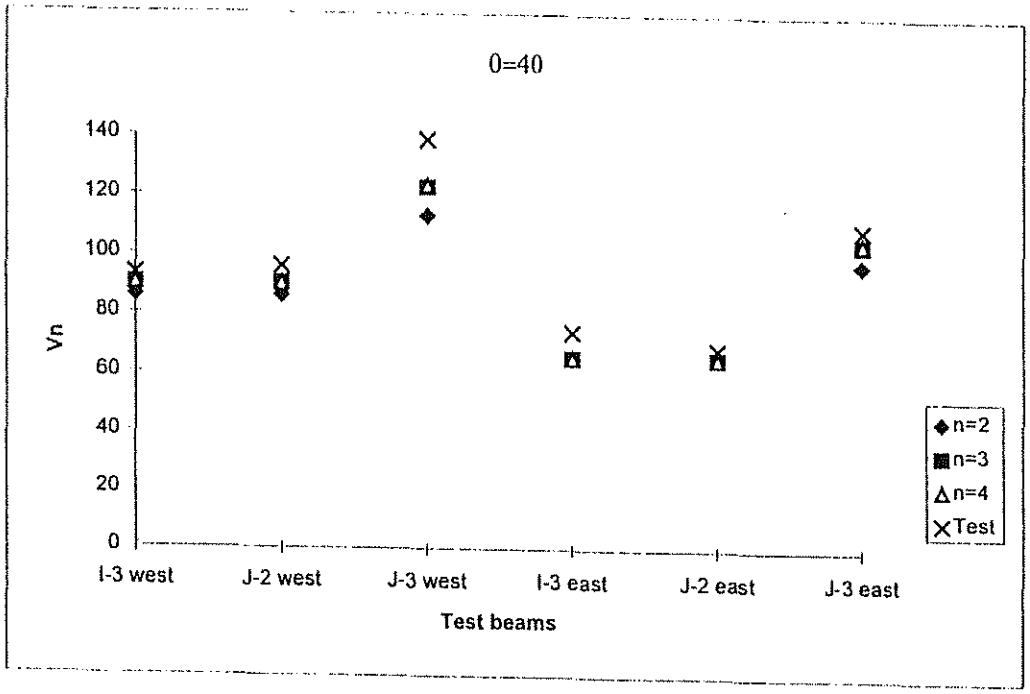

Fig.3.16: Predicted Nominal Shear Capacity of 3 Truss Models vs. Test Results.

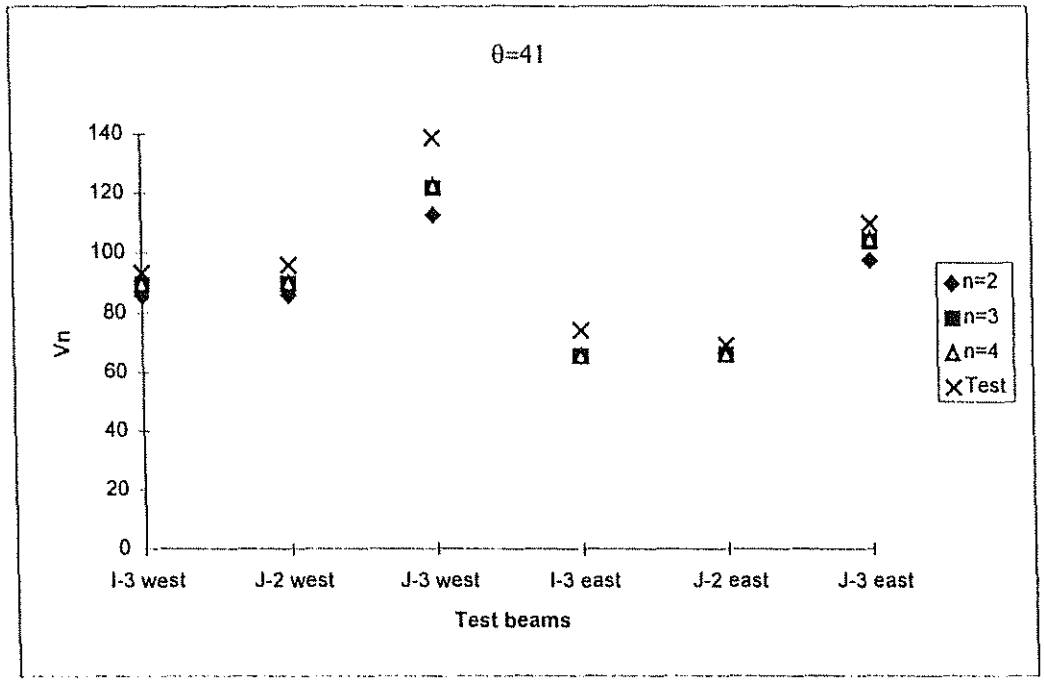

Fig. 3.17: Predicted Nominal Shear Capacity of 3 Truss Models vs. Test Results.

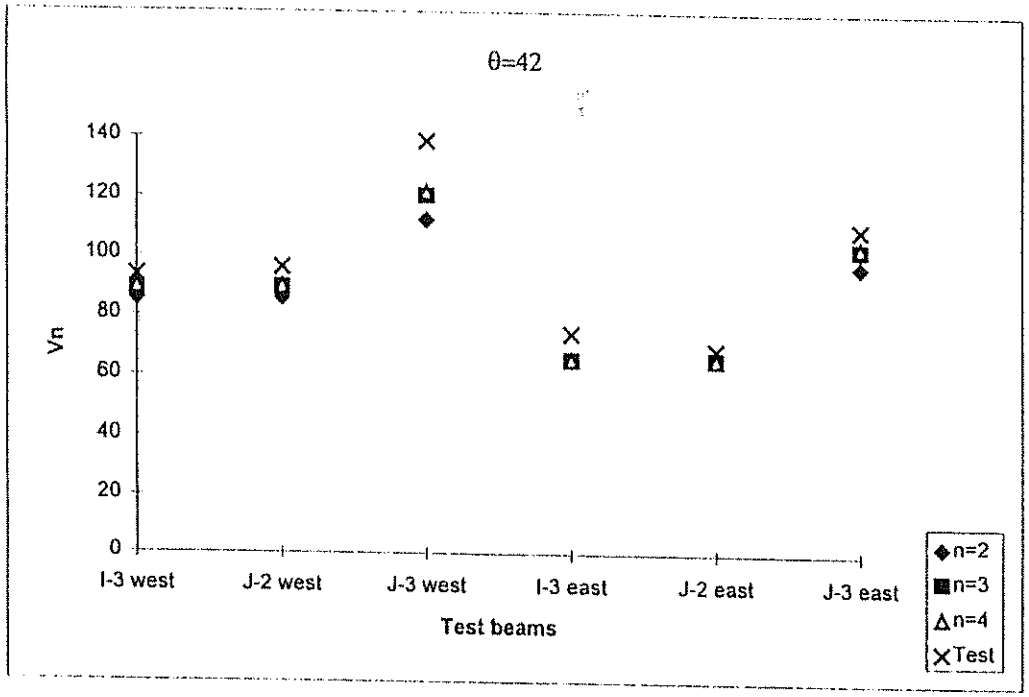

Fig. 3.18: Predicted Nominal Shear Capacity of 3 Truss Models vs. Test Results.

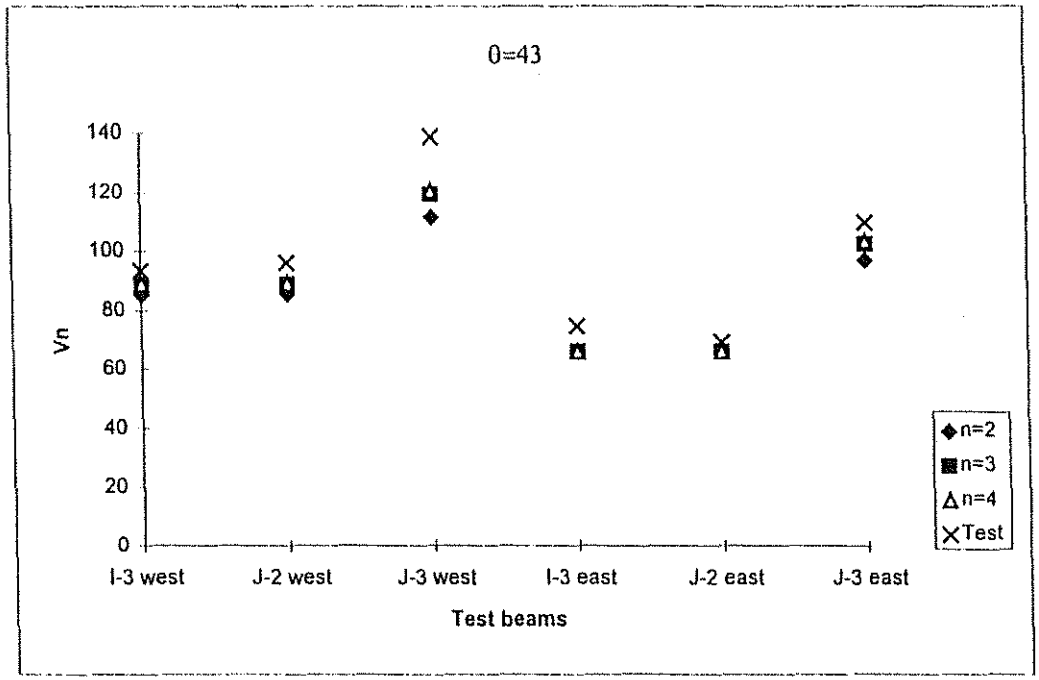

Fig. 3.19: Predicted Nominal Shear Capacity of 3 Truss Models vs. Test Results.

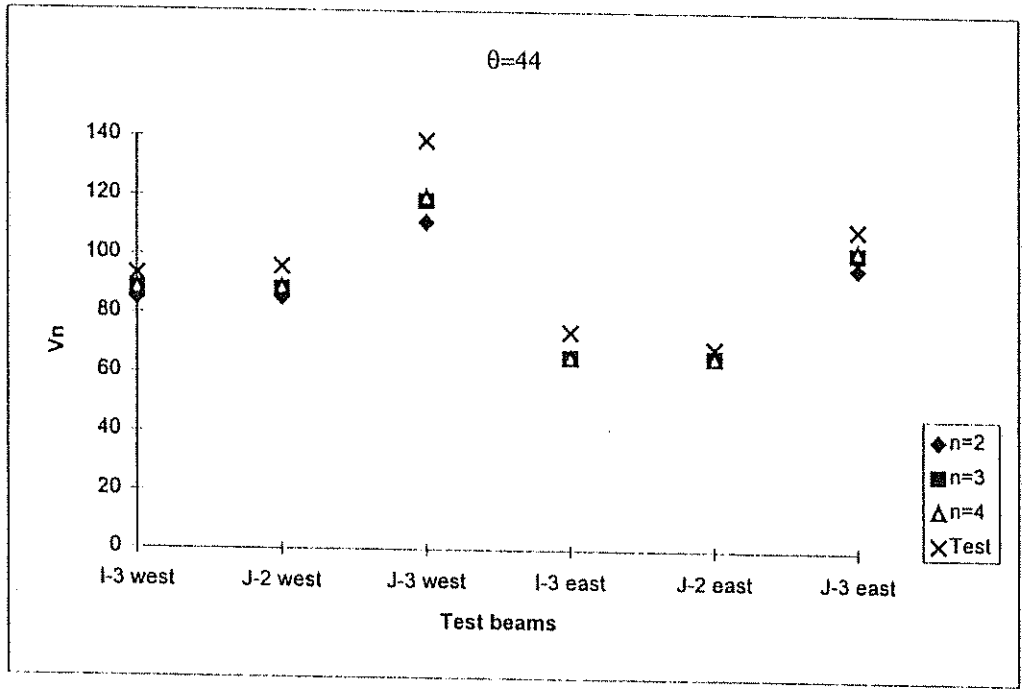

Fig. 3.20: Predicted Nominal Shear Capacity of 3 Truss Models vs. Test Results.

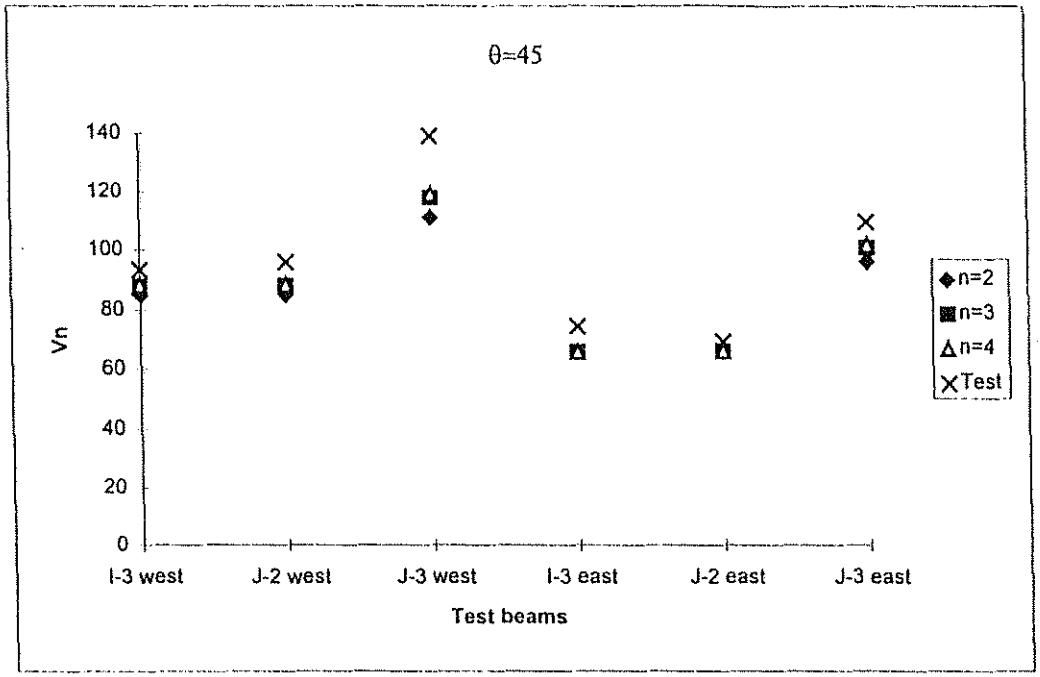

Fig. 3.21: Predicted Nominal Shear Capacity of 3 Truss Models vs. Test Results.

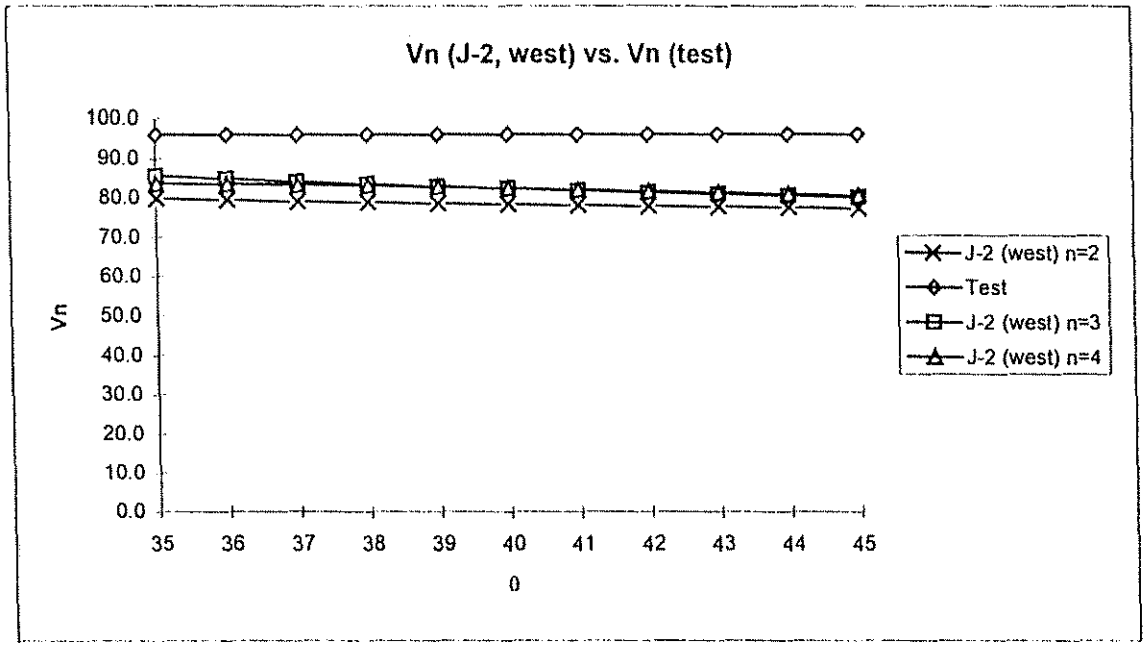

Fig. 3.22: Predicted Nominal Shear Capacity of 3 Truss Models vs. Test Results.

CHAPTER 4
Analysis and Evaluation

4.1 Introduction

It has been shown in Chapter 2 where the various building code shear prediction methods were discussed, that there are significant difference between the ACI empirical approach and other methods available elsewhere. These other methods are rational in nature. That is, they are based on concepts of equilibrium and material performance that together are used to formulate an analysis model that can be used to predict capacity. This approach forms the basis for the EC 2, CEB MC 90, DIN 1045 and the AASHTO/MCFT methods.

The question remains as to how well these various methods perform in actual application. Accordingly, this chapter will address the performance of these methods. The four building code methods; ACI, EC 2, CEB MC 90 and AASHTO/MCFT; plus the approach developed in this study will be employed to evaluate the performance of "typical" reinforced concrete members. One set will be simple and fixed ended rectangular beams under point and distributed loading. Moreover, two levels of flexural reinforcement at 0.75% and 1.0% will be used. These correspond to the lightly reinforced systems tested by Pasley. This "calibration" will be used to ascertain how closely these methods agree. The second larger analysis group will be for the reevaluation of the Pasley data. Here all the methods will be employed to determine the capacities of the various test configurations and then the results will be compared to the experimental data.

While this comparison is not all inclusive, it will show how these other approaches taken to shear predictions available in North America and Europe perform when applied to typical US flexural systems. Moreover, the application of strut an tie analysis also will be evaluated both for accuracy and ease of application.

It has been shown in Chapter 2 where various European and North American shear provisions and experimental investigations were discussed that these are significant differences between the ACI 318 and European approaches for shear design. In Chapter 3 various Strut and Tie Models were applied and the limit states were determined by a comparison with the beam failure loads of Pasley's report (21). In this Chapter examples were calculated to compare ACI 318-95, EC 2, CEB, and the achieved shear equation of Chapter 3 based on the Pasley report (21).

4.2 Sample Beam Evaluation of Rectangular Simple and Fixed End Systems

For this comparison rectangular beams with different support and loading conditions were analyzed. Beam 1 was simply supported and Beam 2 was fixed at both ends. The first loading condition was a point load, P, at the centerline of the beam and the second loading condition was a linear distributed load, p, which was constant over the total length of the beam. The length was 8 m with an effective depth, d, of 500 mm and a width, b, of 200 mm. The compressive strength, f_c', was assumed to be 30 MPa and the steel yield strength, f_y, was 420 MPa. The shear reinforcement corresponded to the Pasley test with a ρ_v of 0.08%.

The beam set up and configuration is shown in Fig. 4.1. The results of these calculations can be seen in Tables 4.1 through 4.4 and results are graphically depicted in Figs. 4.2 through 4.4.

Review of the data reveals that the effects of end condition is not significant for any of the analysis methods except for ACI. Here there is a decease in shear capacity of approximately 10% when the ends are fixed as compared to simple supports. There should be some decease due to loss of bond capacity and the ACI equations do predict this trend. For purposes of comparison, only the simple supported results will be discussed.

The first comparisons is for beams without shear reinforcement. In Fig. 4.2, it can be seen that the capacities are only slightly increased by increasing reinforcement ratio. Moreover, the ACI prediction is close to that from Hofer/McCabe while the CEB prediction is 25% higher and the EC 2 is 25% lower. This range of predictions is large. The results obtained from the EC 2 are safe and it is possible that a reduction factor is already included in the design equations considering flexural reinforcement ratio, ρ_w, cross section, k, and an efficiency factor, ν. The CEB Code, a model Code and the basis of the EC 2, is unconservative in regions of low longitudinal reinforcement ratios. Instead of using variables depending on flexural reinforcement ratio, cross section and efficiency factor in the equations to calculate the capacity of the compression strut and tension tie, as in the EC 2, the CEB Code equations include

constants which are for all cases an upper limit for the EC 2 shear equations for beams without shear reinforcement.

The next set of comparisons is found in Fig. 4.3 and is for beams with shear reinforcement where the capacity of the concrete, V_n, is predicted using standard, simplified methods. Here the EC 2 and Hofer/McCabe predictions are within 5% of each other. The predicted shear capacity of ACI 318-95 is nearly 25% higher than the Hofer/McCabe prediction. Once again, however, the CEB predicted capacity is higher, this time by approximately 40%. This discrepancy in CEB results is questionable and the comparison showed that the CEB Code may not be useful for beams with low flexural reinforcement ratios without special factors.

The last comparison is based on the four shear capacity prediction methods using the detailed procedures found in these codes. The results also show that the ACI and Hofer/McCabe methods are within 10% of each other. Once again the CEB prediction is significantly higher than the ACI prediction while the EC 2 capacity is about 30% of the ACI values. The wide range in capacities is caused by different assumptions. The ACI 318-95 assumes that the shear capacity consists of the capacity of shear reinforcement and of an uncracked concrete capacity. The CEB Code assumes also two capacities, based on a variable inclination of the compression strut, with the difference that the concrete contribution is variable and equal to zero in regions where the shear forces are high. The EC 2 occurs conservative in this comparison. It is assumed that the shear capacity of the tension tie, based on a

variable inclination of the compression strut, is given by the capacity of the shear reinforcement itself. Therefore, for low flexural reinforcement ratios the capacity of the tension tie is significant small.

The results of this comparison show that even with simple straightforward RC sections there is a spread in the predicted shear strengths. The strut and tie model developed for this study closely predicts the shear capacities of these sections and compares quite favorably with ACI across the range of problems and with EC 2. The high values predicted by CEB are somewhat unexpected but do point out the variation in predictions that can occur with shear.

4.3 Pasley Data Reevaluation Using Shear Provisions of Different Building Codes

The reevaluation of the Pasley test data is the subject of this section. The data obtained by test will be compared to the predicted capacities from ACI, EC 2, CEB MC 90 and AASHTO/MCFT. In all cases there are simple and detailed procedures that will be applied and the results compared to the test values. Examples of the procedures utilized in the calculation of the shear capacities are presented in Tables 4.16 to 4.19. In these tables, it can be seen that the calculations are detailed and represent significant amounts of calculation in comparison to that required by the ACI Building Code. The question, therefore, is whether or not this additional amount of effort provides the engineer with improved levels of accuracy.

The results of the analyses of the Pasley beams using the four building codes analyses, ACI, EC 2, CEB MC 90 and AASHTO/MCFT, plus the Hofer/McCabe equation is found in Tables 4.8 to 4.15. A summary of the results is found in Table 4.16 and 4.17. In addition these results also are plotted in Figs. 4.5 to 4.13.

It can be seen from the results that once again there is a spread in the predicted shear capacities as predicted by the various code expressions. If the results are examined, there are trends in the data. In the first set of plots, Figs. 4.5 and 4.6, the ACI results for the east and west spans are found. Here selected results are plotted for tests I-1 and 2 and J-1, 2 and 3. The test differences are discussed in Appendix A and refer to the amount of longitudinal and shear steel in each test. For each test, three points are plotted, the ACI standard method, ACI detailed and the test results. It can be seen here that the ACI predictions are generally conservative and within 10% of the test values. However, there are cases where the ACI predictions are greater than the test values, and in some cases the error is 5%.

The EC 2 results are found in Figs. 4.7 and 4.8. Here it can be seen that the standard method generally predicts shear capacities that are 25% lower than the test data. In the case of the detailed method, however, the predictions become unrealistic in most cases. The predicted capacities are less than one-half the value obtained by test. It also is interesting to note that the predicted shear capacity for the systems without shear reinforcement lies at nearly a constant value for all the cases, while the detailed method actually produces a total shear capacity that is lower with steel than

without. This rather unexpected result is caused by the formulation of the equations and the role of the uncracked concrete in the overall section capacity. In short, the engineer must be aware that the detailed equation may not produce "better" results than the standard method.

The CEB MC 90 predictions are actually quite consistent and produce results that are similar to the experimental data, although the values are higher than the experimental data by about 15%. The detailed method also produced results that are close to the standard method, but slightly higher than those obtained by the standard method, as would be expected for a more complex method. Another observation is that the angle of inclination of the compression strut is approximately 40° and this value matches observations at the time of testing.

The summary of the analysis of the experimental results using the building code expressions reveals that the methods that are available in Europe generally require more effort than the ACI procedures to produce a design. In addition the predicted strengths using the standard methods produce values that are generally conservative by a larger amount than does the ACI expressions. In some cases both the ACI and the CEB equations produce capacity predictions that are unconservative. It is interesting to note that the ACI predictions are generally right on top of the data points or slightly above or below. The EC 2 and CEB equations produce results that are clearly conservative, in general, and different than the test points indicating that the code expressions already have a reduction factor or some form of adjustment

factor within the equation to produce conservative results. It is apparent that an engineer using the EC 2 or CEB expressions must be aware of the applicability of the equations being used and the limitations that the analysis has. Moreover, it must not be assumed that detailed procedures will produce results that are more economical than the standard methods.

Comparison of the Sample Beams and Pasley Data to the Prediction of Shear Capacity by ACI, EC 2, CEB and Hofer/McCabe Equation

Two Problems Evaluated

I. Example of a Rectangular Cross Section

II. Pasley Data from (21)

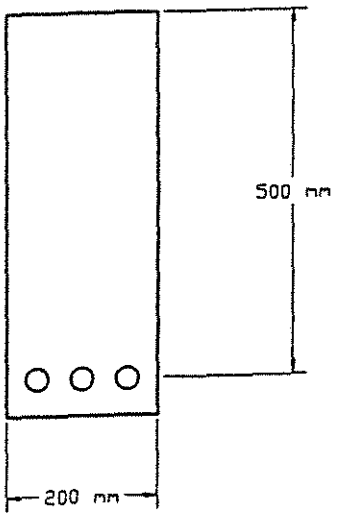

$f_c' = 30$ MPa

$f_y = 420$ MPa

$\rho_w = 0.75$ %

$\rho_w = 1.00$ %

$\rho_v = 0.08$ %

LOADING

(a) Uniformly Distributed Load (p)

(b) Point Load (P)

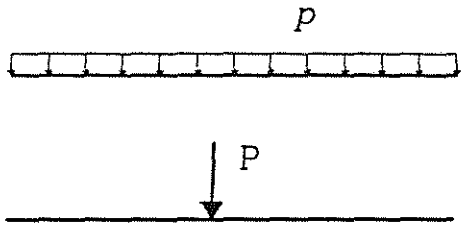

BEAM END CONDITIONS

(a) Simply Supported Beam

(b) Fixed End Beam

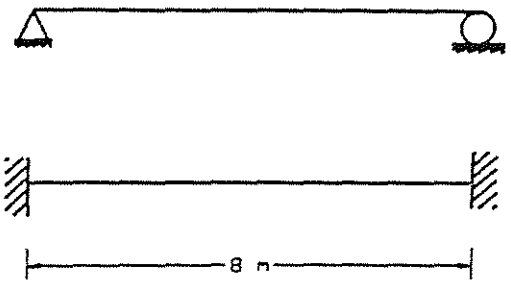

Fig. 4.1 Example: Rectangular Beam.

Table 4.1 Sample Beams - Allowable load based on shear capacity using ACI 318-92 rules at d off support

Simply supported

Load	Beam	A_s	ρ_w	ρ_v	Without ShearReinf. V_u	V_n	With Shear Reinf. V_u	M_u	With Shear Reinf. $V_{n(std)}$	$V_{n(detailed)}$	$P_{n(no)}$	$P_{n(reinf.)}$
		[mm^2]	[-]	[-]	[kN]	[kN]	[kN]	[kNm]	[kN]	[kN]	[kN]	[kN]
Poi nt	1	750.000	0.0075	0.0008	91.2871	91.2871	124.0000	62.0000	124.8871	124.7032	182.6	248.0
Point	1	1000.000	0.0100	0.0008	91.2871	91.2871	124.0000	62.0000	124.8871	128.9889	182.6	248.0

Load	Beam	A_s	ρ_w	ρ_v	Without ShearReinf. V_u	V_n	With Shear Reinf. V_u	M_u	With Shear Reinf. $V_{n(std)}$	$V_{n(detailed)}$	$p_{n(no)}$	$p_{n(reinf.)}$
		[mm^2]	[-]	[-]	[kN]	[kN]	[kN]	[kNm]	[kN]	[kN]	[kN/m]	[kN/m]
Linear	1	750.000	0.0075	0.0008	91.2871	91.2871	123.2000	66.0000	124.8871	123.8461	26.1	35.2
Linear	1	1000.000	0.0100	0.0008	91.2871	91.2871	124.6000	66.7500	124.8871	127.8461	26.1	35.6

Fixed end system

Load	Beam	A_s	ρ_w	ρ_v	Without ShearReinf. V_u	V_n	With Shear Reinf. V_u	M_u	With Shear Reinf. $V_{n(std)}$	$V_{n(detailed)}$	$P_{n(no)}$	$P_{n(reinf.)}$
		[mm^2]	[-]	[-]	[kN]	[kN]	[kN]	[kNm]	[kN]	[kN]	[kN]	[kN]
Point	1	750.000	0.0075	0.0008	91.2871	91.2871	115.0000	172.5000	124.8871	116.1318	182.6	230.0
Point	1	1000.000	0.0100	0.0008	91.2871	91.2871	117.5000	176.2500	124.8871	117.5604	182.6	235.0

Load	Beam	A_s	ρ_w	ρ_v	Without ShearReinf. V_u	V_n	With Shear Reinf. V_u	M_u	With Shear Reinf. $V_{n(std)}$	$V_{n(detailed)}$	$p_{n(no)}$	$p_{n(reinf.)}$
		[mm^2]	[-]	[-]	[kN]	[kN]	[kN]	[kNm]	[kN]	[kN]	[kN/m]	[kN/m]
Linear	2	750.000	0.0075	0.0008	91.2871	91.2871	114.4500	242.6613	124.8871	114.8781	26.1	32.7
Linear	2	1000.000	0.0100	0.0008	91.2871	91.2871	115.5000	246.1250	124.8871	115.8684	26.1	33.0

Table 4.2 Sample Beams - Allowable load based on shear capacity using EC 2 rules at d off support

Simply supported

Load	Beam	ρ_l	V_u	Without ShearReinf.		With Shear Reinf.			With Shear Reinf.		$P_{n(no)}$	$P_{n(reinf.)}$
				V_{r1}	V_{r2}	V_u	$V_{r2(std)}$	$V_{r3(std)}$	$V_{r2(detailed)}$	$V_{r3(detailed)}$		
		[-]	[kN]	[kN]	[kN]	[kN]	[kN]	[kN]	[kN]	[kN]	[kN]	[kN]
Point	1	0.0075	55.7570	55.7570	825.0000	85.9970	825.0000	85.9970	806.9718	37.3433	111.5	172.0
Point	1	0.0100	59.4741	59.4741	825.0000	89.7141	825.0000	89.7141	806.9718	37.3433	118.9	179.4

Load	Beam	ρ_l	V_u	Without ShearReinf.		With Shear Reinf.			With Shear Reinf.		$p_{n(no)}$	$p_{n(reinf.)}$
				V_{r1}	V_{r2}	V_u	$V_{r2(std)}$	$V_{r3(std)}$	$V_{r2(detailed)}$	$V_{r3(detailed)}$		
		[-]	[kN]	[kN]	[kN]	[kN]	[kN]	[kN]	[kN]	[kN]	[kN/m]	[kN/m]
Linear	1	0.0075	27.8785	55.7570	825.0000	42.9985	825.0000	85.9970	806.9718	37.3433	15.9	24.6
Linear	1	0.0100	29.7371	59.4741	825.0000	44.8571	825.0000	89.7141	806.9718	37.3433	17.0	25.6

Fixed end system

Load	Beam	ρ_l	V_u	Without ShearReinf.		With Shear Reinf.			With Shear Reinf.		$P_{n(no)}$	$P_{n(reinf.)}$
				V_{r1}	V_{r2}	V_u	$V_{r2(std)}$	$V_{r3(std)}$	$V_{r2(detailed)}$	$V_{r3(detailed)}$		
		[-]	[kN]	[kN]	[kN]	[kN]	[kN]	[kN]	[kN]	[kN]	[kN]	[kN]
Point	2	0.0075	55.7570	55.7570	825.0000	85.9970	825.0000	85.9970	806.9718	37.3433	111.5	172.0
Point	2	0.0100	59.4741	59.4741	825.0000	89.7141	825.0000	89.7141	806.9718	37.3433	118.9	179.4

Load	Beam	ρ_l	V_u	Without ShearReinf.		With Shear Reinf.			With Shear Reinf.		$p_{n(no)}$	$p_{n(reinf.)}$
				V_{r1}	V_{r2}	V_u	$V_{r2(std)}$	$V_{r3(std)}$	$V_{r2(detailed)}$	$V_{r3(detailed)}$		
		[-]	[kN]	[kN]	[kN]	[kN]	[kN]	[kN]	[kN]	[kN]	[kN/m]	[kN/m]
Linear	2	0.0075	55.7570	55.7570	825.0000	85.9970	825.0000	85.9970	806.9718	37.3433	15.9	24.6
Linear	2	0.0100	59.4741	59.4741	825.0000	89.7141	825.0000	89.7141	806.9718	37.3433	17.0	25.6

Table 4.3 Sample Beams - Allowable load based on shear capacity using CEB Code rules at d off support

Simply supported

Load	Beam	V_u	Without Shear Reinf. V_{r1}	V_{r2}	V_u	With Shear Reinf. $V_{r2(std)}$	$V_{r3(std)}$	With Shear Reinf. $V_{r2(detailed)}$	$V_{r3(detailed)}$	0	$P_{n(no)}$	$P_{n(reinf.)}$
		[kN]	[kN]	[kN]	[kN]	[kN]	[kN]	[kN]	[kN]	[grad]	[kN]	[kN]
Point	1	123.5050	123.5050	900.0000	153.7450	900.0000	153.7450	886.3270	159.5436	40.0000	247.0	307.5
Point	1	123.5050	123.5050	900.0000	153.7450	900.0000	153.7450	886.3270	159.5436	40.0000	247.0	307.5

Load	Beam	V_u	Without Shear Reinf. V_{r1}	V_{r2}	V_u	With Shear Reinf. $V_{r2(std)}$	$V_{r3(std)}$	With Shear Reinf. $V_{r2(detailed)}$	$V_{r3(detailed)}$	0	$P_{n(no)}$	$P_{n(reinf.)}$
		[kN]	[kN]	[kN]	[kN]	[kN]	[kN]	[kN]	[kN]	[grad]	[kN/m]	[kN/m]
Linear	1	61.7525	123.5050	900.0000	76.8725	900.0000	153.7450	886.3270	159.5436	40.0000	35.3	43.9
Linear	1	61.7525	123.5050	900.0000	76.8725	900.0000	153.7450	886.3270	159.5436	40.0000	35.3	43.9

Fixed end system

Load	Beam	V_u	Without Shear Reinf. V_{r1}	V_{r2}	V_u	With Shear Reinf. $V_{r2(std)}$	$V_{r3(std)}$	With Shear Reinf. $V_{r2(detailed)}$	$V_{r3(detailed)}$	θ	$P_{n(no)}$	$P_{n(reinf.)}$
		[kN]	[kN]	[kN]	[kN]	[kN]	[kN]	[kN]	[kN]	[grad]	[kN]	[kN]
Point	1	123.5050	123.5050	900.0000	153.7450	900.0000	153.7450	886.3270	159.5436	40.0000	247.0	307.5
Point	1	123.5050	123.5050	900.0000	153.7450	900.0000	153.7450	886.3270	159.5436	40.0000	247.0	307.5

Load	Beam	V_u	Without Shear Reinf. V_{r1}	V_{r2}	V_u	With Shear Reinf. $V_{r2(std)}$	$V_{r3(std)}$	With Shear Reinf. $V_{r2(detailed)}$	$V_{r3(detailed)}$	θ	$P_{n(no)}$	$P_{n(reinf.)}$
		[kN]	[kN]	[kN]	[kN]	[kN]	[kN]	[kN]	[kN]	[grad]	[kN/m]	[kN/m]
Linear	1	123.5050	123.5050	900.0000	153.7450	900.0000	153.7450	886.3270	159.5436	40.0000	35.3	43.9
Linear	1	123.5050	123.5050	900.0000	153.7450	900.0000	153.7450	886.3270	159.5436	40.0000	35.3	43.9

Table 4.4 Sample Beams - Allowable load based on shear capacity using Hofer/McCabe rules at d off support

Simply supported

Load	Beam	ρ_w	V_u	Without ShearReinf. $V_{(tension)}$	Without ShearReinf. $V_{(comp.)}$	V_u	With Shear Reinf. $V_{(tension)}$	With Shear Reinf. $V_{(comp.)}$	$P_{n(no)}$	$P_{n(reinf.)}$
		[-]	[kN]	[kN]	[kN]	[kN]	[kN]	[kN]	[kN]	[kN]
Point	1	0.0075	83.0723	83.0723		97.8618	97.8618		166.1	195.7
Point	1	0.0100	83.1630	83.1630		97.9526	97.9526		166.3	195.9

Load	Beam	ρ_w	V_u	Without ShearReinf. $V_{(tension)}$	Without ShearReinf. $V_{(comp.)}$	V_u	With Shear Reinf. $V_{(tension)}$	With Shear Reinf. $V_{(comp.)}$	$p_{n(no)}$	$p_{n(reinf.)}$
		[-]	[kN]	[kN]	[kN]	[kN]	[kN]	[kN]	[kN/m]	[kN/m]
Linear	1	0.0075	41.5361	83.0723		48.9309	97.8618		23.7	28.0
Linear	1	0.0100	41.5815	83.1630		48.9763	97.9526		23.8	28.0

Fixed end system

Load	Beam	ρ_w	V_u	Without ShearReinf. $V_{(tension)}$	Without ShearReinf. $V_{(comp.)}$	V_u	With Shear Reinf. $V_{(tension)}$	With Shear Reinf. $V_{(comp.)}$	$P_{n(no)}$	$P_{n(reinf.)}$
		[-]	[kN]	[kN]	[kN]	[kN]	[kN]	[kN]	[kN]	[kN]
Point	1	0.0075	83.0723	83.0723		97.8618	97.8618		166.1	195.7
Point	1	0.0100	83.1630	83.1630		97.9526	97.9526		166.3	195.9

Load	Beam	ρ_w	V_u	Without Shear Reinf. $V_{(tension)}$	Without Shear Reinf. $V_{(comp.)}$	V_u	With Shear Reinf. $V_{(tension)}$	With Shear Reinf. $V_{(comp.)}$	$p_{n(no)}$	$p_{n(reinf.)}$
		[-]	[kN]	[kN]	[kN]	[kN]	[kN]	[kN]	[kN/m]	[kN/m]
Linear	1	0.0075	83.0723	83.0723		97.8618	97.8618		23.7	28.0
Linear	1	0.0100	83.1630	83.1630		97.9526	97.9526		23.8	28.0

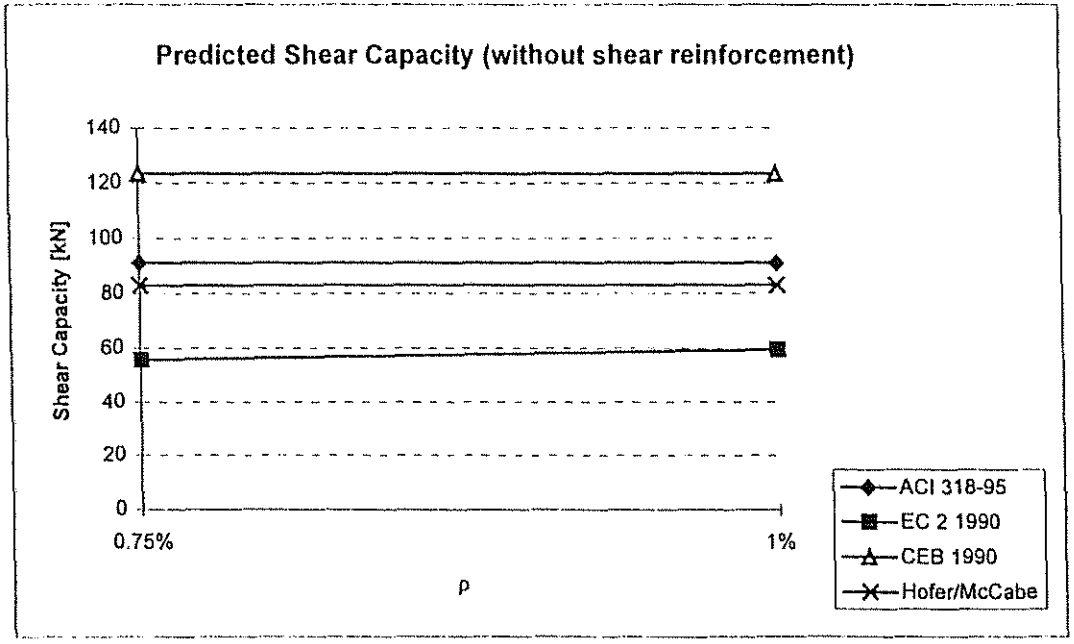

Fig. 4.2 Predicted shear capacity, V_n, for beams without shear reinforcement.

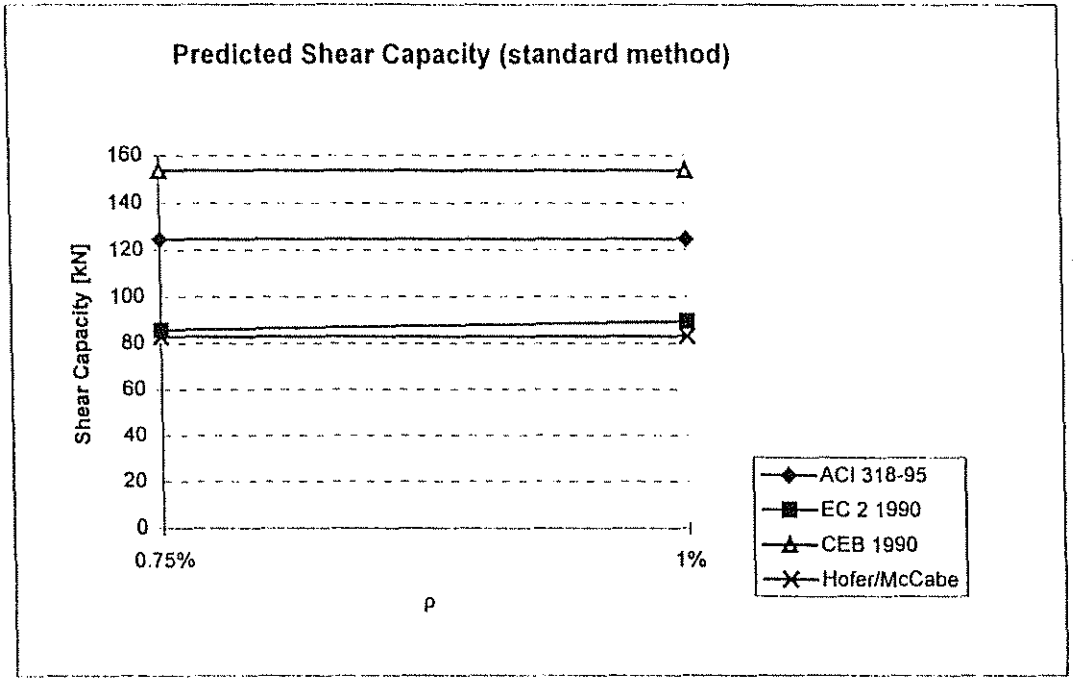

Fig. 4.3 Predicted shear capacity, V_n, for beams with shear reinforcement using standard method.

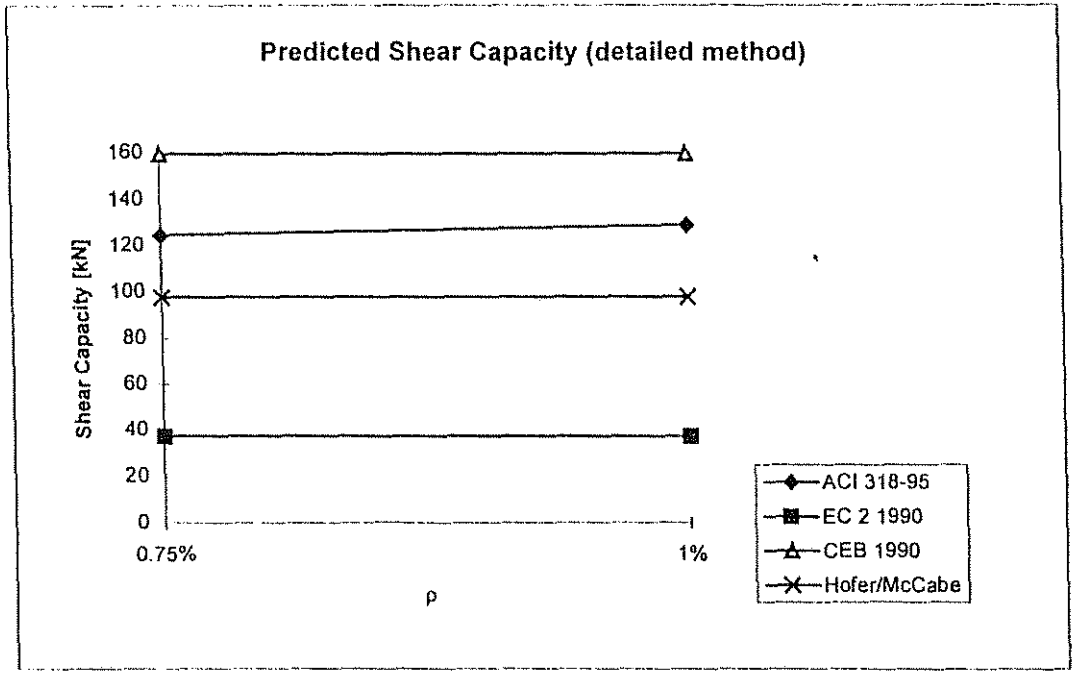

Fig. 4.4 Predicted shear capacity, V_n, for beams with shear reinforcement using detailed method.

Table 4.5: Measured Shear Strength by SM Report #26.

Load	Failure region	Pos/Neg	Beam	V_n(test) [kN]	v_n(test) [MPa]
1	east	negative	I-1	68.0544	0.9032
1	west	negative	I-1	66.2752	0.8826
1	east	negative	I-2	104.5280	1.3583
2	east	negative	I-3	74.2816	0.9653
2	west	negative	I-3	93.4080	1.2135
1	east	positive	J-1	53.3760	0.6895
1	west	negative	J-1	66.7200	0.8895
1	west	positive	J-1	64.4960	0.8343
1	east	negative	J-1	66.2752	0.8826
2	east	negative	J-2	68.9440	0.8964
2	west	negative	J-2	96.0768	1.2480
2	east	negative	J-3	109.4208	1.4342
2	west	negative	J-3	138.7776	1.8341

Beam (west)	V_n(test) [kN]	Beam (east)	V_n(test) [kN]
I-1	66.2752	I-1	68.0544
I-2	0.0000	I-2	104.5280
I-3	93.4080	I-3	74.2816
J-1	66.7200	J-1	66.2752
J-2	96.0768	J-2	68.9440
J-3	138.7776	J-3	109.4208

bw= 190.5 [mm]

$$\theta_{ACI} = 45^{\circ}$$

$$\cot\theta_{EC} = 1.25 - 3\frac{\sigma_{cp,eff}}{f_{cd}} \Rightarrow \theta_{EC} \cong 39^{\circ}$$

$$\cot\theta_{CEB} = \sqrt{\left[\frac{b_w s f_{cd2}}{A_{sw} f_{ywd}} - 1\right]} \le 3 \rightarrow f_{cd2} = 0.60\left[1 - \frac{f_{ck}}{250}\right] f_{cd} \Rightarrow \theta_{CEB}$$

Table 4.6: Pasley Data - Beam Properties in the Positive Moment Region.

Load	West	Positive Moment Region d	ρ_w	ρ_v	$\rho_v * f_{vy}$	f'_c	$V_{(support)}$	$V_{(mid.supp.)}$	$M_{(support)}$	$M_{(mid.supp.)}$
		[mm]	[-]	[-]	[MPa]	[MPa]	[kN]	[kN]	[kNm]	[kNm]
1	I-1	407.6700	0.0099	0.0000	0.0000	31.8549	33.8048	23.1296	0.0000	89.2361
1	I-2	404.3680	0.0100	0.0008	0.2351	30.4759	0.0000	0.0000	0.0000	0.0000
2	I-3	406.1460	0.0099	0.0008	0.2337	30.8207	50.2624	43.1456	0.0000	107.2370
1	J-1	406.4000	0.0073	0.0000	0.0000	31.0965	34.2496	23.1296	0.0000	89.5299
2	J-2	406.9080	0.0099	0.0008	0.2344	30.9586	57.8240	51.1520	0.0000	122.9327
2	J-3	381.7620	0.0184	0.0015	0.5654	30.5449	112.0896	105.8624	0.0000	239.0628
Load	**East**	**d**	ρ_w	ρ_v	$\rho_v * f_{vy}$	f'_c	$V_{(support)}$	$V_{(mid.supp.)}$	$M_{(support)}$	$M_{(mid.supp.)}$
		[mm]	[-]	[-]	[MPa]	[MPa]	[kN]	[kN]	[kNm]	[kNm]
1	I-1	407.6700	0.0099	0.0000	0.0000	31.8549	34.2496	23.5744	0.0000	90.4000
1	I-2	405.3840	0.0099	0.0008	0.2351	30.4759	52.4864	41.8112	0.0000	145.6909
2	I-3	408.4320	0.0099	0.0000	0.0000	30.8207	39.1424	32.0256	0.0000	83.6313
1	J-1	406.4000	0.0073	0.0000	0.0000	31.0965	32.0256	21.3504	0.0000	83.0776
2	J-2	406.9080	0.0099	0.0000	0.0000	30.9586	37.3632	31.1360	0.0000	108.9772
2	J-3	385.0640	0.0184	0.0008	0.3951	30.5449	81.3984	75.1712	0.0000	173.5228

Table 4.7: Pasley Data - Beam Properties in the Negative Moment Region.

Load	West	Negative Moment Region d	ρ_w	ρ_v	$\rho_v * f_{vy}$	f'_c	$V_{(support)}$	$V_{(mid.supp.)}$	$M_{(support)}$	$M_{(mid.supp.)}$
		[mm]	[-]	[-]	[MPa]	[MPa]	[kN]	[kN]	[kNm]	[kNm]
1	I-1	394.2080	0.0102	0.0000	0.0000	31.8549	66.2752	56.9344	98.6829	89.2361
1	I-2	403.6060	0.0100	0.0008	0.2351	30.4759	0.0000	0.0000	0.0000	0.0000
2	I-3	403.6060	0.0100	0.0008	0.2337	30.8207	93.4080	84.0672	131.6902	57.5848
1	J-1	393.7000	0.0076	0.0000	0.0000	31.0965	66.7200	57.3792	99.2592	89.5299
2	J-2	403.3520	0.0074	0.0008	0.2344	30.9586	96.0768	88.9600	100.1067	81.1679
2	J-3	400.0500	0.0074	0.0015	0.5654	30.5449	138.7776	131.6608	92.6261	204.6091
Load	**East**	**d**	ρ_w	ρ_v	$\rho_v * f_{vy}$	f'_c	$V_{(support)}$	$V_{(mid.supp.)}$	$M_{(support)}$	$M_{(mid.supp.)}$
		[mm]	[-]	[-]	[MPa]	[MPa]	[kN]	[kN]	[kNm]	[kNm]
1	I-1	394.2080	0.0102	0.0000	0.0000	31.8549	68.0544	58.7136	102.6040	90.4000
1	I-2	403.6060	0.0100	0.0008	0.2351	30.4759	104.5280	95.1872	159.1718	145.6909
2	I-3	403.6060	0.0100	0.0000	0.0000	30.8207	74.2816	64.9408	106.6381	41.4936
1	J-1	393.7000	0.0076	0.0000	0.0000	31.0965	62.7168	53.3760	94.4793	83.0776
2	J-2	403.3520	0.0074	0.0000	0.0000	30.9586	70.2784	60.9376	100.1067	39.6743
2	J-3	397.0020	0.0075	0.0008	0.3951	30.5449	109.4208	102.7488	92.6939	137.5210

Table 4.8: Pasley Data - ACI 318-89 Results in the Positive Moment Region.

ACI Load	West	Positive Moment Region d	A_s	ρ_w	ρ_v	$\rho_v * f_{vy}$	f'_c	V_u	M_u	$V_{n(std)}$	$V_{n(detailed)}$	$V_{c(std)}$	V_c
		[mm]	[mm^2]	[-]	[-]	[MPa]	[MPa]	[MPa]	[kNm]	[kN]	[kN]	[kN]	[kN]
1	I-1	407.6700	767.669	0.0099	0.0000	0.0000	31.8549	32.3770	11.9353	73.0534	77.1930	73.0534	77.1930
1	I-2	404.3680	767.669	0.0100	0.0008	0.2351	30.4759	0.0000	0.0000	88.9877	0.0000	70.8759	0.0000
2	I-3	406.1460	767.669	0.0099	0.0008	0.2337	30.8207	48.9980	19.0524	89.6738	93.1621	71.5891	75.0774
1	J-1	406.4000	567.688	0.0073	0.0000	0.0000	31.0965	32.7669	11.9373	71.9537	72.4824	71.9537	72.4824
2	J-2	406.9080	767.669	0.0099	0.0008	0.2344	30.9586	56.6364	21.8820	90.0557	93.6419	71.8837	75.4698
2	J-3	381.7620	1335.357	0.0184	0.0015	0.5654	30.5449	111.0497	39.9235	108.1077	122.8974	66.9893	81.7790
Load	East	d	A_s	ρ_w	ρ_v	$\rho_v * f_{vy}$	f'_c	V_u	M_u	$V_{n(std)}$	$V_{n(detailed)}$	$V_{c(std)}$	V_c
		[mm]	[mm^2]	[-]	[-]	[MPa]	[MPa]	[MPa]	[kNm]	[kN]	[kN]	[kN]	[kN]
1	I-1	407.6700	767.669	0.0099	0.0000	0.0000	31.8549	32.8218	12.0910	73.0534	77.2030	73.0534	77.2030
1	I-2	405.3840	767.669	0.0099	0.0008	0.2351	30.4759	51.0666	19.3769	89.2113	93.0630	71.0540	74.9057
2	I-3	408.4320	767.669	0.0099	0.0000	0.0000	30.8207	37.8709	14.9421	71.9920	75.3767	71.9920	75.3767
1	J-1	406.4000	567.688	0.0073	0.0000	0.0000	31.0965	30.6022	11.0770	71.9537	72.5523	71.9537	72.5523
2	J-2	406.9080	767.669	0.0099	0.0000	0.0000	30.9586	36.2548	19.3979	71.8837	71.6195	71.8837	71.6195
2	J-3	385.0640	1335.357	0.0184	0.0008	0.3951	30.5449	80.3495	29.2290	96.5499	111.3897	67.5687	82.4085

Table 4.9: Pasley Data - ACI 318-89 Results in the Negative Moment Region.

ACI Load	West	Negative Moment Region d	A_s	ρ_w	ρ_v	$\rho_v * f_{vy}$	f'_c	V_u	M_u	$V_{n(std)}$	$V_{n(detailed)}$	$V_{c(std)}$	V_c
		[mm]	[mm^2]	[-]	[-]	[MPa]	[MPa]	[MPa]	[kNm]	[kN]	[kN]	[kN]	[kN]
1	I-1	394.2080	767.669	0.0102	0.0000	0.0000	31.8549	65.0671	74.3787	70.6411	65.0779	70.6411	65.0779
1	I-2	403.6060	767.669	0.0100	0.0008	0.2351	30.4759	0.0000	0.0000	88.8200	0.0000	70.7424	0.0000
2	I-3	403.6060	767.669	0.0100	0.0008	0.2337	30.8207	91.7588	98.2726	89.1130	83.9171	71.1414	65.9455
1	J-1	393.7000	567.688	0.0076	0.0000	0.0000	31.0965	65.5135	74.8739	69.7051	63.1133	69.7051	63.1133
2	J-2	403.3520	567.688	0.0074	0.0008	0.2344	30.9586	94.8211	68.1218	89.2687	84.5620	71.2555	66.5488
2	J-3	400.0500	567.688	0.0074	0.0015	0.5654	30.5449	137.5322	40.6099	113.2865	116.3563	70.1984	73.2682
Load	**East**	**d**	**A_s**	**ρ_w**	**ρ_v**	**$\rho_v * f_{vy}$**	**f'_c**	**V_u**	**M_u**	**$V_{n(std)}$**	**$V_{n(detailed)}$**	**$V_{c(std)}$**	**V_c**
		[mm]	[mm^2]	[-]	[-]	[MPa]	[MPa]	[MPa]	[kNm]	[kN]	[kN]	[kN]	[kN]
1	I-1	394.2080	767.669	0.0102	0.0000	0.0000	31.8549	66.8463	24.9619	70.6411	74.4116	70.6411	74.4116
1	I-2	403.6060	767.669	0.0100	0.0008	0.2351	30.4759	103.2911	40.3689	88.8200	92.3255	70.7424	74.2479
2	I-3	403.6060	767.669	0.0100	0.0000	0.0000	30.8207	72.6324	26.1535	71.1414	75.7522	71.1414	75.7522
1	J-1	393.7000	567.688	0.0076	0.0000	0.0000	31.0965	61.5103	22.9344	69.7051	70.0649	69.7051	70.0649
2	J-2	403.3520	567.688	0.0074	0.0000	0.0000	30.9586	68.6303	24.6636	71.2555	72.0166	71.2555	72.0166
2	J-3	397.0020	567.688	0.0075	0.0008	0.3951	30.5449	108.2621	39.9807	99.5432	100.0446	69.6635	70.1648

Table 4.10: Pasley Data - EC 2 Results in the Positive Moment Region.

EC 2		Positive Moment Region					No Shear Reinf.		With Shear Reinf.		With Shear Reinf.	
Load	West	d	f'_c	τ_r	k	ρ_1	V_{r1}	V_{r2}	$V_{r2(std)}$	$V_{r3(std)}$	$V_{r2(detailed)}$	$V_{r3(detailed)}$
		[mm]	[MPa]	[]	[]	[-]	[kN]	[kN]	[kN]	[kN]	[kN]	[kN]
1	I-1	407.6700	31.8549	0.3517	1.1923	0.0099	51.9779	601.9624				
1	I-2	404.3680	30.4759	0.3415	1.1956	0.0100	50.3224	578.5228	578.5228	66.6230	565.8807	20.1295
2	I-3	406.1460	30.8207	0.3441	1.1939	0.0099	50.7213	585.7900	585.7900	66.9975	572.9891	20.0995
1	J-1	406.4000	31.0965	0.3461	1.1936	0.0073	47.7183	589.9077				
2	J-2	406.9080	30.9586	0.3451	1.1931	0.0099	50.9354	588.7704	588.7704	67.2903	575.9043	20.1966
2	J-3	381.7620	30.5449	0.3420	1.2182	0.0184	58.6613	547.0719	547.0719	95.6679	535.1170	45.6993
Load	East	d	f'_c	τ_r	k	ρ_1	V_{r1}	V_{r2}	$V_{r2(std)}$	$V_{r3(std)}$	$V_{r2(detailed)}$	$V_{r3(detailed)}$
		[mm]	[MPa]	[]	[]	[-]	[kN]	[kN]	[kN]	[kN]	[kN]	[kN]
1	I-1	407.6700	31.8549	0.3517	1.1923	0.0099	51.9779	601.9624				
1	I-2	405.3840	30.4759	0.3415	1.1946	0.0099	50.2800	579.9764	579.9764	66.6215	567.3025	20.1801
2	I-3	408.4320	30.8207	0.3441	1.1916	0.0099	50.9091	589.0872				
1	J-1	406.4000	31.0965	0.3461	1.1936	0.0073	47.7183	589.9077				
2	J-2	406.9080	30.9586	0.3451	1.1931	0.0099	50.9354	588.7704				
2	J-3	385.0640	30.5449	0.3420	1.2149	0.0184	59.0083	551.8037	551.8037	85.0914	539.7455	32.2100

Table 4.11: Pasley Data - EC 2 Results in the Negative Moment Region.

EC 2		Negative Moment Region					No Shear Reinf.		With Sh. Reinf.		With Shear Reinf.	
Load	West	d	f'_c	τ_r	k	ρ_1	V_{r1}	V_{r2}	$V_{r2(std)}$	$V_{r3(std)}$	$V_{r2(detailed)}$	$V_{r3(detailed)}$
		[mm]	[MPa]	[]	[]	[-]	[kN]	[kN]	[kN]	[kN]	[kN]	[kN]
1	I-1	394.2080	31.8549	0.3517	1.2058	0.0102	51.2111	582.0845				
1	I-2	403.6060	30.4759	0.3415	1.1964	0.0100	50.2596	577.4327	577.4327	66.5295	564.8144	20.0916
2	I-3	403.6060	30.8207	0.3441	1.1964	0.0100	50.6379	582.1266	582.1266	66.8124	569.4057	19.9738
1	J-1	393.7000	31.0965	0.3461	1.2063	0.0076	47.0947	571.4731				
2	J-2	403.3520	30.9586	0.3451	1.1966	0.0074	47.4678	583.6251	583.6251	63.6797	570.8715	20.0201
2	J-3	400.0500	30.5449	0.3420	1.2000	0.0074	46.7876	573.2789	573.2789	85.5669	560.7514	47.8884
Load	East	d	f'_c	τ_r	k	ρ_1	V_{r1}	V_{r2}	$V_{r2(std)}$	$V_{r3(std)}$	$V_{r2(detailed)}$	$V_{r3(detailed)}$
		[mm]	[MPa]	[]	[]	[-]	[kN]	[kN]	[kN]	[kN]	[kN]	[kN]
1	I-1	394.2080	31.8549	0.3517	1.2058	0.0102	51.2111	582.0845				
1	I-2	403.6060	30.4759	0.3415	1.1964	0.0100	50.2596	577.4327	577.4327	66.5295	564.8144	20.0916
2	I-3	403.6060	30.8207	0.3441	1.1964	0.0100	50.6379	582.1266				
1	J-1	393.7000	31.0965	0.3461	1.2063	0.0076	47.0947	571.4731				
2	J-2	403.3520	30.9586	0.3451	1.1966	0.0074	47.4678	583.6251				
2	J-3	397.0020	30.5449	0.3420	1.2030	0.0075	46.6735	568.9111	568.9111	73.5653	556.4790	33.2085

Table 4.12: Pasley Data - CEB Results in the Positive Moment Region.

CEB Load	West	Positive Moment Region d	f'c	τr	No Shear Reinf. Vr1	Vr2	With Shear Reinf. Vr2(std)	Vr3(std)	With Shear Reinf. Vr2(detailed)	Vr3(detailed)	θ
		[mm]	[MPa]	[]	[kN]	[kN]	[kN]	[kN]	[kN]	[kN]	[deg]
1	I-1	407.6700	31.8549	0.5142	99.8293	742.1663					
1	I-2	404.3680	30.4759	0.4992	96.1420	704.2868	704.2868	112.4426	621.8483	110.5345	31.0000
2	I-3	406.1460	30.8207	0.5030	97.2916	715.3856	715.3856	113.5678	631.6480	111.6626	31.0000
1	J-1	406.4000	31.0965	0.5060	97.9324	722.2387					
2	J-2	406.9080	30.9586	0.5045	97.7647	719.9346	719.9346	114.1195	635.6646	112.2051	31.0000
2	J-3	381.7620	30.5449	0.5000	90.9041	666.4183	666.4183	127.9106	588.4125	123.5789	31.0000
Load	**East**	**d**	**f'c**	**τr**	**Vr1**	**Vr2**	**Vr2(std)**	**Vr3(std)**	**Vr2(detailed)**	**Vr3(detailed)**	**θ**
		[mm]	[MPa]	[]	[kN]	[kN]	[kN]	[kN]	[kN]	[kN]	[deg]
1	I-1	407.6700	31.8549	0.5142	99.8293	742.1663					
1	I-2	405.3840	30.4759	0.4992	96.3835	706.0564	706.0564	112.7251	623.4108	110.8123	31.0000
2	I-3	408.4320	30.8207	0.5030	97.8392	719.4122					
1	J-1	406.4000	31.0965	0.5060	97.9324	722.2387					
2	J-2	406.9080	30.9586	0.5045	97.7647	719.9346					
2	J-3	385.0640	30.5449	0.5000	91.6903	672.1824	672.1824	117.7734	593.5018	114.7203	31.0000

Table 4.13: Pasley Data - CEB Results in the Negative Moment Region.

CEB Load	West	Negative Moment Region d	f'_c	τ_r	No Shear Reinf. V_{r1}	V_{r2}	With Shear Reinf. $V_{r2(std)}$	$V_{r3(std)}$	With Shear Reinf. $V_{r2(detailed)}$	$V_{r3(detailed)}$	θ
		[mm]	[MPa]	[]	[kN]	[kN]	[kN]	[kN]	[kN]	[kN]	[deg]
1	I-1	394.2080	31.8549	0.5142	96.5328	717.6586					
1	I-2	403.6060	30.4759	0.4992	95.9608	702.9596	702.9596	112.2307	620.6765	83.9344	31.0000
2	I-3	403.6060	30.8207	0.5030	96.6831	710.9117	710.9117	112.8576	627.6977	84.7273	31.0000
1	J-1	393.7000	31.0965	0.5060	94.8720	699.6687					
2	J-2	403.3520	30.9586	0.5045	96.9103	713.6431	713.6431	113.1222	630.1094	84.9267	31.0000
2	J-3	400.0500	30.5449	0.5000	95.2587	698.3426	698.3426	134.0380	616.5999	66.5938	31.0000
Load	**East**	**d**	**f'_c**	**τ_r**	**V_{r1}**	**V_{r2}**	**$V_{r2(std)}$**	**$V_{r3(std)}$**	**$V_{r2(detailed)}$**	**$V_{r3(detailed)}$**	**θ**
		[mm]	[MPa]	[]	[kN]	[kN]	[kN]	[kN]	[kN]	[kN]	[deg]
1	I-1	394.2080	31.8549	0.5142	96.5328	717.6586					
1	I-2	403.6060	30.4759	0.4992	95.9608	702.9596	702.9596	112.2307	620.6765	83.9344	31.0000
2	I-3	403.6060	30.8207	0.5030	96.6831	710.9117					
1	J-1	393.7000	31.0965	0.5060	94.8720	699.6687					
2	J-2	403.3520	30.9586	0.5045	96.9103	713.6431					
2	J-3	397.0020	30.5449	0.5000	94.5330	693.0218	693.0218	121.4247	611.9020	74.6551	31.0000

Table 4.14: Pasley Data - Hofer/McCabe Results in the Positive Moment Region.

H/McC		Positive Moment Region			No Shear Reinf.		With Shear Reinf.	
Load	West	d	f'_c	ρ_1	$V_{(tension)}$	$V_{(comp.)}$	$V_{(tension)}$	$V_{(comp.)}$
		[mm]	[MPa]	[-]	[kN]	[kN]	[kN]	[kN]
1	I-1	407.6700	31.8549	0.0099	79.9068			
1	I-2	404.3680	30.4759	0.0100	76.0418		74.8890	
2	I-3	406.1460	30.8207	0.0099	77.0234		75.7409	
1	J-1	406.4000	31.0965	0.0073	72.0708			
2	J-2	406.9080	30.9586	0.0099	77.5132		76.2103	
2	J-3	381.7620	30.5449	0.0184	88.9167		96.3456	
Load	East	d	f'_c	ρ_1	$V_{(tension)}$	$V_{(comp.)}$	$V_{(tension)}$	$V_{(comp.)}$
		[mm]	[MPa]	[-]	[kN]	[kN]	[kN]	[kN]
1	I-1	407.6700	31.8549	0.0099	79.9068			
1	I-2	405.3840	30.4759	0.0099	76.0189		74.8889	
2	I-3	408.4320	30.8207	0.0099	77.4569			
1	J-1	406.4000	31.0965	0.0073	72.0708			
2	J-2	406.9080	30.9586	0.0099	77.5132			
2	J-3	385.0640	30.5449	0.0184	89.6858		91.6801	

Table 4.15: Pasley Data - Hofer/McCabe Results in the Negative Moment Region.

H/McC		Negative Moment Region			No Shear Reinf.		With Shear Reinf.	
Load	West	d	f'_c	ρ_t	$V_{(tension)}$	$V_{(comp.)}$	$V_{(tension)}$	$V_{(comp.)}$
		[mm]	[MPa]	[-]	[kN]	[kN]	[kN]	[kN]
1	I-1	394.2080	31.8549	0.0102	66.3198			
1	I-2	403.6060	30.4759	0.0100	64.9558		72.9130	
2	I-3	403.6060	30.8207	0.0100	65.6906		73.6011	
1	J-1	393.7000	31.0965	0.0076	64.5840			
2	J-2	403.3520	30.9586	0.0074	65.8682		73.7970	
2	J-3	400.0500	30.5449	0.0074	64.4559		83.4219	
Load	East	d	f'_c	ρ_t	$V_{(tension)}$	$V_{(comp.)}$	$V_{(tension)}$	$V_{(comp.)}$
		[mm]	[MPa]	[-]	[kN]	[kN]	[kN]	[kN]
1	I-1	394.2080	31.8549	0.0102	66.3198			
1	I-2	403.6060	30.4759	0.0100	64.9558		72.9130	
2	I-3	403.6060	30.8207	0.0100	65.6906			
1	J-1	393.7000	31.0965	0.0076	64.5840			
2	J-2	403.3520	30.9586	0.0074	65.8682			
2	J-3	397.0020	30.5449	0.0075	63.9676		77.1197	

Table 4.16: Pasley Data - Summary of the Results.

ACI

standard method

Beam	west Vn	east Vn
I-1	70.6411	70.6411
I-2	88.8200	88.8200
I-3	89.1130	71.1414
J-1	69.7051	69.7051
J-2	89.2687	71.2555
J-3	113.2865	99.5432

detailed method

west Vn	east Vn
65.0779	74.4116
	92.3255
83.9171	75.7522
63.1133	70.0649
84.5620	72.0166
116.3563	100.0446

EC 2

no shear reinf.

Beam	west Vn	east Vn
I-1	51.2111	51.2111
I-2	50.2596	50.2596
I-3	50.6379	50.6379
J-1	47.0947	47.0947
J-2	47.4678	47.4678
J-3	46.7876	46.6735

standard method

west Vn	east Vn
66.5295	66.5295
66.8124	
63.6797	
85.5669	73.5653

detailed method

west Vn	east Vn
20.0916	20.0916
19.9738	
20.0201	
47.8884	33.2085

CEB

no shear reinf.

Beam	west Vn	east Vn
I-1	96.5328	96.5328
I-2	95.9608	95.9608
I-3	96.6831	96.6831
J-1	94.8720	94.8720
J-2	96.9103	96.9103
J-3	95.2587	94.5330

standard method

west Vn	east Vn
112.2307	112.2307
112.8576	
113.1222	
134.0380	121.4247

detailed method

west Vn	east Vn
83.9344	83.9344
84.7273	
84.9267	
66.5938	74.6551

Table 4.17: Pasley Data - Summary of the Results.

Hofer/McCabe

	Beam	west Vn	east Vn
no shear reinf.	I-1	66.3198	66.3198
	I-2	64.9558	64.9558
	I-3	65.6906	65.6906
	J-1	64.5840	64.5840
	J-2	65.8682	65.8682
	J-3	64.4559	63.9676

	west Vn	east Vn
shear reinf.	0.0000	0.0000
	72.9130	72.9130
	73.6011	0.0000
	0.0000	0.0000
	73.7970	0.0000
	83.4219	77.1197

SM-Report #26

	Beam	west Vn	east Vn
test data	I-1	66.2752	68.0544
	I-2	0.0000	104.5280
	I-3	93.4080	74.2816
	J-1	66.7200	66.2752
	J-2	96.0768	68.9440
	J-3	138.7776	109.4208

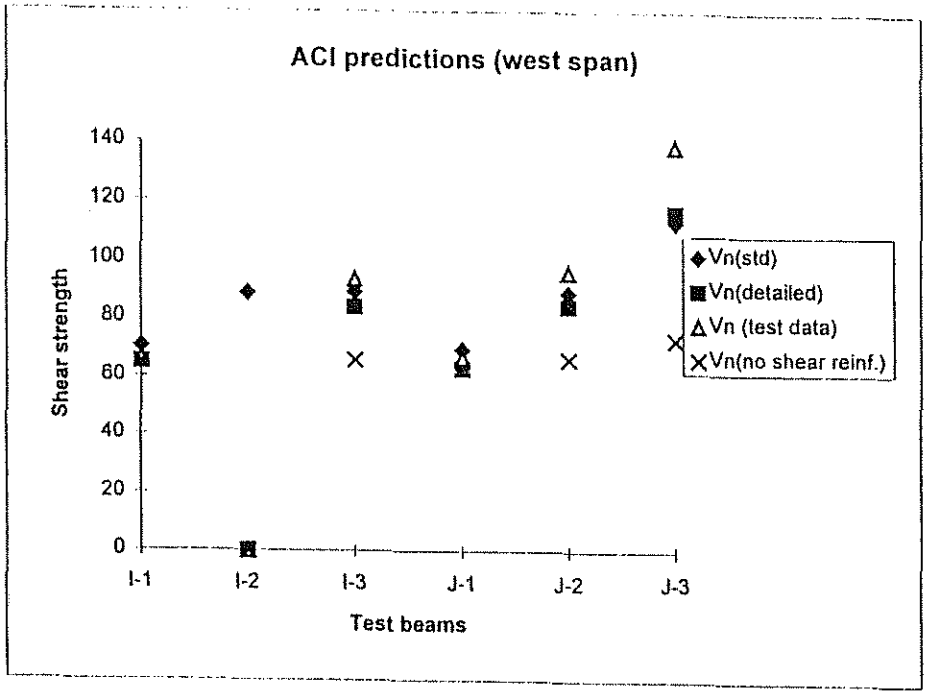

Fig. 4.5: ACI 318-89 Predictions versus Test Results.

* (a) Indicates that beam #i did not fail in the test region, therefore no data exist, which may be also used in shear equations Vn = ...
(b) Indicates that beam #i has no shear reinforcement.

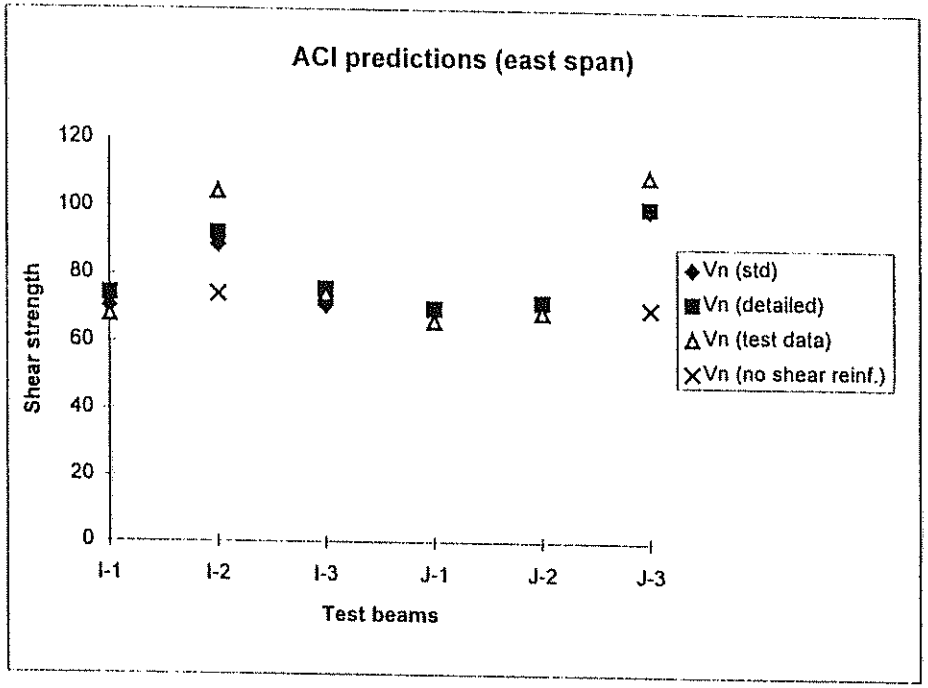

Fig. 4.6: ACI 318-89 Predictions versus Test Results.

* (a) Indicates that beam #i did not fail in the test region, therefore no data exist, which may be also used in shear equations Vn = ...
(b) Indicates that beam #i has no shear reinforcement.

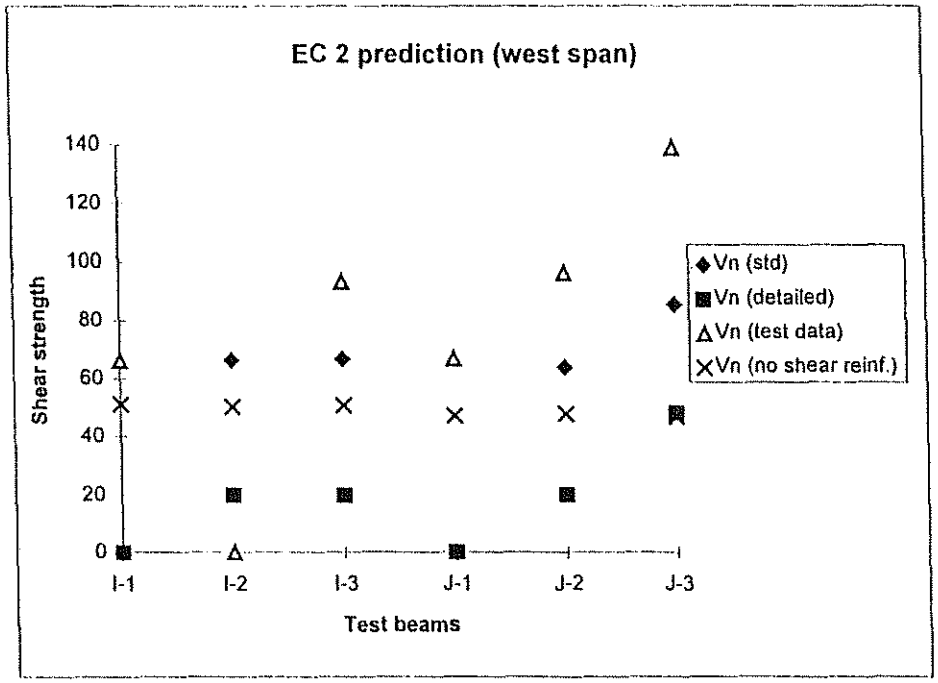

Fig. 4.7: EC 2 Predictions versus Test Results.

* (a) Indicates that beam #i did not fail in the test region, therefore no data exist, which may be also used in shear equations Vn = ...
(b) Indicates that beam #i has no shear reinforcement.

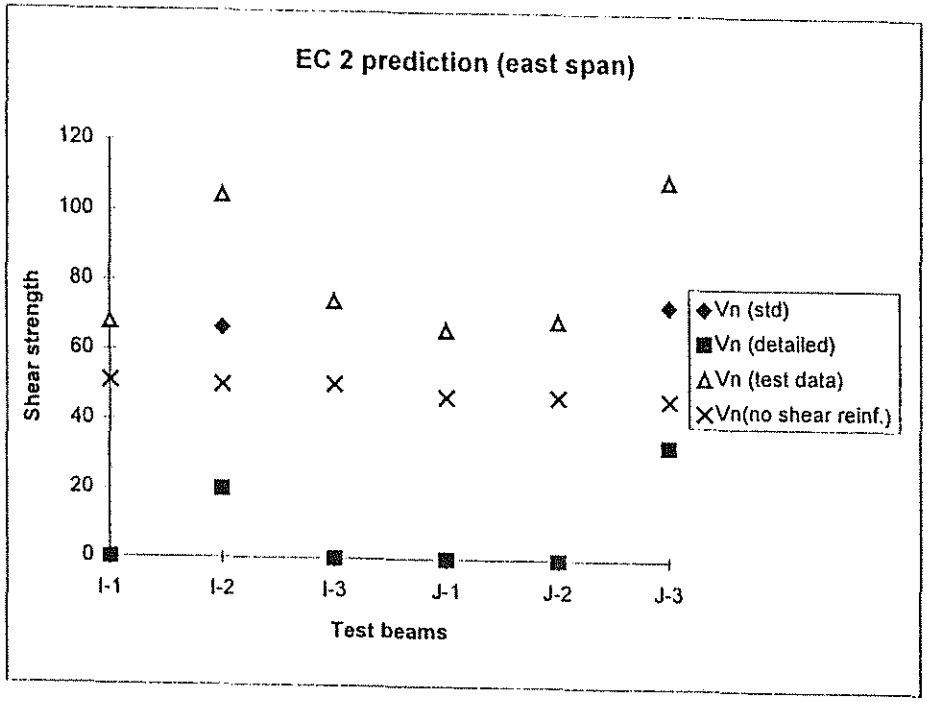

Fig. 4.8: EC 2 Results versus Test Results.

* (a) Indicates that beam #i did not fail in the test region, therefore no data exist, which may be also used in shear equations Vn = ...
(b) Indicates that beam #i has no shear reinforcement.

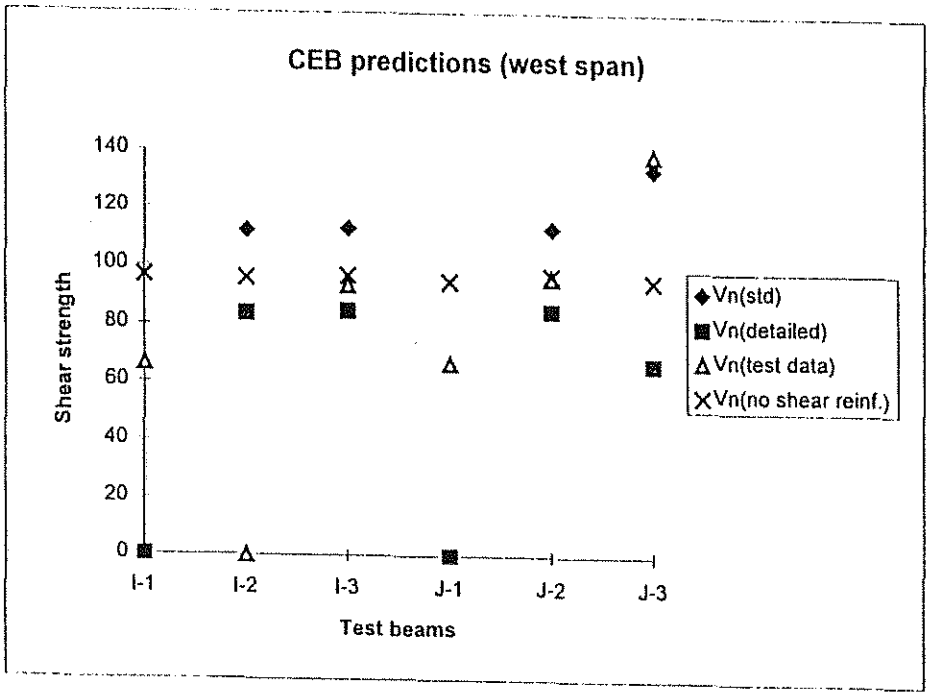

Fig. 4.9: CEB Predictions versus Test Results.

* (a) Indicates that beam #i did not fail in the test region, therefore no data exist, which may be also used in shear equations Vn = ...

(b) Indicates that beam #i has no shear reinforcement.

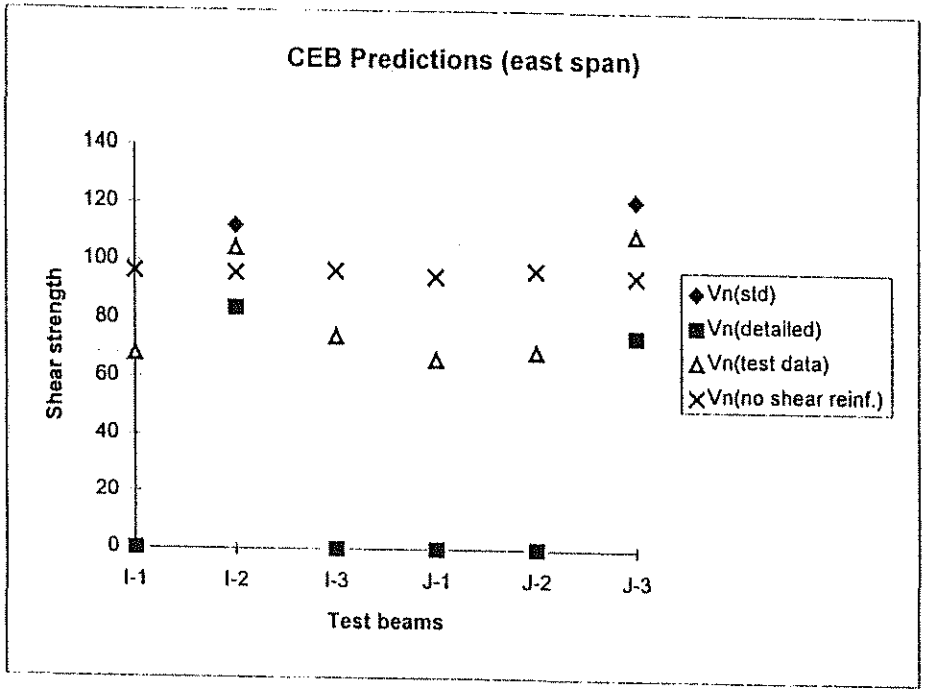

Fig. 4.10: CEB Predictions versus Test Results.

* (a) Indicates that beam #i did not fail in the test region, therefore no data exist, which may be also used in shear equations Vn = ...

(b) Indicates that beam #i has no shear reinforcement.

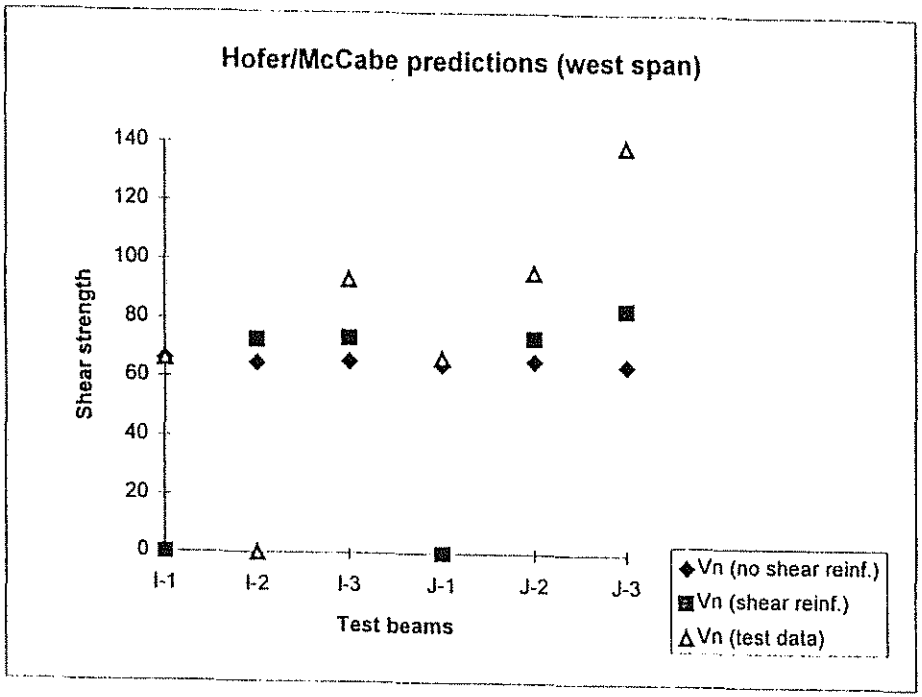

Fig. 4.11: Hofer/McCabe Predictions versus Test Results.

* (a) Indicates that beam #i did not fail in the test region, therefore no data exist, which may be also used in shear equations Vn = ...
(b) Indicates that beam #i has no shear reinforcement.

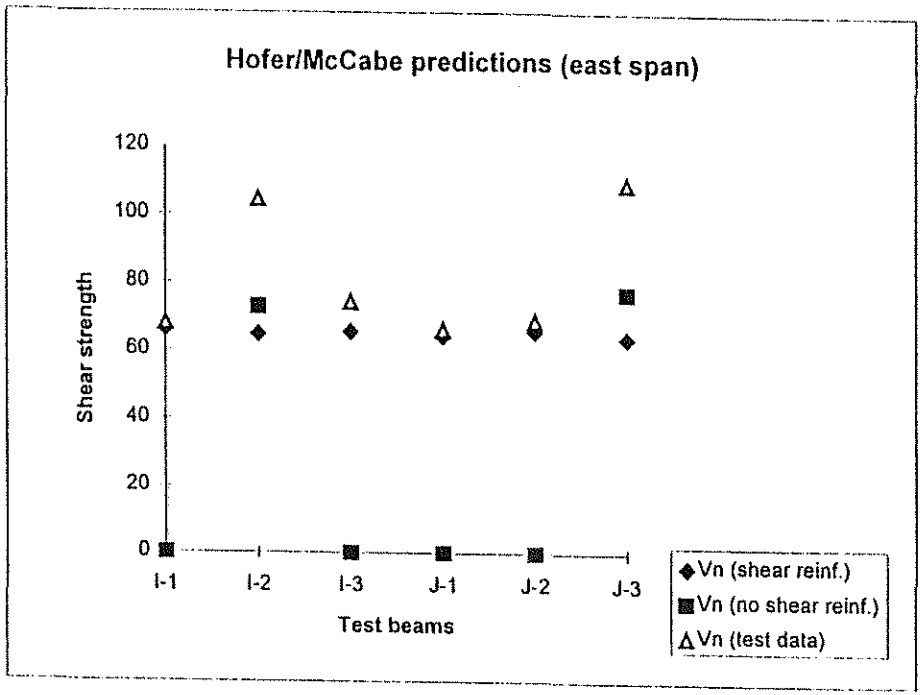

Fig. 4.12: Hofer/McCabe Predictions versus Test Results.

* (a) Indicates that beam #i did not fail in the test region, therefore no data exist, which may be also used in shear equations Vn = ...
(b) Indicates that beam #i has no shear reinforcement.

Table 4.18: Example Using ACI 318-89, Beam I-3 West, Positive Moment Region (21)

Unfactored Capacities

Member Requiring Design Shear Reinforcement

Standard Procedure

Shear strength of the concrete

$$V_c = \frac{1}{6}\sqrt{f'_c}\, b_w d$$

$f'_c = 30.82065 \cong 30.82$ MPa

$b_w = 190.5$ mm

$d = 406.146$ mm

$$V_c = \frac{1}{6}\sqrt{(30.82)} \times 190.5 \times 406.146 \times 10^{-3} = 71.59 \text{ kN}$$

Capacity of the shear reinforcement

$$V_s = \frac{A_v}{s} f_y d$$

$$a_{sw} = \frac{A_v}{s} = 0.1524 \text{ mm} = 1.524 \text{ cm}^2/\text{m}$$

$$V_s = 0.1524 \times 292.18 \times 406.146 \times 10^{-3} = 18.08 \text{ kN}$$

Nominal capacity of the cross section

$$V_n = V_c + V_s = 71.59 + 18.08 = 89.67 \text{ kN}$$

More Detailed Approach

Shear strength of the concrete

$$V_c = \left[\left[\sqrt{f'_c} + 120\rho_w \frac{V_u d}{M_u}\right]\frac{1}{7}\right] b_w d \le 0.3\sqrt{f'_c} b_w d$$

$$\frac{V_u d}{M_u} \le 1.0$$

$M_u = 19.05$ kNm

$V_u = 49.00$ kN

$\rho_w = 0.0099$

$$V_c = \left[\left[\sqrt{(30.82)} + 120 \times 0.0099 \times \frac{49.00 \times 0.406146}{19.05}\right]\frac{1}{7}\right] \times 190.5 \times 406.146 \times 10^{-3}$$

$= 75.08$ kN

Capacity of the shear reinforcement

$$V_s = \frac{A_v}{s} f_y d$$

$$a_{sw} = \frac{A_v}{s} = 0.1524 \text{ mm} = 1.524 \text{ cm}^2/\text{m}$$

$$V_s = 0.1524 \times 292.18 \times 406.146 \times 10^{-3} = 18.08 \text{ kN}$$

Nominal capacity of the cross section

$$V_n = V_c + V_s = 75.08 + 18.08 = 93.16 \text{ kN}$$

Table 4.19: Example Using EC 2, Beam I-3 West, Positive Moment Region (21)

Unfactored Capacities

Member Requiring Design Shear Reinforcement

Standard Procedure

Check the capacity of the compression strut

$$V_{r2} = 0.5\nu f_{ck} b_w z$$

$$f_{ck} = 30.82065 \cong 30.82 \text{ MPa}$$

$$\nu = 0.7 - f_{ck} / 200 = 0.7 - 30.82 / 200 = 0.55 \geq 0.5$$

$$b_w = 190.5 \text{ mm}$$

$$z = 0.9d = 0.9 \times 406.146 = 365.5 \text{ mm}$$

$$V_{r2} = 0.5 \times 0.55 \times 30.82 \times 190.5 \times 365.5 \times 10^{-3} = 590.13 \text{ kN}$$

Check the capacity of the shear reinforcement

$$V_{r3} = V_c + V_w$$

$$V_c = V_{r1} = \tau_{rk} k(1.2 + 40\rho_l) b_w d$$

$$\tau_{rk} = 0.035 f_{ck}^{\frac{2}{3}} = 0.035 \times 30.82^{\frac{2}{3}} = 0.344$$

$$k = 1.6 - d = 1.6 - 0.406146 = 1.194 \geq 1.0$$

$$\rho_l = \rho_w = 0.0099$$

$$V_c = 0.344 \times 1.194 \times (1.2 + 40 \times 0.0099) \times 190.5 \times 406.146 \times 10^{-3} = 50.72 \text{ kN}$$

$$V_w = \left(\frac{A_{sw}}{s}\right) z f_{ywd} = a_{sw} z f_{ywd}$$

$$a_{sw} = \rho_v b_w = 0.0008 \times 190.5 = 0.1524\,[\text{mm}] = 1.524\,[\text{cm}^2/\text{m}]$$

$$f_{ywd} = \frac{\rho_v f_{vy}}{\rho_v} = \frac{0.233741}{0.0008} = 292.18\ \text{MPa}$$

$$V_w = 0.1524 \times 365.5 \times 292.18 / 1000 = 16.275\ \text{kN}$$

$$V_{r3} = 50.72 + 16.275 = 67.0\ \text{kN}$$

Detailed Procedure

$$\cot\theta = 1.25 - 3\frac{\sigma_{cp,eff}}{f_{cd}} = 1.25 \Rightarrow \theta \cong 39^\circ$$

Check the capacity of the compression strut

$$V_{r2} = 0.5\nu f_{ck} b_w z / (\cot\theta + \tan\theta)$$

$$f_{ck} = 30.82065 \cong 30.82 \text{ MPa}$$

$$\nu = 0.7 - f_{ck} / 200 = 0.7 - 30.82 / 200 = 0.55 \geq 0.5$$

$$b_w = 190.5 \text{ mm}$$

$$z = 0.9d = 0.9 \times 406.146 = 365.5 \text{ mm}$$

$$V_{r2} = 0.55 \times 30.82 \times 190.5 \times 365.5 \times 10^{-3} / (\cot 39^\circ + \tan 39^\circ) = 577.23 \text{ kN}$$

Check the capacity of the shear reinforcement

$$V_{r3} = \left(\frac{A_{sw}}{s}\right) z f_{ywd} \cot\theta = a_{sw} z f_{ywd} \cot\theta$$

$$a_{sw} = \rho_v b_w = 0.0008 \times 190.5 = 0.1524 \text{ [mm]} = 1.524 \text{ [cm}^2\text{/m]}$$

$$f_{ywd} = \frac{\rho_v f_{vy}}{\rho_v} = \frac{0.233741}{0.0008} = 292.18 \text{ MPa}$$

$$V_{r3} = 0.1524 \times 365.5 \times 292.18 \times \cot 39^\circ / 1000 = 20.10 \text{ kN}$$

Check requirement:

$$\frac{A_{sw} f_{ywd}}{b_w s} \leq 0.5 \nu f_{cd} \qquad \text{(for 90° stirrups)}$$

$$\frac{0.1524 \times 292.18}{190.5} \leq 0.5 \times 0.55 \times 30.82 / 1.5$$

$0.233744 \leq 5.65$ OK

Table 4.20: Example Using CEB, Beam I-3 West, Positive Moment Region (21)

Unfactored Capacities

Member Requiring Design Shear Reinforcement

Standard Procedure

Check the capacity of the compression strut

$V_{r2} = 0.30 f_{ck} b_w d$

$f_{ck} = 30.82065 \cong 30.82 \text{ MPa}$

$f_{cd} = f_{ck} / 1.5 = 30.82 / 1.5 = 20.55 \text{ MPa}$

$b_w = 190.5 \text{ mm}$

$d = 406.146 \text{ mm}$

$V_{r2} = 0.30 \times 30.82 \times 190.5 \times 406.146 / 1000 = 715.37 \text{ kN}$

Check the capacity of the shear reinforcement

$V_{r3} = V_c + V_w$

$V_c = 2.5 \tau_{rk} b_w d$

$\tau_{rk} = 0.25 f_{ctk}$

$$f_{ctk,min} = f_{ctko,min}\left[\frac{f_{ck}}{f_{ck,o}}\right]^{\frac{2}{3}}, \; f_{cko,min} = 0.95 \text{ MPa}, \; f_{cko} = 10 \text{ MPa}$$

$$\tau_{rk} = 0.25 \times 0.95 \times \left(\frac{30.82}{10}\right)^{\frac{2}{3}} = 0.503$$

$$f_{ck} = 30.82065 \cong 30.82 \text{ MPa}$$

$$b_w = 190.5 \text{ mm}$$

$$d = 406.146 \text{ mm}$$

$$V_c = 2.5 \times 0.503 \times 190.5 \times 406.146 / 1000 = 97.29 \text{ kN}$$

$$V_w = \left(\frac{A_{sw}}{s}\right) z f_{ywd} = a_{sw} z f_{ywd}$$

$$a_{sw} = \rho_v b_w = 0.0008 \times 190.5 = 0.1524 \text{ [mm]} = 1.524 \text{ [cm}^2\text{/m]}$$

$$f_{ywd} = \frac{\rho_v f_{vy}}{\rho_v} = \frac{0.233741}{0.0008} = 292.18 \text{ MPa}$$

$$V_w = 0.1524 \times 365.5 \times 292.18 / 1000 = 16.275 \text{ kN}$$

$$V_{rd3} = 97.29 + 16.275 = 113.565 \text{ kN}$$

Refined Procedure

$$\cot\theta = \sqrt{\left[\frac{b_w s f_{cd2}}{A_{sw} f_{ywd}} - 1\right]} \le 3 \Rightarrow \sqrt{\left[\frac{190.5 \times 10.81}{0.1524 \times 292.18} - 1\right]} = 6.73 \le 3$$

$\Rightarrow \theta \cong 30.96^\circ$ (lower limit)

with $f_{ck} = 30.82065 \cong 30.82$ MPa

$f_{cd} = f_{ck} / 1.5 = 30.82 / 1.5 = 20.55$ MPa

$$f_{cd2} = 0.60\left[1 - \frac{f_{ck}}{250}\right] f_{cd} = 0.60\left[1 - \frac{30.82}{250}\right] \times 20.55 = 10.81 \text{ MPa}$$

Check the capacity of the compression strut

$V_{r2} = 0.30 f_{ck} b_w d \sin 2\theta$

$b_w = 190.5$ mm

$d = 406.146$ mm

$$V_{r2} = 0.30 \times 30.82 \times 190.5 \times 406.146 / 1000 \times \sin\left(2 \times 30.96^\circ\right) = 631.16 \text{ kN}$$

Check the capacity of the shear reinforcement

$V_{r3} = V_{c2} + V_w$

$$V_w = \left(\frac{A_{sw}}{s}\right) z f_{ywd} \cot\theta = a_{sw} z f_{ywd} \cot\theta$$

$$a_{sw} = \rho_v b_w = 0.0008 \times 190.5 = 0.1524\ [\text{mm}] = 1.524\ [\text{cm}^2/\text{m}]$$

$$f_{ywd} = \frac{\rho_v f_{vy}}{\rho_v} = \frac{0.233741}{0.0008} = 292.18\ \text{MPa}$$

$$V_w = 0.1524 \times 365.5 \times 292.18 \times \cot 41.81^\circ / 1000 = 18.20\ \text{kN}$$

$$V_{c2} = V_c = 97.29\ \text{kN}$$

$$V_{r3} = 18.20 + 97.29 = 115.49\ \text{kN}$$

CHAPTER 5
Summary and Conclusions

5.1 Summary

The purpose of this study was to compare the nominal shear strength of continuous lightly reinforced beams based on the test results obtained by Pasley et al. (SM-Report #26) with current shear provisions of the ACI 318-95, Eurocode 2 (1990), CEB Model Code 1990 and a strut and tie model developed herein.

Six two-span T-beams with and without shear reinforcement were tested concerning the primary variables of longitudinal reinforcement, ρ_w, varying nominal stirrups strength, $\rho_w f_{vy}$, and variations in shear span-to-depth ratio, a/d.

The test results proved that the ACI 318-95 overpredicts the concrete shear capacity of lightly reinforced beams without shear reinforcement. Negative moment regions experienced fewer cracks at wider spacing than in the positive moment regions, most likely due to the reduced bond capacity from the top-bar effect. On the other hand the stirrup contribution to the shear strength exceeded in the test results the ACI 318-95 predictions.

Based on these test results it was studied to predict the shear capacity by a truss model with a variable inclination, θ, between 35° and 45°.

These test results yielded to the Hofer/McCabe equation, Eq. 3.13, which represents the predicted shear capacity of the tension strut in the truss model. The first example, a lightly reinforced continuous T-beam, showed how close the Hofer/McCabe equation is in comparison to the test results the European and North

American Codes which were discussed before. The second example, a lightly reinforced continuous rectangular beam, showed a second set of comparisons of the Hofer/McCabe equation, European and North American Codes.

5.2 Conclusions

The usefulness of a design method depends on its accuracy judged from comparison with test results, its applicability to different problems, its ease of handling and last but not least on its scientific foundation. "At present a study of different methods is nearly hopeless undertaking. For the many test points plot like a 'Milky Way' allowing almost any interpretation." "Nevertheless, a comparison with test results allows at least to find out if a procedure is on the safe side." (11, pg. 111)

Truss models approaches have been generalized to all parts of the structure in form of a Strut and Tie Model. The main advantages are that the flow of the internal forces is available to the designer and that the effect of shear and moment are accounted simultaneously. The design of shear regions and transitions may be conducted in a consistent manner. It is shown that the shear strength of reinforced concrete beams may be determined by a Strut and Tie Model with variable inclination, θ, of the compression field based on the theory of plasticity to derive the interaction between bending moment and shear. The comparison shows that a clear truss model gives close results to the Pasley test data. The predictions of the shear capacity by the ACI 318-95 was close to the test results. Generally it may be noted

that one set of test beams is not a proof whether or not an equation which predicts the shear capacity of nonprestressed concrete members is accurate or not.

Consequently, the application of the EC 2 and the CEB-Code, which are based on a truss model, might be successfully used to adjust the current ACI shear provisions which are scheduled to be changed in the next edition of the Building Code.

The standard and the more detailed procedures of the EC 2 give similar results for low shear stresses. Even for the two procedures of the CEB Code these results are close. At high shear values the procedure with a variable inclination θ may lead to a considerable reduction in the shear reinforcement using a low value of $\tan\theta$. Additional horizontal steel in the tension zone is required if the inclination θ of the compression strut is not equal 45°.

The plots of V_n(CEB) versus V_n(test) in Fig. 4.7 and 4.10 show that the CEB Code overpredicts the shear capacity of beams without shear reinforcement and a low ratios of longitudinal steel. At the same time plots of V_n(EC 2) versus V_n(test) in Fig. 4.7 and 4.8 indicate that the Eurocode is conservative to some extent.

The shear capacity prediction given by the MCFT (21) are conservative compared to the test results of Pasley, the EC 2 and the CEB-Code predictions. The efficiency of the immense calculation process involved in the MCFT is, therefore, somewhat questionable. The theory seems to be too complex for use in routine design of simple or continuous beams. It may be more applicable for the analysis of

members having unusual or complex geometry or loading. The plots of v_n (test) versus v_n (MCFT, response procedure) showed that the difference between the level of the predicted and actual strengths was relatively constant. According to Pasley, the response procedure predicted the nominal shear capacity of beams with stirrups better than of those without stirrups. The study also showed that the prediction of the MCFT design procedure was better for beams without stirrups than for those with stirrups. Both procedures were not as accurate as ACI 318-89 in predicting the nominal shear capacity of the members due to conservative initial assumptions. The MCFT design procedure appeared to be more conservative as nominal shear strength increased.

The Hofer/McCabe equation is based on the test results and an assumed strut and tie truss model. Using principles of geometry, simplifying assumptions the predicted shear capacity of the compression/tension strut is derived. According to low ratios of shear reinforcement or no shear reinforcement it was assumed that the tension strut will yield first. Therefore, the first example shows that the Hofer/McCabe equation is close to the test results because it is based on these results. The second example shows that the Hofer/McCabe equation is close to the ACI equation for the cases of no shear reinforcement (Fig. 4.2) and the detailed method (Fig. 4.4). Using the standard method (Fig. 4.3) the Hofer/McCabe equation results lie between the ACI and the EC 2 prediction or 75% of the predicted shear capacity of the ACI equation. Because the Hofer/McCabe equation is based on one test series its

general applicability is questionable. It is meant to be an attempt to reflect the complexity of predicted shear capacities of continuous reinforced concrete members.

It is now generally recognized that the ACI Building Code shear design does not always produce a conservative design. The shear capacity equations are essentially empirical and the approach lacks a proper physical model for the behavior of beams subjected to both bending and shear.

During the past decades considerable research has been conducted to understand the behavior of structural concrete members. Based on a solid foundation of research the ACI-ASCE Committee 426 pays attention to the development of design approaches based on rational behavioral models, generally applicable, rather than on empirical evidence alone. The behavior of beams failing in shear may be expressed in terms of a mechanical model to visualize the shear flow in a beam which can be used in shear design. Consequently the shear capacities of the compression strut and the tension tie of the truss model have to be checked independently.

REFERENCES

1. ACI, "Standard Building Regulations for the Use of Reinforced Concrete", *American Standard Specification No. 23*, Vol. 16, Feb. 1920, pp. 283-322.
2. ACI-ASCE Committee 326, "Shear and Diagonal Tension", *ACI Journal, Proceedings*, 59, Jan., Feb., and March 1962, 1-30, 277-344, 352-396.
3. ACI-ASCE Committee 426, "The Shear Strength of Reinforced Concrete Members" - Chapters 1 to 4, *Journal of Structural Division*, ASCE 99, ST6, June 1973.
4. ACI-ASCE Committee 426, "Suggested Revisions to Shear Provisions for Building Codes", Abstract, *ACI Journal, Proceedings*, Sept. 1987, 74-150.
5. ACI-ASCE Committee 426, "Suggested Revisions to Shear Provisions for Building Codes", Detroit, Michigan: *American Concrete Institute*, 1979, 82pp.
6. ACI Code metric (revised 1992).
7. Boris Bresler and James G. MacGregor, "Review of Concrete Beams Failing in Shear", *Journal of the Structural Division*, ASCE, 93, ST1, Feb. 1967.
8. M. P. Collins and D. Mitchell, "Shear and Torsion Design of Prestressed and Non-Prestressted Concrete Beams", *Journal of the Prestressed Concrete Institute*, Vol. 25, No. 5, Sept.-Oct. 1980, pp. 32-100.
9. Comité Euro-International du Béton (CEB), Thomas Telford, *CEB-FIP Model Code*, 1990, Design Code.
10. CEB, "Shear and Torsion", *Explanatory and Viewpoint Papers on Model Code*, Ch. 11 and 12, Prep. By CEB Comm. V., CEB-Bulletin 12, Paris, June 1978.
11. Concrete Design, "US and European Practices", *ACI-CEB-PCI-FIB Symposium*, Copyright 1979, ACI, Detroit, Michigan.
12. *Eurocode 2* (1990).
13. P. M. Ferguson, J. E. Breen, J. O. Jirsa, *Reinforced Concrete Fundamentals*, 5th Edition, John Wiley & Sons, 1988.
14. F. Leonhardt, "Vorlesungen über den Massivbau", *Teil 1: Grundlagen zur Bemessung im Stahlbetonbau*, Springer-Verlag, 3. Auflage, 1984.
15. J.G. MacGregor, *Reinforced Concrete*, Prentice Hall, Englewood Cliffs, NJ, 1988.
16. P. Marti, "Truss Models in Detailing", *Conc. Int.*, Vol. 7, No. 12, 1985, pp 66-73.
17. P. Marti, "Basic Tools of Reinforced Concrete Beam Design", *ACI Journal*, Proceedings, 82, Jan.-Feb., 1985, 46-56.
18. D. Mitchell and M. P. Collins, "Diagonal Compression Field Theory - A Rational Model for Structural Concrete in Pure Tension", *ACI Journal*, Proceedings, Vol. 71, No. 8, Aug. 1974, pp. 396-408.

19. E. Mörsch, "Seine Theorie und Anwendung" (Reinforced Concrete Theory and Application), *Der Eisenbetonbau,* Konrad Wittwer Verlag, Stuttgart, 1912.
20. A. H. Nielson, G. Winter, "Design of Concrete Structures", 11th Edition, McGraw Hill, 1991.
21. G. P. Pasley et al., "Shear Strength of Continuous Lightly Reinforced T-Beams", *SM-Report No. 26*, Dec. 1990.
22. W. Ritter, "Die Bauweise Hennebique", *Schweizerische Bauzeitung*, Vol. 33, No. 7, Feb. 1899, pp. 59-61, Zürich.
23. H. G. Schäfer, "Eurocode 2 Commentary", University of Dortmund, Germany.
24. J. Schlaich, K. Schäfer and M. Jennewein, "Toward a Consistant Design of Structural Concrete", *J. Prestressed Concr. Inst.*, Vol. 32, No. 3, 1987, pp. 74-150.
25. WIT40, "Bautabellen für Ingenieure", *Schneider*, 9.Auflage, Werner Verlag, 1990.
26. WIT40, Bautabellen für Ingenieure mit europäischen und nationalen Vorschriften, *Schneider*, 11.Auflage, Werner Verlag, 1995.
27. A. N. Talbot, "Tests of Reinforced Concrete Beams, Resistance to Web Stresses Series of 1907 and 1908", *Bulletin 29*, University of Illinois, Engineering Experiment Station, Jan. 1909, pp. 85.
28. Frank J. Vecchio and Michael P. Collins, "The Compression Field Theory for Reinforced Concrete Elements Subjected to Shear", *ACI Journal* , Proceedings, 83, March-April 1986, 219-231, Disc. 84, January-February 1987, 87-90.
29. Frank J. Vecchio and Michael P. Collins, "Predicting the Response of Reinforced Concrete Beams Subjected to Shear Using Modified Compression Field Theory", *ACI Structural Journal*, 85, May-June 1988, 258-268.
30. C.-K. Wang, C. G. Salmon, "Reinforced Concrete Design", 5th Edition, 1992.
31. J. C. Walraven, "Fundamental Analysis of Aggregate Interlock", *Proceedings, ASCE*, Vol. 107, ST11, Nov. 1981, pp. 2245-2270.
32. M. O. Whitney, "Tests of Plain and Reinforced Concrete Series of 1906", *Bulletin of the University of Wisconsin*, Engineering Series, Vol. 4, No. 1, Nov. 1907, pp. 1-66.
33. M. O. Whitney, "Tests of Plain and Reinforced Concrete Series of 1907", *Bulletin of the University of Wisconsin*, Engineering Series, Vol. 4, No. 2, Nov. 1908, pp. 1-66.

APPENDIX A
Summary of Experimental Investigation

A.1 General

The basis for this thesis is the experimental investigation by Pasley, Gogoi, Darwin and McCabe at the University of Kansas in 1990 (21). The research was focused on the shear strength of continuous T-beams with light flexural reinforcement to identify how these typical members perform under shear loading. Primary emphasis was given to the behavior of the negative moment regions of the test beams. The details of the experimental work are described in this chapter.

A.2 Test Specimen

The test specimens were two-span continuous T-beams; each span was 6.26 m (20.5 ft) long. The beams were 457.2 mm (18 in) deep, with a web thickness of 190.5 mm (7.5 in). The flanges of the T-beams were 609.6 mm (24 in) wide and 101.6 mm (4 in) thick. The middle support was a simply supported transverse girder with a span of 1.04 m (41 in). Beam dimensions and properties are shown in Figs. A.1 and A.2.

The end supports of the test beams were rollers. The middle support, the transverse girder was pinned at each end. To reduce friction two layers of 0.8 mm (1/32 in) thick Teflon sheets were used between the bearing surfaces of the pin supports.

The test regions in the beams extended from the faces of the transverse girder to the points of maximum positive bending in both spans. Two series of T-beams

were tested, I and J. The I series had top longitudinal steel consisting of 2 #6 bars and 1 #5 bar for a reinforcement ratio, ρ_w, of 1.0% while the top longitudinal steel for the J series consisted of 2 #6 bars only with a ρ_w of 0.75%.

The intent of the experimental investigation was to fail the test specimen in shear in the negative moment. To prevent a failure mechanism prior to shear failure the system was designed with sufficient bottom steel. The I series had equal steel in the top and the bottom of the section. The J series had positive moment ratio values ρ_w of 0.75% (2 #6 bars), 1.0% (2 #6 and 1 #5 bars) and 1.83% (4 #6 and 1 #5 bars), respectively.

After the formation of a plastic hinge at the middle support, moment redistribution was achieved in beams I-2, J-2 and J-3 by a combination of top and bottom steel. Because the beams were longer than a single length of steel, Class A splices were employed. Top bars had a splice length of 685.8 mm (27 in) and were staggered far away from the face of the transverse girder to remove the splice from the test region of the section. The bottom bars had a splice length of 482.6 mm (19 in).

A.3 Materials

Concrete

An air-entrained concrete mixture was used supplied by a local ready-mix plant for these test beams. The ingredients were Type 1 Portland Cement, 19 mm (3/4 in) nominal maximum size coarse aggregate. The air content of the concrete varied between 3 and 4 %. The compressive strength of the concrete ranged between 30.34 MPa (4400 psi) and 31.72 MPa (4600 psi) based on compression cylinder tests per ASTM C 318-88. Concrete mixture proportions and properties are presented in Table A.2.

Steel

Flexural reinforcement in the test beams consisted of ASTM A615, Grade 60 (420 MPa), No. 3, 5 and 6 deformed steel bars. Shear reinforcement in the test regions was provided by smooth bars with diameters of 4.19 and 5.64 mm (0.165 and 0.222 in), spaced at 177.8 mm (7 in), not exceeding the spacing requirement per ACI 318-89.

In case of two point loads per span, stirrups were provided at a spacing of 444.5 mm (17.5 in) to hold the longitudinal steel in place in the positive moment region. The flanges of the beams were reinforced transversely with No. 3 bars spaced at 177.8 mm (7 in).

A.4 Specimen Preparation

Micro Measurements Type EA-06-060LZ-VZ0 strain gages were installed at midheight on the test stirrups and at points of maximum bending on the flexural steel, to measure strains in the stirrups and flexural.

Precision Type W240-120 paper backed strain gages were placed on the top and bottom surfaces of the T-beams to measure concrete strains.

A.5 Loading Systems

Two loading configurations, a single point load per span and two point loads per span, were applied to the tests:

One set of T-beams (I-1, I-2, J-1) were subjected to the single point loading, the second set (I-3, J-2, J-3) to the two point loading. Shear span to depth ratios, a/d, in the negative moment regions of the beams ranged from 3.2 to 3.8. Higher values of a/d were obtained in beams tested under single point span Loading. The two point loading system produced a/d ratios close to those of uniform loading.

Steel rods of 38 mm (1.5 in) diameter were used to load the beams. Each rod had a load capacity of 420 MPa (60 ksi). Load cells were installed at the steel rods and below the transverse girder to measure loads and reactions. A set of hydraulic jacks were used to apply the test load on the steel rods.

A.6 Instrumentation

For this experimental investigation midspan deflections were measured by linear variable differential transformers (LVDTs). Midspan deflections, concrete and steel strain gage readings were recorded by a Hewlett Packard data acquisition system.

A.7 Test Procedure

Readings of all strain gages and LVDTs were taken at zero total load, at 26.7 kN (6 kips) total load and then in incremental steps of 8.9 kN (2 kips) until the beam failed. After failure occurred in one of the spans the beams were unloaded, external stirrups were applied to clamp the failed beam and the test was continued. The beams were loaded up to the load at which the failure occurred and then incrementally loaded in steps of 8.9 kN (2 kips) until the second span failed. Each test took about three hours.

A.8 Test Observations

All beams experienced shear failures in the negative shear span near the girder. Under loading flexure cracks appeared first in sections of maximum bending moment, at the load points and at the middle support. As the load was increased, the

flexure cracks appeared further away from these sections and progressed toward the load points and supports.

Generally fewer cracks were developed in negative shear spans than in positive shear spans implying possible lower bond strength of the top cast flexural reinforcement compared to that of the bottom cast reinforcement. In the negative moment region first visible cracks were flexural cracks near the transverse girder at the top of the flange which propagated vertically. The effect of higher loads produced vertical cracks through the top of the flange which propagated diagonally up to the face of the transverse girder. Close to shear failure in the negative moment region the cracks propagated from the face of the girder parallel to the bottom of the flange intersecting few stirrups and passed diagonally through the flange.

In eleven out of thirteen conducted tests the test beams failed in the negative moment region. The shear capacity predicted by the ACI 318-89 was in five out of eleven failures[1] higher than the actual shear capacity.

[1] The test beams, continuous beams, were loaded until a failure occurred. The span which failed was fixed by external stirrups, reloaded until the beam failed again intending to obtain a shear failure in both of the spans.

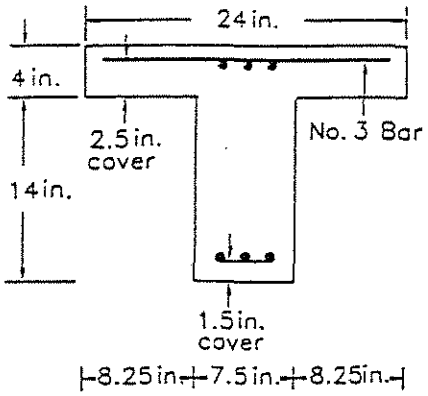

Fig. A.1 Cross section of beams without stirrups in test region.

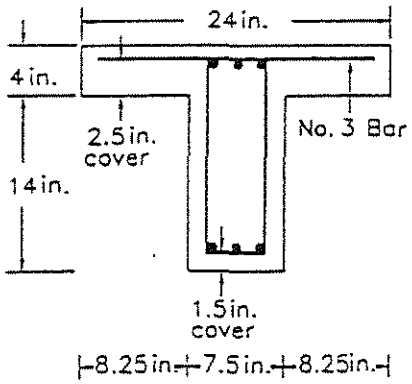

Fig. A.2 Cross section of beams with stirrups in test region.

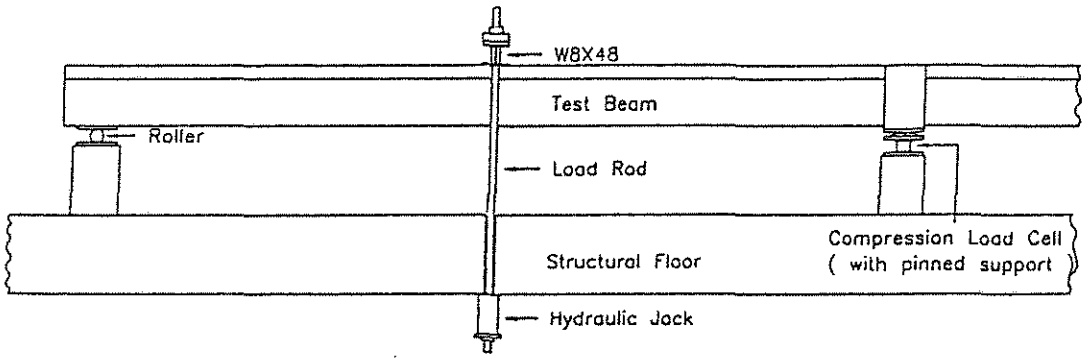

Fig. A.3 Single Point Loading System.

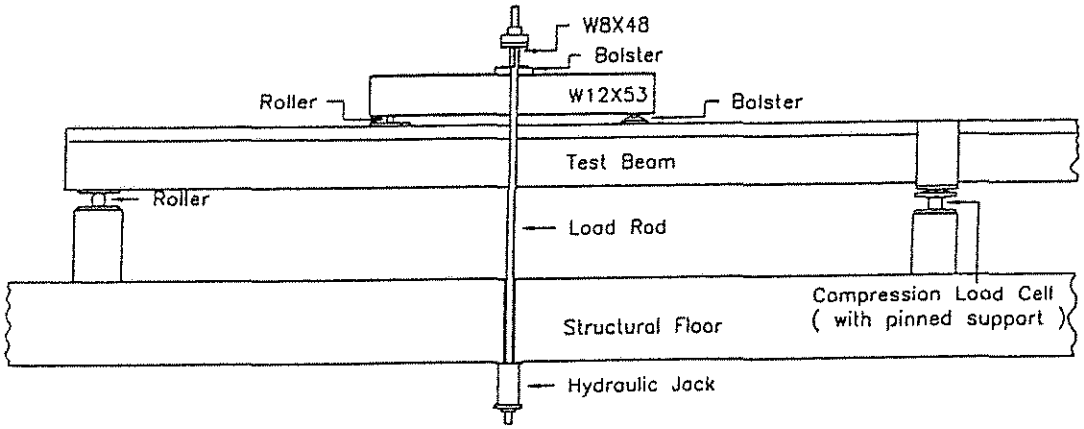

Fig. A.4 Two Point Loading System.

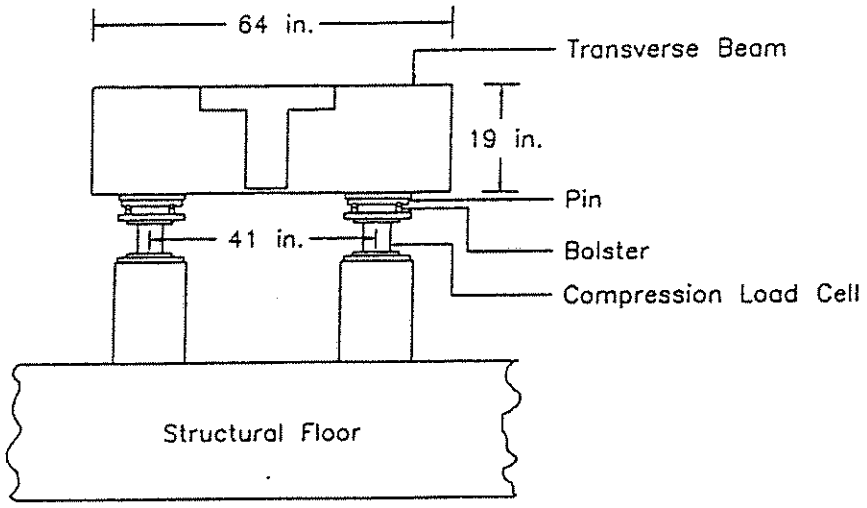

Fig. A.5 Transverse Girder.

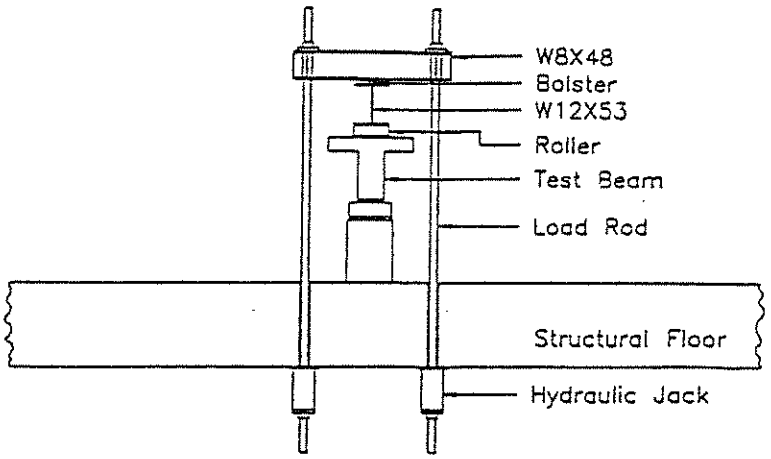

Fig. A.6 Two Point Loading System.

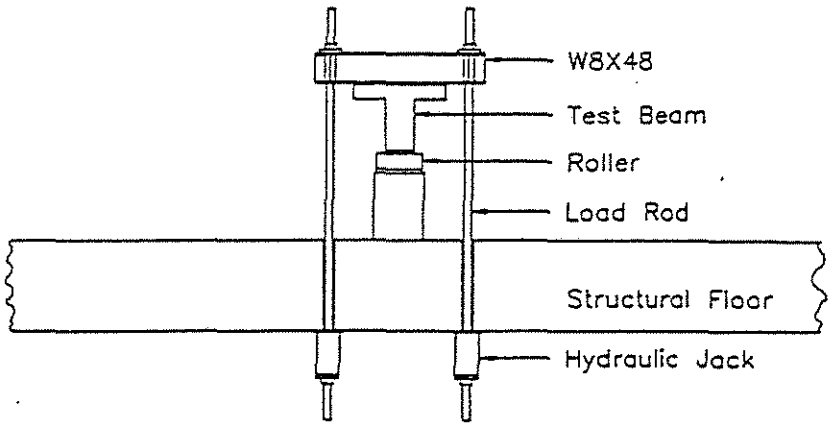

Fig. A.7 Single Point Loading System.

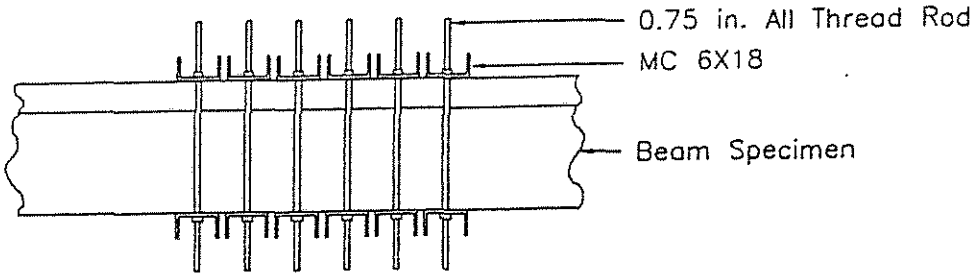

Fig. A.8 External Stirrups.

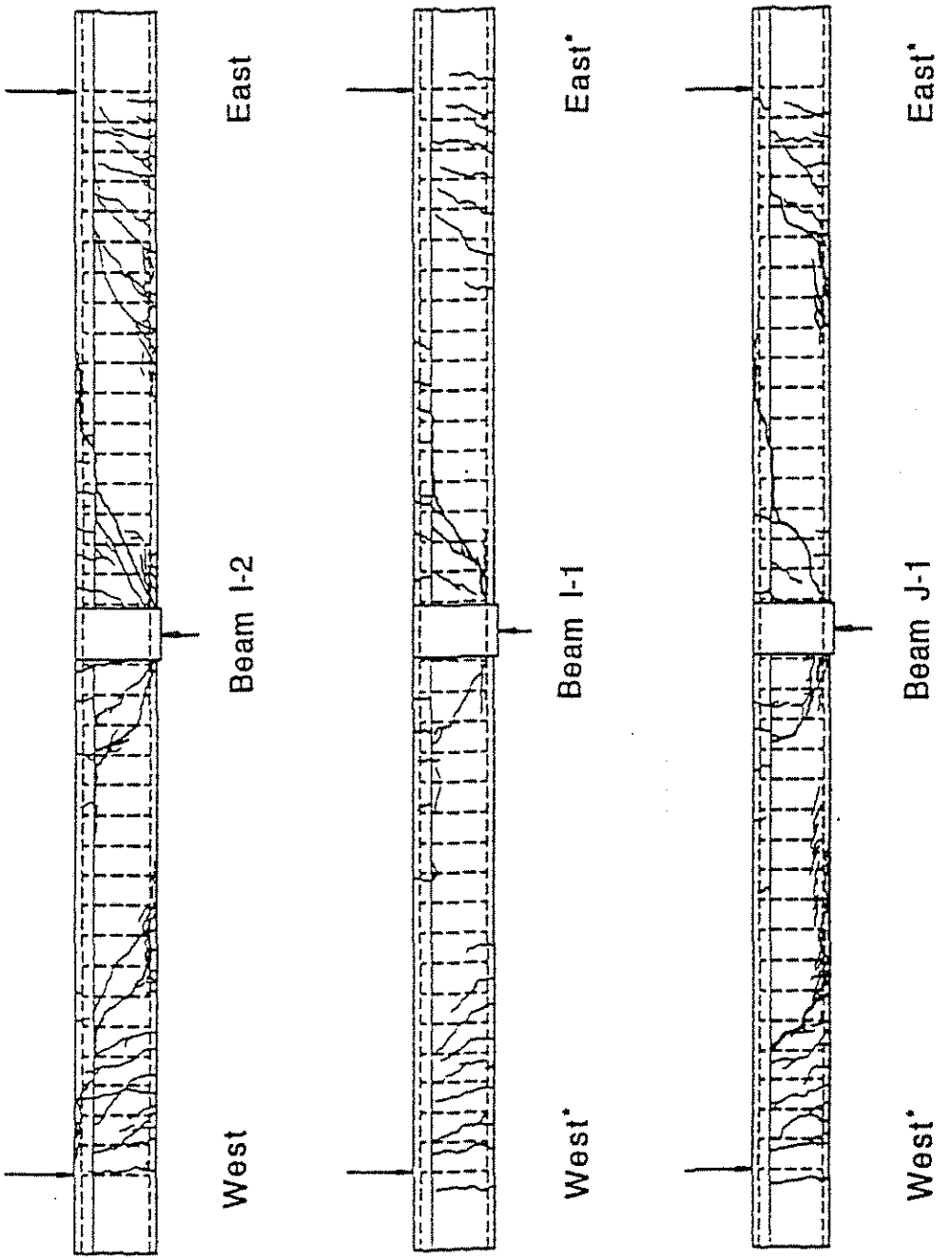

Fig. A.9 Crack Patterns, Beams I-1, I-2 and J-1 (*indicates span without stirrups).

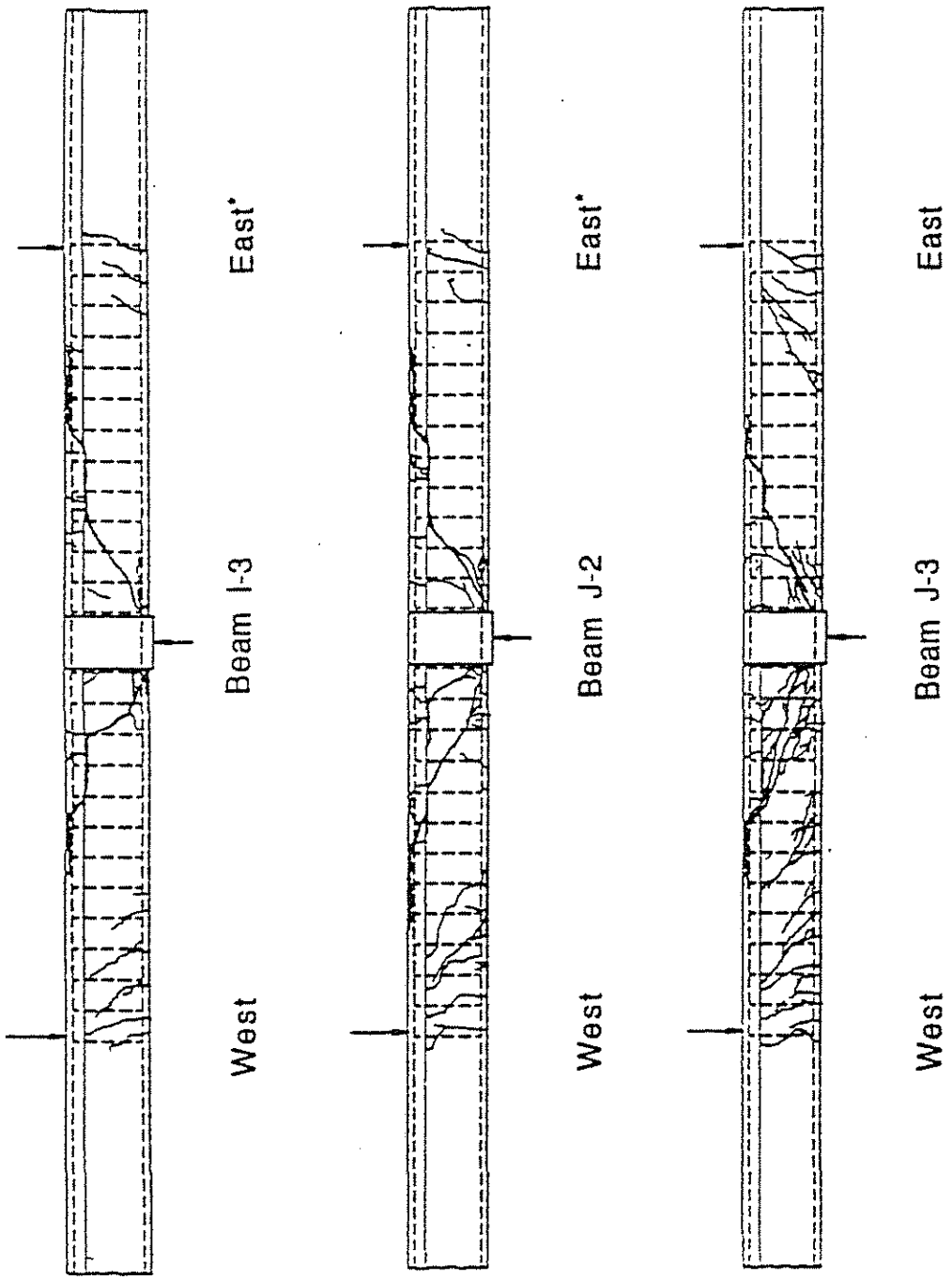

Fig. A.10 Crack Patterns, Beams I-3, J-2 and J-3 (*indicates span without stirrups).

Table A1: Results obtained from MCFT Response Procedure (21).

Load	Beam	Failure Region	θ	Horizontal Projection	$V_{n(MCFT)}$ [kN]	$v_{n(MCFT)}$ [MPa]	$\frac{v_{n(test)}}{v_{n(MCFT)}}$
1	I-1	east	50.00	0.84d	55.60	737.70	1.22
1	I-1	west	50.00	0.84d	55.60	737.70	1.20
1	I-2	east**	40.70	1.16d	93.85	1220.31	1.11
2	I-3	east	50.10	0.84d	56.93	737.70	1.31
2	I-3	west**	40.40	1.17d	96.52	1254.78	0.97
1	J-1*	east	57.60	0.63d	45.81	592.92	1.16
1	J-1	west	54.10	0.72d	48.04	641.18	1.39
1	J-1*	west	57.60	0.63d	45.81	592.92	1.41
1	J-1	east	54.10	0.72d	48.04	641.18	1.38
2	J-2	east	54.10	0.72d	49.82	648.07	1.38
2	J-2	west**	43.40	1.06d	85.40	1110.00	1.12
2	J-3	east**	41.10	1.13d	90.29	1192.73	1.20
2	J-3	west**	44.20	1.03d	94.74	1240.99	1.48

* positive moment region failure
** beams containing stirrups

Note: k1 from Step 3 equal to 0.8 for shear reinforcement.

Ratio is given for different cases as listed below:

$$\frac{v_n(test)}{v_n(MCFT)}$$

Mean (I-series beams, ρ_w=1.00%): 1.16
Coefficient of variation: 0.11

Mean (J-series beams, ρ_w=0.75%): 1.32
Coefficient of variation: 0.10

Mean (all beams): 1.26
Coefficient of variation: 0.12

Mean (beams without stirrups): 1.31
Coefficient of variation: 0.08

Mean (beams with stirrups): 1.18
Coefficient of variation: 0.16

Table A2: Results obtained from MCFT Response Procedure (21).

Load	Beam	Failure Region	θ	Horizontal Projection	$V_{n(MCFT)}$ [kN]	$v_{n(MCFT)}$ [MPa]	$\frac{v_{n(test)}}{v_{n(MCFT)}}$
1	I-2	east**	39.30	1.22d	98.75	1282.36	1.06
2	I-3	west**	38.90	1.24d	101.41	1316.83	0.92
2	J-2	west**	43.20	1.06d	85.85	1116.90	1.12
2	J-3	east**	41.30	1.14d	90.29	1192.73	1.20
2	J-3	west**	45.00	1.00d	95.19	1247.89	1.47

* positive moment region failure
** beams containing stirrups

Note: k1 from Step 3 equal to 0.4 for shear reinforcement.

		$\frac{v_n(test)}{v_n(MCFT)}$
Mean (beams with stirrups):	1.18	
Coefficient of variation:	0.16	

Table A3: Results obtained from MCFT Design Procedure (21).

Load	Beam	Failure Region	θ	Horizontal Projection	$V_{n(MCFT)}$ [kN]	$v_{n(MCFT)}$ [MPa]	$\frac{v_{n(test)}}{v_{n(MCFT)}}$
1	I-1	east	48.00	0.9d	54.71	730.81	1.24
1	I-1	west	48.00	0.9d	54.71	730.81	1.21
1	I-2	east**	43.00	1.07d	73.84	958.32	1.42
2	I-3	east	49.00	0.87d	56.04	730.81	1.32
2	I-3	west**	43.00	1.07d	75.62	985.90	1.23
1	J-1*	east	50.00	0.84d	51.15	661.86	1.04
1	J-1	west	50.00	0.84d	49.37	654.97	1.36
1	J-1*	west	50.00	0.84d	51.15	661.86	1.26
1	J-1	east	50.00	0.84d	49.37	654.97	1.35
2	J-2	east	50.00	0.84d	51.15	668.76	1.34
2	J-2	west**	45.00	1.00d	69.39	903.17	1.38
2	J-3	east**	45.00	1.00d	77.84	1027.27	1.40
2	J-3	west**	45.00	1.00d	89.85	1178.94	1.56

* positive moment region failure
** beams containing stirrups

Ratio is given for different cases as listed below:

$$\frac{v_n(test)}{v_n(MCFT)}$$

Mean (I-series beams, ρ_w=1.00%): 1.28
Coefficient of variation: 0.07

Mean (J-series beams, ρ_w=0.75%): 1.34
Coefficient of variation: 0.11

Mean (all beams): 1.32
Coefficient of variation: 0.10

Mean (beams without stirrups): 1.27
Coefficient of variation: 0.08

Mean (beams with stirrups): 1.40
Coefficient of variation: 0.08

APPENDIX B

CONVERSION TABLE

To convert from	to	multiply by
	Length	
foot	meter (m)	0.3048E*
inch	centimeter (cm)	2.54E*
	Area	
square foot	square meter (m^2)	0.0929
square inch	square centimeter (cm^2)	6.451
	Force	
kip	newton (N)	4448
pound force	newton (N)	4.448
	Stress (Force per Area)	
psi	newton/square meter (N/m^2)	6895
psf	newton/square meter (N/m^2)	47.88
	Bending Moment	
inch-pound-force	newton-meter (Nm)	0.1130
foot-pound-force	newton-meter (Nm)	1.356

* E indicates that the factor given is exact.